

Exosomes as Mediators of Cell-to-Cell Communication in Prostate Cancer

Isla Bruce

A thesis submitted in partial fulfilment of the requirements of
Edinburgh Napier University, for the award of Master by Research

August 2020

Declaration

I certify

- a) That this thesis is a result of my own independent work.
- b) This work has not been submitted for any other degree or professional qualification.

Signed:



Isla Bruce

Acknowledgments

Firstly, I would like to extend my thanks to my amazing supervisory team Dr Jenny Fraser and Dr Amy Poole. They have provided me with invaluable training, knowledge and guidance and I am eternally grateful for their support during my MRes. I feel extremely fortunate to have worked with such empowering women in science.

I'd like to acknowledge the postgraduate community at Napier with special thanks to Alice, Connan and Dave, you have all been an incredible support and I am so grateful to have met you. My fellow researchers and the technical staff of 3.C.16 were also of tremendous support during my research.

To my parents, it appears I am biomed homozygous, there was no avoiding it, thank you for both being my inspiration. Thank you for always encouraging me to strive for greatness and teaching me to be the best version of myself. Together we endured a lot during my degree, I am so grateful to have made it through stronger than ever. Scott, thank you for being so understanding and for all your love and support throughout my degree – I couldn't have done it without you.

This thesis is dedicated to the late Agnes Bruce and Elizabeth Whittet.

Abstract

Prostate cancer (PCa) is dependent on androgens for growth. Androgen deprivation therapy (ADT) curtails PCa progression, however this powerful selective pressure leads to aggressive, castrate resistant PCa. One castrate resistant prostate cancer subtype, neuroendocrine (NE) PCa, is characterised by increased abundance of NE cells. Transdifferentiation into androgen independent NE-like cells is thought to allow PCa epithelial cells to escape potent ADT, causing resistance. NE-like cells are thought to promote growth of surrounding tumour cells through paracrine communication. Exosomes are small extracellular vesicles released from all cells. They can be endocytosed by neighbouring cells and modify cellular function through their cargo (proteins and RNAs). Exosomes have been proposed to promote PCa NE-transdifferentiation (NEtD); by an unknown mechanism. This project aimed to isolate and characterise exosomes from NE-like cells and investigate their potential role in driving neuroendocrine PCa.

LNCaP cells were cultured in media containing charcoal-stripped FCS to deplete androgens as an *in vitro* model of AD (androgen deprivation) to promote NEtD. NEtD was confirmed by analysing LNCaP morphology, immunoblotting and qRT-PCR, investigating markers of the androgen receptor and NEtD. Exosomes are prevalent in FCS and may mask exosomes released from NE-like LNCaP cells, therefore exosomes were depleted from FCS/charcoal-stripped FCS by differential centrifugation. Exosome depletion did not affect LNCaP NEtD morphology or expression of androgen receptor and NEtD markers. However, AD increased expression of markers of the exosomal machinery (ALIX, CD9, HSP70, TSG101, RAB27A, VAMP7) as seen by qRT-PCR, suggesting AD may enhance exosome production. Exosomes were isolated from LNCaP and NE-like LNCaP culture medium to analyse exosome size, number and content by dynamic light scattering and immunoblotting. AD increased exosomal number and CD9 expression, suggesting NEtD is associated with increased exosome release. Exosome release from LNCaP cells was reduced by GW4869 and enhanced by Monensin. GW4869 regressed NEtD in AD LNCaP cells while Monensin induced NEtD in control LNCaP cells and enhanced AD LNCaP cells.

Table of Contents

Declaration	I
Acknowledgments	II
Abstract	III
Table of Contents.....	IV
List of Figures	XI
List of Tables.....	XIII
Abbreviations	XIV
1. Chapter 1: Introduction	1
1.1 Cell-to-cell communication.....	1
1.2 Extracellular vesicles	1
1.2.1 Exosome biogenesis	2
1.2.2 Microvesicle biogenesis.....	4
1.2.3 Extracellular vesicle content	5
1.2.4 Extracellular vesicle uptake	6
1.2.5 Extracellular vesicle isolation.....	6
1.2.6 Physical characterisation of extracellular vesicles	8
1.2.7 Biochemical and molecular characterisation of extracellular vesicles.....	9
1.3 Prostate cancer	11
1.3.1 The androgen receptor	12
1.3.2 Treatment options for PCa	12
1.3.3 Castrate resistant prostate cancer.....	14
1.3.4 Neuroendocrine cells in the prostate	15
1.3.5 Neuroendocrine prostate cancer (NEPC).....	16
1.3.6 Proposed factors involved in NETD of PCa.....	18

1.4	Exosomes in cancer	18
1.4.1	PCa patients and exosomes.....	20
1.4.2	Exosomes and NEtD in PCa	21
1.4.3	<i>In vitro</i> model of NEtD PCa	22
1.5	Overall aims.....	24
1.6	Thesis Hypothesis	24
2.	Chapter 2: Materials and Methods	25
2.1	Reagents and chemicals	25
2.2	Cell culture techniques	25
2.2.1	LNCaP cells.....	25
2.2.2	LNCaP culture conditions	25
2.2.3	Depletion of exosomes from Foetal Calf Serum by differential ultracentrifugation	25
2.2.4	Androgen deprivation of LNCaP cells.....	26
2.2.5	Exosome depletion of LNCaP cells	26
2.2.6	Sub Culturing LNCaP cells	26
2.2.7	Cryopreservation of LNCaP cells.....	27
2.2.8	Reviving LNCaP cells	27
2.2.9	Counting LNCaP cells	28
2.2.10	LNCaP morphology/microscopy	28
2.2.11	Harvesting cells	28
2.3	Assessing exosomes	29
2.3.1	Exosome isolation from conditioned culture medium.....	29
2.3.2	Assessing exosomes via Dynamic Light Scattering.....	30
2.3.3	Exosome Lysis	30
2.4	Synthetic inhibition and induction of exosome release	30
2.4.1	Stock solutions	30

2.5	MTT assay.....	31
2.6	Protein analysis	32
2.6.1	Cell lysis	32
2.6.2	Protein quantification by Bradford analysis.....	32
2.6.3	Preparation of protein for immunoblotting.....	33
2.6.4	Sodium Dodecyl Sulphate – Polyacrylamide Gel Electrophoresis (SDS-PAGE).....	33
2.6.5	Immunoblotting.....	34
2.7	RNA extraction, quantification and reverse transcription	36
2.7.1	Preparing DEPC treated water	36
2.7.2	RNA extraction	36
2.7.3	RNA quantification by Nanodrop 2000 (Spectrophotometer).....	37
2.7.4	Microfluidic analysis of RNA by Bioanalyzer 2100.....	37
2.7.5	Reverse transcription of RNA	38
2.8	Quantification of gene expression	39
2.8.1	Oligonucleotide design and preparation	39
2.8.2	qPCR.....	39
2.8.3	Identification of reference genes.....	40
2.8.4	Quantification of fold change in gene expression	42
2.9	Statistical analysis	42
3.	Chapter 3: Establishing a model for the analysis of exosomes derived from NEtD LNCaP cells	43
3.1	Introduction.....	43
3.2	Study aims and research questions.....	46
3.2.1	Overall aim:	46
3.2.2	Objectives.....	46
3.2.3	Research questions:.....	46
3.3	Results.....	46

3.3.1	Analysing the effect of exosome depletion on NEtD of LNCaP model – cell morphology analysis	46
3.3.2	Analysing the effect of exosome depletion on expression of molecular markers of AD-induced NEtD of LNCaP cells	48
3.3.3	Identifying stable reference genes for exosome depleted AD-induced NEtD LNCaP model	51
3.3.4	Analysing the effect of exosome depletion on the expression of key genes associated with NEtD	54
3.3.5	Conclusions	57
3.4	Discussion	58
3.4.1	Establishing a model to assess exosomes released from NEtD LNCaP cells	58
3.4.2	The consequence of exosome depletion of FCS	61
3.4.3	Androgen deprivation and exosome depletion	62
3.4.4	Exosome depletion of FCS may cause reduction in total RNA concentration	65
3.5	Conclusions and future work	65
4.	Chapter 4: Isolation and characterisation of exosomes from AD-induced neuroendocrine transdifferentiated LNCaP cells	67
4.1	Introduction	67
4.1.1	Exosomes and PCa/ NEtD	67
4.1.2	Isolation and characterisation of exosomes released from NEtD LNCaP cells	68
4.2	Study aim and research questions	69
4.2.1	Overall aim:	69
4.2.2	Objective:	69
4.2.3	Research Questions:	69
4.3	Results	70

4.3.1	Identification of exosomal associated markers in androgen deprived LNCaP cell model	70
4.3.2	Identifying the presence of exosomes isolated from AD-induced NEtD LNCaP cells	72
4.3.3	Analysing exosomes isolated from AD-induced NEtD LNCaP cells.....	75
4.3.4	Characterising exosomal machinery markers in AD-induced NEtD LNCaP cells	77
4.4	Discussion	79
4.4.1	The potential role of exosomes in PCa and NEtD	79
4.4.2	PCa exosomes and associated cargo	80
4.4.3	PCa exosomes and pre-metastatic niche formation	82
4.4.4	PCa exosomes and cellular stress	83
4.4.5	Exosomes as biomarkers in PCa.....	84
4.4.6	The impact of methodology on exosome isolation.....	85
4.4.7	Characterisation of exosomes released from NEtD LNCaP cells	87
4.4.8	Biochemical analysis of exosomes released from NEtD LNCaP cells.....	88
4.5	Conclusion.....	89
5.	Chapter 5: Manipulation of exosome release from control and AD-induced neuroendocrine transdifferentiated LNCaP cells	90
5.1	Introduction.....	90
5.1.1	The role of GW4869 in the blockade of exosome release	90
5.1.2	The role of Monensin in the induction of exosome release.....	92
5.1.3	Employing GW4869 and Monensin to manipulate exosomes release in disease	94
5.1.4	Employing GW4869 and Monensin to manipulate exosome release in PCa	95
5.2	Study aims and research questions.....	96

5.2.2	Overall aim:	96
5.2.3	Objectives:.....	96
5.2.4	Research Questions:	96
5.3	Results.....	97
5.3.2	Effect on cell viability after treatment of control and AD-induced NEtD LNCaP cells with different concentrations of GW4869 and Monensin.....	97
5.3.3	Exosomes released from AD LNCaP cells promote NEtD.....	100
5.3.4	Analysing the effect of GW4869 and Monensin treatment on the profile of exosomes released from LNCaP cells	102
5.3.5	Analysing the effect of GW4869 and Monensin treatment on the expression of key genes associated with AR signalling and NEtD	107
5.3.6	Analysing the effect of GW4869 and Monensin treatment on the expression of key genes of exosome machinery	110
5.4	Discussion	113
5.4.2	GW4869 as an inhibitor of exosome release.....	114
5.4.3	Monensin may manipulate exosome release via multiple mechanisms.....	115
5.4.4	The use of Monensin to enhance exosome release	117
5.4.5	Manipulating exosome release alters LNCaP cell morphology..	118
5.4.7	Manipulating exosome release alters the profile of extracellular vesicles isolated from LNCaP cells.....	120
5.4.8	Limitations of exosome manipulation via GW4869 and Monensin.....	122
5.4.9	Alternative methods of exosome manipulation	123
5.5	Conclusions	124
6.	Chapter 6: Relevance, research conclusions, and future direction ..	125
6.1	Relevance of research.....	125

6.1.1	Exosome depletion of FCS is an appropriate <i>in vitro</i> model to assess exosomes released from LNCaP and NEtD LNCaP cells.....	126
6.1.2	Androgen deprivation induces exosome machinery markers	126
6.1.3	Extracellular vesicle manipulation indicates a role for exosomes in NEtD in LNCaP cells.....	128
6.2	Research limitations	129
6.3	Future Directions	129
6.3.1	Exosomes as biomarkers in AD-induced NEtD LNCaP cells.....	129
6.3.2	Do exosomes drive NEtD in LNCaP cells?	130
6.3.3	Do differential time points affect the cargo within AD LNCaP cell exosomes?	131
6.3.4	Are drivers of NEtD present in exosomes released from PCa cells?.....	132
6.4	Final conclusions	133
	References.....	134

List of Figures

Figure 1.1: Exosome Biogenesis.	3
Figure 1.2: Microvesicle Biogenesis.	4
Figure 1.3: Progression of prostate cancer to castrate resistant prostate cancer.	15
Figure 1.4: Neuroendocrine transdifferentiation of prostate cancer.	17
Figure 1.5: Proposed involvement of exosomes in NEtD PCa.	22
Figure 1.6: Schematic diagram indicating how ultracentrifugation can deplete exosomes from FCS.	23
Figure 3.1: Schematic highlighting the potential effects of exosome depletion of serum on culture of LNCaP cells.	45
Figure 3.2: Exosome depletion does not affect AD induced NE-transdifferentiation of LNCaP cells.	47
Figure 3.3: Exosome depletion may affect expression of NEtD-associated markers in LNCaP cells.	49
Figure 3.4: Identifying stable reference genes in exosome-depleted model of AD-induced NEtD in C, dC, AD and dAD LNCaP cells.	53
Figure 3.5: Assessing the effect of exosome depletion on NEtD LNCaP cells.	56
Figure 4.1: Exosome isolation, precipitation and purification.	68
Figure 4.2: Assessing the effect of exosome depletion on expression of exosomal markers in NEtD LNCaP cells.	71
Figure 4.3: Analysing the profile of extracellular vesicle populations secreted by AD LNCaP cells.	74
Figure 4.4: Analysing the profile of markers of exosomes isolated from control and AD LNCaP cells.	76
Figure 4.5: Analysing exosome machinery in LNCaP cells.	78
Figure 5.1: Manipulation of extracellular vesicle release via GW4869.	91
Figure 5.2: Manipulation of exosome release via Monensin.	93
Figure 5.3: Analysing the effect of GW4869 and Monensin on LNCaP cell viability.	98

Figure 5.4: Monensin induces a neuroendocrine-like phenotype in control LNCaP cells.	101
Figure 5.5: Manipulation of exosome release alters the profile of extracellular vesicles isolated from LNCaP cells.	105
Figure 5.6: Manipulation of exosome release alters the size and number of extracellular vesicles isolated from LNCaP cells.	106
Figure 5.7: Assessing the effect of GW4869 or Monensin treatment on key genes associated with NEtD in LNCaP cells.	109
Figure 5.8: Assessing the effect of GW4869 or Monensin treatment on genes associated with exosomes in LNCaP cells.	112
Figure 6.1: Differential expression of exosome machinery genes induced by AD	128

List of Tables

Table 2.1: Primary antibodies used within this study for immunoblotting	36
Table 2.2: Secondary antibodies used within this study for immunoblotting	37
Table: 2.3: Oligonucleotides used for qRT-PCR analysis in this study	42

Abbreviations

ACTB	Beta Actin
AD	Androgen Deprivation
ADT	Androgen Deprivation Therapy
ALIX	ALG-2 Interacting Protein X
AmPS	Ammonium Peroxodisulphate
AR	Androgen Receptor
ARE	Androgen Response Element
AR-V7	Androgen Receptor Splice Variant 7
ASCL1	Achaete-Scute Complex-Like 1
BCL2	Beta Cell Lymphoma 2
BSA	Bovine Serum Albumin
C	Control
cDNA	Complementary Deoxyribonucleic acid
CHGA	Chromogranin A
CRPC	Castrate Resistant Prostate Cancer
CrgA	Chromogranin A
CS-FCS	Charcoal Stripped Foetal Calf serum
C_T	Cycle Threshold
dAD	Exosome Depleted Androgen Deprived
dC	Exosome Depleted Control
DEPC	Diethylpyrocarbonate
dH₂O	Distilled Water
DHT	Dihydrotestosterone
DLS	Dynamic Light Scattering
DMSO	Dimethyl sulfoxide
DNA	Deoxyribonucleic acid
EIF4A2	Eukaryotic Translation Initiation Factor
ENO2	Enolase 2
ESCRT	Endosomal Sorting Complex Required for Transport
EV	Extracellular Vesicle

FCS	Foetal Calf Serum
GAPDH	Glyceraldehyde 3-Phosphate Dehydrogenase
GnRH	Gonadotropin Releasing Hormone
hASH1	Human Achaete-scute Homolog 1
Hsp70	Heat Shock Protein 70
IHC	Immunohistochemistry
ILV	Intraluminal Vesicle
ISEV	International Society for Extracellular Vesicles
kDa	Kilodaltons
KLK3	Kallikrein Related Peptidase 3
LSB	Loading Sample Buffer
mCRPC	Metastatic Castrate Resistant Prostate Cancer
mRNA	Messenger Ribonucleic acid
miRNA	Micro Ribonucleic acid
MISEV	Minimal Information for Studies of Extracellular Vesicles
MS	Mass Spectrometry
MTT	3-(4,5-Dimethylthiazol-2-yl)-2,5 Diphenyltetrazolium Bromide
MVB	Multivesicular Body
NCBI	National Centre for Biotechnology Information
NDRG1	N-Myc Downstream Regulated 1
NE	Neuroendocrine
NEPC	Neuroendocrine Prostate Cancer
NEtD	Neuroendocrine Transdifferentiation
NGS	Next Generation Sequencing
nSMase	Neural Sphingomyelinase
NSE	Neuron Specific Enolase
NTA	Nanoparticle Tracking Analysis
NTC	No Template Control
PARP	ADP Ribose Polymerase Protein
PBS	Phosphate Buffered Saline
PBS-T	Phosphate Buffered Saline - Tween
PC3	Pro-Caspase

PCa	Prostate Cancer
PSA	Prostate Specific Antigen
PTOV1	Prostate tumour overexpressed 1
qRT-PCR	Quantitative Reverse Transcriptase Polymerase Chain Reaction
RAB27A	Ras-Associated Binding Protein 27A
RAB7	Ras- Associated Binding Protein 7
REST	RE-1 Silencing Transcription Factor
RIN	RNA Integrity Number
RNA	Ribonucleic Acid
RIPA	Radioimmunoassay Precipitation Assay
RNP	Ribonucleoprotein
RPL13A	Ribosomal Protein L13a
RPMI	Roswell Park Memorial Institute Cell Culture Medium
RT	Reverse Transcription
SD	Standard Deviation
SDHA	Succinate Dehydrogenase Complex Sub-Unit A
SEM	Standard Error of the Mean
SNARE	Soluble N-Ethylmale-Imide-Sensitive Factor-Attachment Protein Receptors
SYP	Synaptophysin
TEM	Transmission Electron Microscopy
TMPRSS2	Transmembrane protease serine 2
TSG101	Tumour Susceptibility Gene 101
TUBB3	Beta Tubulin Class III
tRPS	Tuneable Resistive Pulse Sensing
TNM	Tumour Node Metastasis
TXNIP	Thioredoxin-interacting Protein
VAMP7	Vesicle Associated Membrane Protein 7
YWHAZ	14,3,3 Protein Zeta/Delta

1. Chapter 1: Introduction

1.1 Cell-to-cell communication

In multicellular systems, cell-to-cell communication is essential to maintain homeostasis, coordinate development and promote environmental adaptation and survival via migration, proliferation, differentiation and apoptosis of cells (Mittelbrunn and Sánchez-Madrid, 2012; Turturici *et al.*, 2014; Vader *et al.*, 2014). Classically, cells communicate by direct cell-to-cell contact, using adhesion molecules, gap junctions or released via soluble factors such as cytokines, chemokines, growth factors, neurotransmitters and their specific recognition cell-surface receptors for proximal (autocrine, paracrine) or distal (endocrine) communication (Mittelbrunn and Sánchez-Madrid, 2012; Tetta *et al.*, 2013).

1.2 Extracellular vesicles

Extracellular vesicles (EVs) are endogenous heterogenous lipid membrane-bound vesicles, ranging from 30 – 2000 nm in diameter, released by all cells (Willms *et al.*, 2016). Cell-derived EVs convey multifaceted biological messages between cells via their cargo, consisting of proteins, lipids and nucleic acids (Théry, 2011). Thus, EVs are widely accepted to provide a novel form of intercellular communication with exciting potential to reform the understanding of cellular communication in disease (Vader *et al.*, 2014). EVs can be categorised into, exosomes and microvesicles; based on intracellular origin or mechanism of release (Willms *et al.*, 2016). Intraluminal vesicles are formed by inward budding of the endosomal membrane during maturation of multivesicular endosomes to form multivesicular bodies and are secreted by fusion of multivesicular bodies with the plasma membrane, known as exosomes (Figure 1.1; Van Niel *et al.*, 2018). Microvesicles are produced by direct outward budding and fission of the plasma membrane and are more heterogeneous in size (50 – 1000 nm); (Vader *et al.*, 2014).

1.2.1 Exosome biogenesis

Exosome biogenesis occurs through the Endosomal Sorting Complex Required for Transport (ESCRT) pathway and the ceramide-mediated pathway (Figure 1.1; Bebelman et al., 2018). Sorting and packaging of ubiquitinated proteins is performed by tumour susceptibility gene 101 (TSG101) and ESCRT accessory protein ALG-interacting protein X (ALIX); (Figure 1.1; Schmidt and Teis, 2012). Intraluminal vesicles are formed by invaginations in the endosomal membrane, initiating maturation of early endosomes to multivesicular bodies (MVBs), which are degraded by lysosomes or transported to the plasma membrane (Figure 1.1; Van Niel et al., 2018). Multivesicular bodies are docked at the plasma membrane via Ras-associated binding protein 27A (RAB27A) (Figure 1.1; Ostrowski et al., 2010). Then, Soluble N-ethylmale-imide-sensitive factor-Attachment Protein Receptors (SNARE) proteins such as vesicle associated membrane protein 7 (VAMP7), induce fusion with the plasma membrane (Figure 1.1; Fader et al., 2009) releasing intraluminal vesicles into the extracellular space, as exosomes, which are enriched in tetraspanins (CD9); (Figure 1.1; Andreu and Yáñez-Mó, 2014).

Trajkovic et al. (2008) elucidated ceramide-mediated exosome generation as an alternative exosome biogenesis pathway (Figure 1.1). Hydrolytic removal of the phosphocholine moiety of sphingomyelin via neutral sphingomyelinase produces ceramide (Trajkovic et al., 2008). Generation of ceramide in the limiting membrane of multivesicular bodies induces membrane invaginations and thus, intraluminal vesicle formation (Trajkovic et al., 2008). Ceramide's cone-shaped structure may cause spontaneous membrane curvature of the endosomal membrane promoting domain-based budding, highlighting the role of lipids in exosome biogenesis (Zhang et al., 2019).

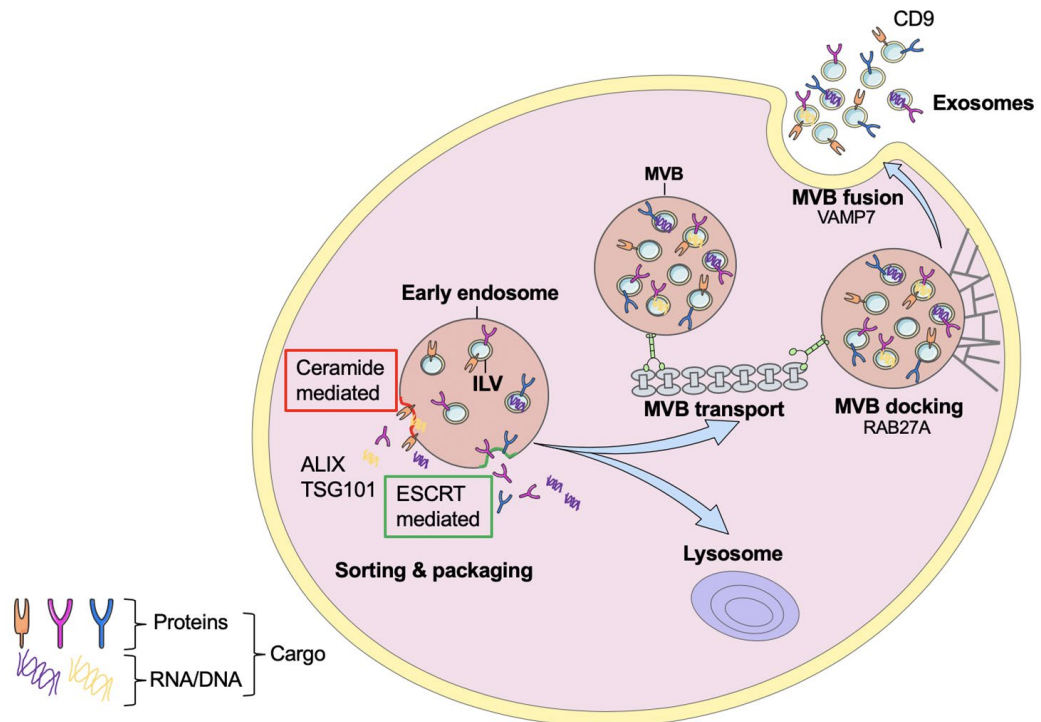


Figure 1.1: Exosome biogenesis. Cargo is sorted and packaged by Endosomal Sorting Complex Required for Transport (ESCRT) or ceramide-mediated pathways. ESCRT-0 identifies and sorts ubiquitinated proteins and recruits ESCRT-1 by binding tumour susceptibility gene 101 (TSG101)/Vps23 subunit. Ubiquitinated proteins are transported to ESCRT-I and ESCRT-II, which drive invaginations in the endosomal membrane to form intraluminal vesicles (ILVs). ESCRT-III then forms a spherical structure to limit the budding neck, the ATPase, VPS4, drives membrane scission leading to intraluminal vesicle release. The accessory protein ALG interacting protein X (ALIX) intersects the canonical ESCRT pathway, contributing to exosomal cargo selection. Multivesicular bodies are transported to the plasma membrane and dock via RAS-associated binding protein 27a (RAB27A). Soluble N-ethylmale-imide-sensitive factor-Attachment Protein Receptors (SNARE) proteins such as vesicle associated membrane protein 7 (VAMP7), induce fusion with the plasma membrane releasing the intraluminal vesicles into the extracellular space as exosomes, enriched with tetraspanin proteins such as CD9, CD63 or CD8. In ceramide-mediated biogenesis, ceramide is produced in the limiting membrane of multivesicular bodies inducing invaginations and thus, intraluminal vesicle formation. Created using Servier Medical Art by Servier.

1.2.2 Microvesicle biogenesis

The precise mechanisms involved in microvesicle formation are unknown (Muralidharan-Chari *et al.*, 2010) however, it is widely accepted that their release arises via direct outward budding and pinching of the plasma membrane (Figure 1.2; Tricarico *et al.*, 2017).

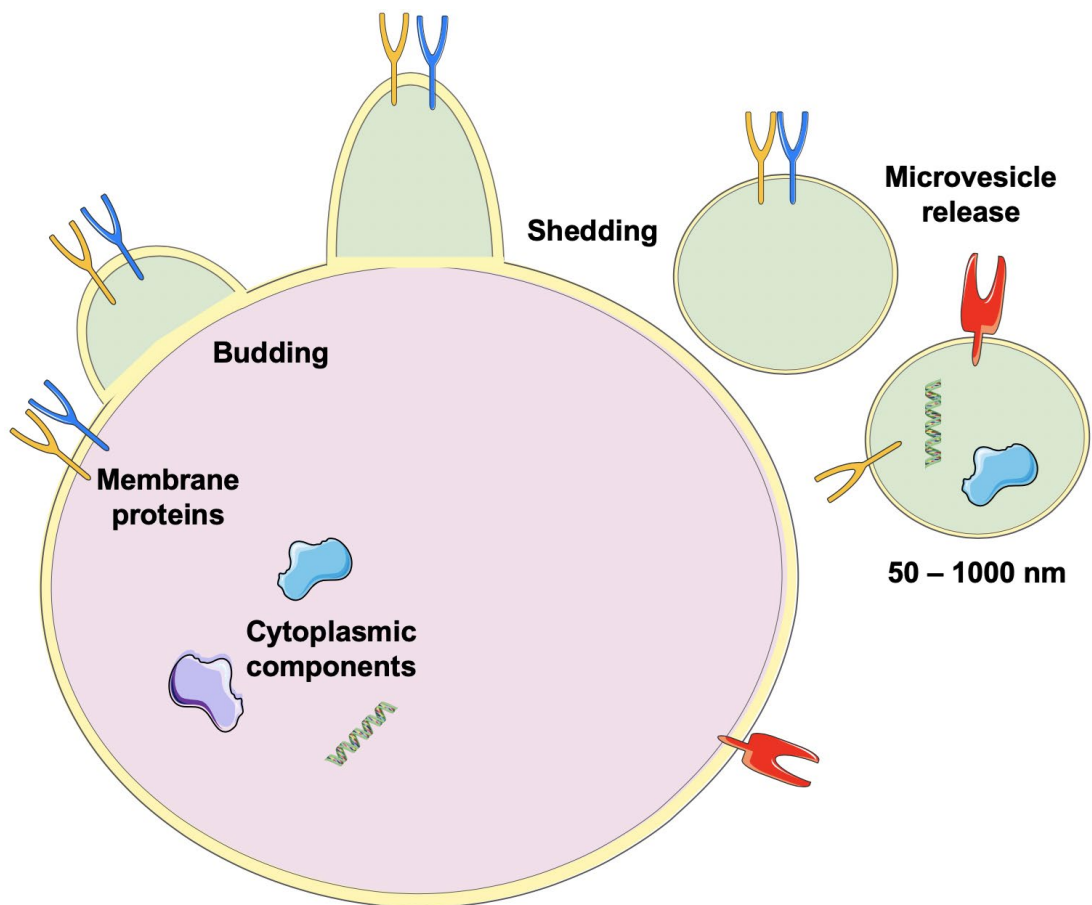


Figure 1.2: Microvesicle biogenesis. Budding of the plasma membrane incorporates cell surface proteins or cytosolic proteins bound to the inner leaflet of the plasma membrane. The vesicles are shed from the plasma membrane and can range from 50-1000 nm and are known as microvesicles. Created using Servier Medical Art by Servier.

There is a partial overlap between exosomes and microvesicles biogenesis as ESCRT machinery is involved in the production of vesicles enriched in cell surface proteins reflecting their plasma membrane origin (Bebelmann *et al.*, 2018).

Acid sphingomyelinase can also induce ceramide-dependant microvesicle assembly (Bianco *et al.*, 2009). There can often be commonality in exosomal and microvesicle cargo (Van Niel *et al.*, 2018). However, cytosolic components are sorted into microvesicles via binding to the inner leaflet of the plasma membrane (Mcgough and Vincent, 2016). Post-translational palmitoylation, prenylation and myristoylation of cargo is responsible for this process (Shen *et al.*, 2011; Yang and Gould, 2013). A sub-population of microvesicles are termed apoptotic bodies and differ from microvesicles via their size (50-5000 nm) and release mechanism (Willms *et al.*, 2016; Van Niel *et al.*, 2018). Microvesicles are released constitutively, however, apoptotic bodies are only released during apoptosis via outward blebbing and fragmentation of the apoptotic cell (Vader *et al.*, 2014). Unlike exosomes and microvesicles, apoptotic bodies contain nuclear and cytoplasmic organelle fragments thus, DNA, histones and components of the Golgi apparatus or endoplasmic reticulum are suggested markers for their identification (Vader *et al.*, 2014).

1.2.3 Extracellular vesicle content

EVs were initially proposed as a mechanism to remove cellular waste from cell damage, or by-products of cell homeostasis, and thought to have no significant impact on neighbouring cells (Zhang *et al.*, 2019). It is now known EVs contain complex cargo of proteins, lipids, and nucleic acids that can alter function of recipient cells by exosomal cell-to-cell communication and contribute to functional diversity of EVs (Mathivanan *et al.*, 2012; Kim *et al.*, 2013).

Proteins commonly found in EVs are associated with biogenesis, such as ESCRT components (ALIX, TSG101); heat shock proteins (HSP70, HSP90); proteins responsible for transport and release (annexins, RAB27A, RAB11B); as well as tetraspanins (CD9, 63, 81), which take part in cell penetration, fusion and invasion (Abels and Breakefield, 2016). EVs are enriched in nucleic acids such as small RNAs (miRNAs), which undergo unidirectional transfer between cells, establishing an intercellular trafficking network, which elicits transient or phenotypic changes in recipient cells (Mittelbrunn and Sánchez-Madrid, 2012).

EVs are also enriched in lipids such as cholesterol, sphingomyelin, arachidonic acid and fatty acids, which account for their stability and structural rigidity (Zhang *et al.*, 2019). To some degree, exosomal cargo is cell type dependent, reflecting the cell they are released from (Hessvik and Llorente, 2018).

1.2.4 Extracellular vesicle uptake

Internalisation of EVs and associated cargo by endocytosis can alter or reprogram the recipient cell function at proximal and distal ranges, presenting as a means of cell-to-cell communication (Zhang *et al.*, 2019). EV internalisation may be dependent on recipient cell type, its physiologic state, and whether there is ligand-receptor recognition by the recipient cell (Zaborowski *et al.*, 2015). For example, neurons employ clathrin-dependent endocytosis or phagocytosis (Morelli *et al.*, 2004; Barrès *et al.*, 2010), macropinocytosis by microglia (Feng *et al.*, 2010), phagocytosis or receptor-mediated endocytosis by dendritic cells (Fitzner *et al.*, 2011; Montecalvo *et al.*, 2012), caveolin-mediated endocytosis in epithelial cells (Frühbeis *et al.*, 2013), and cholesterol- and lipid raft-dependent endocytosis in tumour cells (Nanbo *et al.*, 2013; Svensson *et al.*, 2013). EVs can also fuse with the recipient cell membrane to release cargo into the cytoplasm or via ligand-receptor binding to induce signalling in the recipient cells (Turturici *et al.*, 2014). The uptake of EVs by recipient cells highlights their importance in cell-to-cell communication in healthy and diseased states.

1.2.5 Extracellular vesicle isolation

There are multiple methods of EV isolation including differential ultracentrifugation, size-based techniques such as ultrafiltration, precipitation and size exclusion chromatography (Witwer *et al.*, 2013).

The most widely applied method of exosome isolation is differential ultracentrifugation where EVs are separated by particle density, size and shape (Jeppesen *et al.*, 2014). Differential ultracentrifugation uses several centrifugation steps, that sequentially increase in speed and time to pellet sequentially smaller particles (Li *et al.*, 2017). Little or no sample pre-treatment is required and it is

cost-effective (Doyle and Wang, 2019). Differential ultracentrifugation does not exclusively remove EVs from biological fluids, often proteins such as albumin or immunoglobulins can co-sediment with EVs, interfering with EVs analysis (Caradec *et al.*, 2014). Differential ultracentrifugation can also be time-consuming, with limited capacity to process multiple samples at once due to large sample volumes required (Doyle and Wang, 2019).

Other EV isolation methods include size-based techniques such as ultrafiltration, precipitation or, size exclusion chromatography (Witwer *et al.*, 2013). Ultrafiltration employs nanomembranes or molecular weight cut offs to isolate exosomes from culture medium or bodily fluid (Zhang *et al.*, 2018). This can shorten conventional ultracentrifugation time but vesicles can become obstructed or trapped in filters, resulting in exosomal loss (Doyle and Wang, 2019). Like viruses or other small particles, EVs can also be precipitated from biological fluids using polyethylene glycol (PEG) buffer, which displaces water molecules causing EVs to precipitate out of solution (Rider *et al.*, 2016). EVs can then be pelleted by centrifugation (Ludwig *et al.*, 2018). Precipitation can co-isolate non-EV components such as proteins and protein aggregates therefore, it is recommended to combine precipitation with a purifying method (Doyle and Wang, 2019). Size exclusion chromatography uses a porous column, causing particles in sample to eluate at different rates, larger particles will elute more rapidly while smaller particles will elute more slowly, the eluted fraction of a certain time should therefore, contain a population of particles of the same size (Szatanek *et al.*, 2015). Typically, size exclusion is used in conjunction with precipitation or ultracentrifugation to further purify exosomes (Welton *et al.*, 2015).

Currently, there is no standardised approach to exosome isolation (Witwer *et al.*, 2013) and the biochemical overlap between exosomes and other EVs such as microvesicles means many methods do not exclusively isolate exosomes (Li *et al.*, 2017). The international society for extracellular vesicles (ISEV) created a set of recommendations to promote linearization of EV research, they recommend the use of one or more additional technique (ultrafiltration, density gradients or

chromatography) following primary method (differential ultracentrifugation or precipitation) to improve specificity of EVs subtype separation (Théry *et al.*, 2018; Van Niel *et al.*, 2018).

1.2.6 Physical characterisation of extracellular vesicles

Physical characterisation provides information on particle size and/or concentration of EVs via dynamic light scattering (DLS) nanoparticle tracking analysis (NTA) or transmission electron microscopy (TEM); (Doyle and Wang, 2019). DLS employs a monochromatic and coherent laser beam; when the laser hits a particle in suspension, light is scattered in all directions (Szatanek *et al.*, 2017). DLS analyses fluctuations in intensity of scattered light in Brownian motion to estimate particle size and concentration to detect particles from 1 nm to 6 µm (Lane *et al.*, 2015). A shortcoming of DLS is that scattered light intensity is more sensitive to the presence of larger particles; thus, scattered light caused by smaller particles is more difficult to detect so data can be skewed towards larger particles in heterogenous mixtures (Doyle and Wang, 2019). Like DLS, NTA also uses scattered light however, instead of fluctuations in intensity, NTA uses the diffusion coefficient to estimate particle size (Doyle and Wang, 2019). NTA uses a camera attached to a microscope to track particle displacement plotted as a function of time, enabling calculation of particle size and distribution (Szatanek *et al.*, 2017). NTA can also analyse fluorescently labelled exosomes however, expression of the studied marker must be high and the fluorescent signal needs to be very bright in order to be detected (Dragovic *et al.*, 2013, 2015).

Transmission Electron Microscopy (TEM) uses short wavelengths of electrons to resolve characteristic features of exosomes such as their cup-shaped morphology (Raposo and Stoorvogel, 2013). Generally, TEM is employed as a method of visualisation after detection of the size and concentration by other techniques such as DLS or NTA (Zhang *et al.*, 2018).

1.2.7 Biochemical and molecular characterisation of extracellular vesicles

Biochemical and molecular techniques such as immunoblotting, mass spectrometry, flow cytometry or miRNA profiling provide information on cargo isolated from EVs (Doyle and Wang, 2019).

Where possible, when performing EV protein analysis five different categories of proteins should be employed including; transmembrane or GPI-anchored proteins localised in the plasma membrane or endosome such as non-tissues specific tetraspanins (CD63) or tissue specific tetraspanin such as CD9 (absent from NK, B and some mesenchymal stem cells), TSPAN8 (epithelial cells) or ERBB2; cytosolic proteins such as those associated with ESCRT-I/II/III (TSG101, ALIX, VSP4A/B, flotillin-1/2 or Hsp70); proteins that are major constituents of non-EV membranes, which can often be co-isolated (albumin, protein/nucleic acid aggregates); proteins localised on intracellular compartments such as the nucleus (histones), mitochondria (cytochrome C) or secretory pathway (calnexin); or secreted luminal proteins that associate with EVs via surface receptors such as cytokines (interleukins) or growth factors (TGFB1/2); (Théry *et al.*, 2018). Using a combination of these markers to characterise EVs will provide a more robust and standardised analysis approach to exosomal proteomic analysis (Bhome *et al.*, 2018).

Immunoblotting is the most commonly used method to detect exosomal proteins due to its wide accessibility (Théry *et al.*, 2018). Immunoblotting requires cell lysis; therefore, this technique can provide data on exosomal cargo that may be involved in cell-to-cell communication. Exosomal cargo therefore, may represent potential biomarkers for disease, which are used to distinguish abnormal biological processes from normal processes (Verma *et al.*, 2011). Immunoblotting is dependent on the use of specific antibodies; therefore, it is necessary to know what proteins you intend to investigate (Doyle and Wang, 2019). Unlike immunoblotting, mass spectrometry (MS) enables high-throughput peptide profiling and identification of previously unknown proteins (Shao *et al.*, 2018).

Validation of protein candidates can then be performed using conventional protein techniques such as immunoblotting to provide an insight to exosomal protein cargo and the potential to use these as biomarkers for disease (Bandu *et al.*, 2019), to provide quantitative and comparative EV proteomic analysis (Shao *et al.*, 2018). Flow cytometry can be considered as a physical and biochemical form of exosome analysis as it allows visual observation of EV populations however, this requires knowledge regarding their protein composition (Doyle and Wang, 2019). The detection limit of most flow cytometers is 300 - 500 nm, which poses a challenge as exosomes have an average diameter of 30 - 100 nm (Shao *et al.*, 2018). Exosomes must, therefore, be immobilised via beads by immunocapture or covalent conjugation (Doyle and Wang, 2019). Once immobilised exosomes are exposed to fluorescently conjugated antibodies against antigens on the exosomal surface (tetraspanin proteins); (Szatanek *et al.*, 2017). When sample passes the laser of the flow cytometer it emits a fluorescent signal, allowing high-throughput analysis and classification of EVs based on antigen expression (Szatanek *et al.*, 2017).

miRNA expression in EVs can be measured by qRT-PCR, microarray hybridization and next-generation sequencing (NGS); (Git *et al.*, 2010). qRT-PCR is scaled up for miRNA profiling, as reactions are carried out in a highly parallel, high-throughput form by performing hundreds of reactions to measure different miRNAs using the same reaction conditions (Pritchard *et al.*, 2012). In microarray hybridization probes can cover more than 1000 mature human miRNAs sequences found in the miRNA database, obtained miRNA array data can be validated via qRT-PCR (Schwarzenbach and Heidi, 2017). The major advantage of NGS are detection of novel and known miRNAs and specific identification of miRNA sequences via bioinformatic analysis (Pritchard *et al.*, 2012). Drawbacks of this method are that miRNA sequence biases can be introduced during library construction and that computational support is needed to analyse the extensive data output (Schwarzenbach and Heidi, 2017).

1.3 Prostate cancer

In the UK, prostate cancer (PCa) is the most prevalently diagnosed cancer in males, with 48,500 new cases identified annually (Cancer Research UK, 2020) it is the most common cause of cancer related death in men (Rawla, 2019). PCa results from expansion of malignant glandular cells forming a tumour known as an adenocarcinoma (Dunn and Kazer, 2011). PCa is dependent on androgens, potent mediators of PCa growth and progression and can metastasise to the lymph nodes and bone (Heinlein and Chang, 2004). PCa can be managed therapeutically however, advanced prostate cancer it is also lethal, which presents as a significant problem and major clinical and social burden (Rawla, 2019).

Currently, PCa is diagnosed by a blood test for the biomarker prostate specific antigen (PSA) or a digital rectal examination (Akbaş *et al.*, 2015). However, PSA and digital rectal examination are considered to be non-specific for PCa and they can result in false positive results as increased serum PSA and enlarged prostate are also associated with prostatitis or benign prostate hyperplasia (Akbaş *et al.*, 2015). There is no reliable or widely available method to distinguish high risk tumours at an earlier stage as PSA is unable to discriminate clinically important cancers from low risk tumours (Pezaro *et al.*, 2014). Population studies have also demonstrated that the normal range of PSA increases with age; thus, PSA concentration requires interpretation with the understanding of the clinical situation (Pezaro *et al.*, 2014). Gleason grading and Tumour Node Metastasis (TNM) staging systems have enabled better characterisation of PCa tumours (Ranno *et al.*, 2005). There is also the potential benefit of reducing over treatment of low grade PCa detected by PSA screening and identifying bespoke treatment options (Epstein *et al.*, 2016).

1.3.1 The androgen receptor

The androgen receptor (AR) is a ligand dependant transcription factor, essential for regulation of male sexual differentiation, development and growth (Culig and Santer, 2014). AR activation occurs via binding of circulating androgen hormone native ligands, testosterone and potent metabolite, 5 α -dihydrotestosterone (DHT); (Tan *et al.*, 2015). DHT binds with high affinity to AR, displacing heat shock proteins, which triggers AR translocation to the nucleus forming dimers that bind to androgen response elements (AREs). Transcription of androgen related genes is initiated such as KLK3, which promotes healthy function of the prostate and transmembrane protease serine 2 (TMPRSS2), known to promote PCa progression upon fusion with the transcription factor erythroblast transformation specific (ETS); (Shang *et al.*, 2002; Heinlein and Chang, 2004; Jin *et al.*, 2013; Tan *et al.*, 2015).

1.3.2 Treatment options for PCa

Treatment options for PCa include surgical tumour removal, radiation, chemotherapy, androgen deprivation therapy (ADT) or a combination of all, depending on whether the PCa is primary, advanced or metastatic (Bono, 2004).

Increased diagnosis of early stage prostate cancer with PSA has increased the use of active surveillance, where serum PSA and prostate biopsies are closely monitored (Dunn and Kazer, 2011). When PCa is primary and localised, radical prostatectomy is considered, where the entire prostate gland is surgically removed (Bill-Axelsson *et al.*, 2014). A limitation to this treatment is that often men present with disease, which has already progressed beyond the prostate gland (Bill-Axelsson *et al.*, 2014). Radiotherapy is also used for localised PCa and is performed as external beam therapy, brachytherapy or a combination of both, depending if the PCa is considered to be of intermediate or high risk (Dietrich *et al.*, 2015). The objective of radiotherapy is to deliver a curative dose of radiation to the prostate without damaging neighbouring tissues such as the bladder, rectum, and bowel (Dunn and Kazer, 2011).

Initially, androgens are essential for PCa growth therefore, removal of androgens through ADT is an effective way to delay PCa progression and improve patient outcomes (Akitake *et al.*, 2018). Decreasing circulating androgens to castrate levels, corresponding to a measurement of <0.5 ng/mL of testosterone, decreases PCa cell proliferation and induces apoptosis (Ritch and Cookson, 2016). ADT can be administered via drugs such as leuprolide, a gonadotropin releasing hormone (GnRH) agonist, that acts on the anterior pituitary to reduce luteinizing hormone by downregulating GnRH receptors. Anti-androgens such as flutamide can also be used alone or in conjunction with castration to block binding of ligands to the AR (Sharifi *et al.*, 2005; Karantanos *et al.*, 2013).

After an initial response to ADT the majority of tumours relapse to a more advanced stage of PCa, castrate-resistant prostate cancer, which has a poor prognosis (Karananos *et al.*, 2013). Initiating synthesis of highly potent second-generation anti-androgens; Abiraterone, which inhibits CYP17A to prevent androgen biosynthesis and Enzalutamide, a pure antagonist of the AR (Hotte and Saad, 2010). The high potency of Abiraterone and Enzalutamide places a strong selective pressure on PCa and causes further therapeutic resistance (Karananos *et al.*, 2013).

When ADT is unable to contain PCa progression to metastatic (m)CRPC, chemotherapeutics become first line treatment. Docetaxel is the leading chemotherapeutic for mCRPC, which binds to β -tubulin to induce apoptosis of the cells (Attard *et al.*, 2006). The life extension of these drugs is poor with overall survival under two years, implementation of chemotherapeutics provides palliative care rather than curative (Petrylak *et al.*, 2004). Radium-223, used for mCRPC is an emitting, bone seeking calcium mimetic able to selectively target and bind to areas of bone turnover in PCa patients with bone metastasis (Ritch and Cookson, 2016).

The only treatment option for PCa with neuroendocrine differentiation are platinum-based therapeutics, most frequently cisplatin is used in combination with etoposide however, these therapeutics do not directly target mechanism of

neuroendocrine mediated PCa survival and drug resistance (Aparicio *et al.*, 2013).

1.3.3 Castrate resistant prostate cancer

Prolonged ADT generates a stressful tumour microenvironment consequently, alternative survival and growth pathways drive PCa to overcome selective pressure, which causes treatment resistance and formation of CRPC (Figure 1.3; Karantanos *et al.*, 2013). CRPC is an advanced, more aggressive and lethal form of PCa that typically forms within 3 years of ADT (Ritch and Cookson, 2016). By definition patients with CRPC have castrate levels of circulating testosterone (< 0.5 ng/mL) however, most tumours remain androgen dependant by constitutive activation of the AR, intratumoral androgen production, AR promiscuity or activation of downstream targets (Beltran *et al.*, 2011). Despite castrate androgen concentrations, expression of androgen-dependant targets, such as a rise in serum PSA means PCa can proliferate in absence of androgens (Saraon *et al.*, 2011). Prognosis for patients with CRPC is usually 18-24 months however, once metastasised this is reduced to less than a year (Sharifi, *et al.*, 2005; Sartor, 2011). It is crucial that new biomarkers for CRPC are identified due to the lack of effective therapies and extremely poor prognosis.

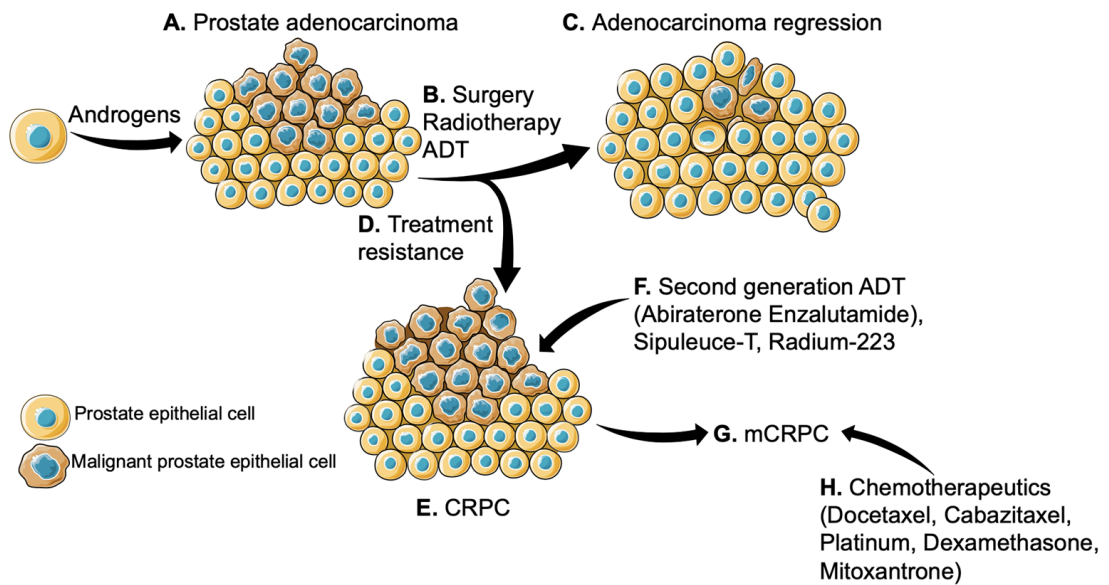


Figure 1.3: Progression of prostate cancer to castrate resistant prostate cancer. **A.** Prostate adenocarcinoma is an androgen-dependent tumour, which arises in the epithelial cells of the prostate. **B.** Surgery, radiotherapy and androgen deprivation therapy (ADT), are the primary treatments for prostate adenocarcinoma. **C.** The adenocarcinoma may respond to treatment showing tumour regression or slowed growth rate. **D.** In response to treatment resistance can occur. **E.** Castrate resistant prostate cancer (CRPC) arises as a result of therapeutic resistance. **F.** Potent second-generation anti-androgens, immunotherapy and radiation implemented to delay disease progression. **G.** Formation of metastatic CRPC (mCRPC) occurs. **H.** Chemotherapeutics involved in palliative treatment to provide modest increase in overall survival. Created using Servier Medical Art by Servier.

1.3.4 Neuroendocrine cells in the prostate

Neuroendocrine (NE) cells are distributed throughout the epithelial layer of the healthy prostate (Liu and True, 2002). These cells function as neuronal and endocrine cells, and are involved in regulating differentiation and growth of normal prostate epithelia (Yuan *et al.*, 2007). NE cells maintain tissue homeostasis by working in a paracrine manner to release potent neuropeptides such as neurotensin, bombesin and serotonin (Abrahamsson, 1999). Release of these peptides is thought to induce growth, survival, motility and metastatic

potential of neighbouring epithelial cells in prostate adenocarcinoma (Amorino and Parsons, 2004; Soundararajan *et al.*, 2018).

1.3.5 Neuroendocrine prostate cancer (NEPC)

Therapy resistance and tumour relapse are very common in advanced PCa, which relates to the extensive intratumoral genetic and phenotypic heterogeneity of PCa (Figure 1.4; Patel *et al.*, 2019). NEPC arises as lethal progression of CRPC and exists in variable differentiation states referred to as the NEPC disease continuum (Figure 1.4; Labrecque *et al.*, 2019). Epithelial PCa cells undergo lineage switching to transdifferentiate into NE-like PCa cells as an adaptive mechanism to evade selective pressure of PCa therapies (ADT, radiotherapy, chemotherapy); (Beltran *et al.*, 2019). In the prostate adenocarcinoma microenvironment, NE cells are thought to release potent neuropeptides to induce neuroendocrine transdifferentiation (NEtD) of neighbouring epithelial prostate cells to NE-like cells (Figure 1.5; Soundararajan *et al.*, 2018). Detection of neuronal biomarkers such as chromogranin A (CrgA/CHGA), neuron specific enolase (NSE/ EN02) and synaptophysin (SYP) and androgen biomarkers such as the AR and PSA by immunohistochemistry (IHC) allows clinical phenotyping of NEPC, however not all NEPC subtypes display a clear staining profile contributing to ineffective treatment and poor patient outcomes (Hu *et al.*, 2015). However, these are not routinely used in the clinic (Dunn and Kazer, 2011). Highlighting the need for novel circulating biomarkers to provide a more accurate diagnosis of NEPC and ability to stratify NEPC from CRPC to provide more effective treatment options.

Labrecque *et al.* (2019) described five phenotypes of NEPC based upon expression of AR or NE biomarkers described in Figure 1.4: ranging from PCa, which has near uniform expression of adenocarcinoma markers to double negative PCa that lack adenocarcinoma or neuronal markers representing distinct disease states or a continuum (Labrecque *et al.*, 2019). Once diagnosed with NEPC the overall survival of patients ranges from 7 months to 2 years (Davies *et al.*, 2018).

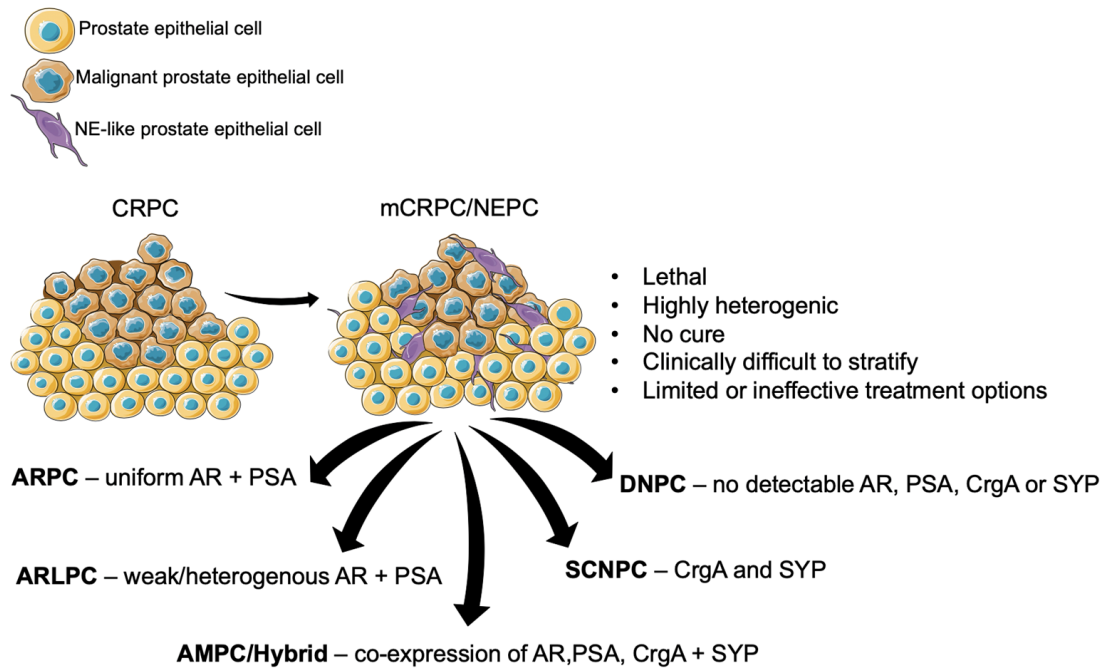


Figure 1.4: Neuroendocrine transdifferentiation of prostate cancer.

Schematic diagram showing the diversity of castrate resistant prostate cancer and neuroendocrine prostate cancer subtypes and the markers expressed in each, AR; androgen receptor, PSA; prostate specific antigen, CrgA; chromogranin, SYP; Synaptophysin. AR PCa has uniform expression of adenocarcinoma markers, AR and PSA and does not express neuronal markers (ARPC). AR low PCa (ARLPC) has weak or heterogeneous AR or PSA with no neuronal markers. Amphicrine or hybrid PCa (AMPC) co-expresses AR, PSA and neuronal markers CrgA and SYP. Small cell or neuroendocrine PCa (SCNPC) displays a neuroendocrine histology with no adenocarcinoma markers. Double negative PCa, lack detectable expression of AR, PSA, CrgA or SYP. Created using Servier Medical Art by Servier.

Currently there is no means of stratifying NEPC from CRPC, thus patient prognosis is extremely poor when PCa reaches this stage (Labrecque *et al.*, 2019). The heterogeneity of PCa, lack of effective therapies and inability to stratify PCa types (CRPC and NEPC) highlights the need for new biomarkers and therapeutic targets for PCa subtypes to improve therapeutic options and patient prognosis (Patel *et al.*, 2019). Lineage plasticity facilitates carcinogenesis, metastasis, and treatment resistance of the tumour (Meacham and Morrison, 2013). Plasticity may display as reversible or irreversible changes of cellular

characteristics, as cells take on alternative morphologic, phenotypic, or epigenetic states (Graf and Enver, 2009). Therapeutic associated lineage plasticity induces differentiated tumour cells to develop different phenotypes, to revert back to a more 'stem-like' state and subsequently re-differentiate towards an alternative cell fate to evade therapeutic pressure (Beltran *et al.*, 2019). Cells undergoing lineage switching preserve the molecular memory of their differentiated cancer cell precursor however, the alternative lineage facilitates subsequent tumour progression (Beltran *et al.*, 2019).

1.3.6 Proposed factors involved in NEtD of PCa

The exact mechanism employed by PCa to shift the epithelial to NE-like phenotype is not fully understood and there have been many genes implicated in this process (Patel *et al.*, 2019). Loss of tumour suppressors RB1 and TP53, leads to alterations in stem cell, developmental, and EMT status, mediated by lineage pluripotency transcription factors SOX2 and EZH2 to facilitate transition from an epithelial to NE-like phenotype (Ku *et al.*, 2017). Down-regulation of REST, a transcriptional repressor of neuronal genes in non-neuronal cells via splicing controlled by SRRM4 (Zhang *et al.*, 2015), as well as activation of lineage associated transcription factors such as N-MYC (Lee *et al.*, 2016), Onecut2 (Guo *et al.*, 2019), and BRN2 (Bhagirath *et al.*, 2019) also are thought to contribute to the epithelial to NE-like transition. Other potential neuronal biomarkers include human achaete-scute homolog 1 (hASH1/ASCL1), regulator of cell commitment and differentiation, AD of LNCaP cells induced NEtD, re-exposure of LNCaP cells to androgen facilitated differentiation back to epithelial state. However, ASCL1 remained localised in the nucleus, revealing the amphicrine status of the tumour and involvement in NEPC lineage plasticity (Fraser *et al.*, 2019).

1.4 Exosomes in cancer

Cancer cells can sort oncogenes, oncoproteins, chemokine receptors, growth factors and immunomodulatory molecules into exosomes (Bebelman *et al.*,

2018). This cargo can be taken up by neighbouring or distal recipient cells leading to neoplastic transition via horizontal gene transfer (Zhang *et al.*, 2019).

Tumour-derived exosomes are known to enhance tumour formation by manipulating the tumour microenvironment, initiating a tumour-promoting niche, tumour angiogenesis, immunosuppression and acquisition of malignant traits (Bebelman *et al.*, 2018). The tumour promoting activity of exosomes is not limited to the local tumour microenvironment and tumour-derived exosomes can enter the circulation to reach distant organs, enabling pre-metastatic niche formation and outgrowth of disseminated tumours (Bebelman *et al.*, 2018; Li and Nabet, 2019). Transfer of the oncogene, MET to bone marrow progenitor cells by metastatic melanoma-derived exosomes directed pre-metastatic niche formation, encouraging lung metastases (Peinado *et al.*, 2012). Uptake of pancreatic cancer cell derived exosomes by Kupffer cells induced TGF- β secretion, upregulation of fibronectin production, enhanced bone marrow-derived macrophage recruitment and pre-metastatic niche formation in the liver (Costa-Silva *et al.*, 2015). This could be prevented by blockade of migration inhibitory factor found in the pancreatic cancer derived exosomes (Costa-Silva *et al.*, 2015).

Cancer patients have an increased number of circulating exosomes compared to healthy individuals, associated with the over expression of ESCRT components, syntenin and heparinase (Bebelman *et al.*, 2018). Increased circulating exosomes may be caused by activation of oncogenic signalling pathways such as EGFR^{vIII} and H-RAS^{v12}, which are thought to induce exosome production in cancer cells (Al-Nedawi *et al.*, 2008; Lee *et al.*, 2014; Takasugi *et al.*, 2017). Environmental stresses can also influence EV release (Wang *et al.*, 2014; Guo *et al.*, 2017). In NEPC, therapeutic stressors force the lineage switching of epithelial cells, thus it is possible this process could be facilitated by stress-induced exosome release. As a result, exosomes can be used as a read-out of the tumour biology as an easily accessible, non-invasive and real-time biomarker of NEPC formation, evolution and/or development.

1.4.1 PCa patients and exosomes

Urinary and plasma exosomes represent an opportunity to identify non-invasive biomarkers for PCa patients, which permit real-time assessment of tumoral characteristics, including genomic and proteomic information (Vlaeminck-Guillem, 2018).

Plasma-derived exosomes are increased in PCa patients compared to benign prostate hyperplasia patients or healthy individuals, this correlates with cancer aggressiveness, metastatic spread and/or Gleason score, providing more evidence for the use of exosomes as biomarkers in PCa (Vlaeminck-Guillem, 2018). Circulating exosomes containing AR splice variant 7 (AR-V7) mRNA was shown as a prognostic marker for CRPC patients and associated with very low levels of castrate androgens (Joncas *et al.*, 2019), evidencing the potential to stratify PCa subtypes via non-invasive real-time exosomal biomarkers. Actinin-4, a cross-linking protein associated with cell motility, cancer invasion and metastasis was significantly upregulated in exosomes from CRPC patients compared to adenocarcinoma patients (Ishizuya *et al.*, 2020), showing the ability to distinguish PCa types via non-invasive, real-time exosomal biomarkers. Vesicle fusion by t-SNARE, syntaxin 6, was increased in exosomes from PCa patients with a higher Gleason score, stage of primary tumour and decreased overall survival (Peak *et al.*, 2020). Further, IHC showed higher syntaxin 6 expression in tissues from Enzalutamide treated patients compared to non-Enzalutamide treated patients (Peak *et al.*, 2020), suggesting exosomes can be employed as biomarkers to stratify PCa stage. Actinin-4, a cross-linking protein associated with cell motility, cancer invasion and metastasis was significantly upregulated in exosomes from CRPC patients compared to adenocarcinoma patients (Ishizuya *et al.*, 2020), showing non-invasive and real-time exosomal biomarkers can distinguish PCa types.

1.4.2 Exosomes and NEtD in PCa

Exosomes released from androgen sensitive (LNCaP) and androgen independent (PC3 and DU145) PCa cell lines increase cellular proliferation of other PCa cells (Soekmadji *et al.*, 2017), can transfer cell-specific cargo (Read *et al.*, 2017; Bhagirath *et al.*, 2019) and initiate formation of the pre-metastatic niche (Itoh *et al.*, 2012).

Exosomes may also mediate NEtD via crosstalk of exosomes released in the tumour microenvironment (Figure 1.5; Lin *et al.*, 2017a). Read *et al.*, (2017) reported that the AR and mutant variant, AR-V7, were secreted in EVs from LNCaP cells and could be transported to the nucleus of AR-null PC3 cells to promote active transcription. Proliferation of recipient PC3 cells was enhanced by the nuclear translocated AR in the absence of androgen (Read *et al.*, 2017). Bhagirath *et al.* (2019) showed the neural transcription factors BRN2 and BRN4 are packaged in exosomes and facilitate NEtD of LNCaP cells by horizontal gene transfer, highlighting the importance of exosomes in progression or maintenance of PCa. There is no cure and limited treatment options for NEPC therefore, understanding how exosomes may contribute to this disease may highlight the use of exosomes for NEPC diagnosis, monitoring of disease progression, targeted therapy or as a drug delivery mechanism.

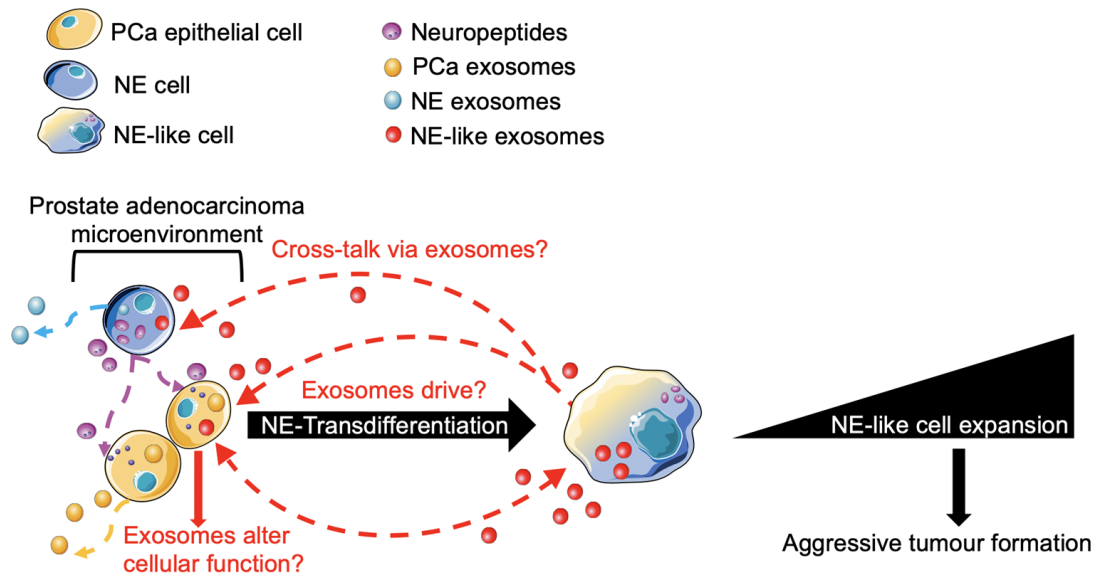


Figure 1.5: Proposed involvement of exosomes in NEtD PCa. Exosomes are released from cells in the prostate adenocarcinoma microenvironment. It is proposed that there is exosome mediated crosstalk via epithelial cells, neuroendocrine cells and NE-like cells. The cargo released from NE-like exosomes may alter cellular function driving NEtD and aggressive tumour formation. Created using Servier Medical Art by Servier.

1.4.3 *In vitro* model of NEtD PCa

The aim of this research was to investigate the potential role of exosomes as a means of cell-to-cell communication involved in potentially driving or maintaining neuroendocrine transdifferentiation (NEtD) in PCa. NEPC can be modelled *in vitro* using charcoal stripped FCS to remove androgens from the culture medium and induce NEtD of LNCaP cells (Shen *et al.*, 1997; Rapa *et al.*, 2008; Fraser *et al.*, 2019). Exosomes are released from all cells and therefore, are present in a significant concentration of many biological fluids (Jeppesen *et al.*, 2014; Lötvald *et al.*, 2014; Szatanek *et al.*, 2015). Depletion of EVs from FCS is necessary to minimise co-isolation of FCS-derived EVs with EVs of interest (Figure 1.6; Szatanek *et al.*, 2015). Depletion of EVs and androgens has not been previously reported in the literature therefore, the NEtD of LNCaP model was further developed to limit FCS exosome interference from PCa exosomes. The impact of AD-induced NEtD stress on exosome machinery and manipulation of exosome

biogenesis was then analysed to investigate the potential communicative role of exosomes in PCa.

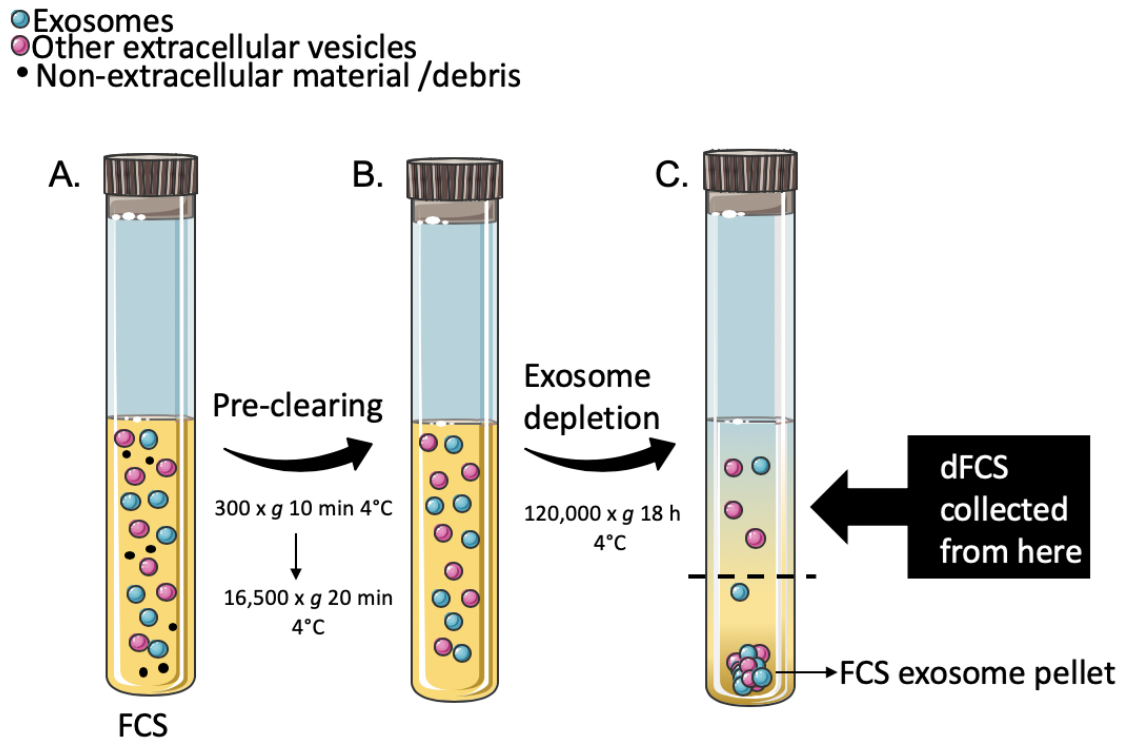


Figure 1.6: Schematic diagram indicating how ultracentrifugation can deplete exosomes from FCS. Firstly, FCS is cleared of any debris and non-exosomal material by centrifuging for 10 minutes at $300 \times g$ $4^{\circ}C$. The supernatant is then transferred into a fresh tube and centrifuged for 20 minutes at $16,500 \times g$ $4^{\circ}C$ to remove larger non-exosomal material. After pre-clearing, FCS is ultracentrifuged for 18 hours overnight at $120,000 \times g$ $4^{\circ}C$ to sediment serum exosomes. After ultracentrifugation, the FCS separates into distinct light to dark layers. The light layer contains exosome-depleted serum, while the dark layer predominantly contains FCS exosomes and other non-EV products such as albumin (Caradec *et al.*, 2014). Created using Servier Medical Art by Servier.

1.5 Overall aims

Aims:

- 1. To establish a robust *in vitro* model to investigate exosome release from AD-induced NEtD LNCaP cells.**
- 2. To investigate the impact of AD stress on exosomal machinery in LNCaP cells**
- 3. To isolate and characterise exosomes released from AD-induced NEtD LNCaP cells.**
- 4. To manipulate exosome release during AD induced NEtD to dissect whether exosomes play a role in NEtD of LNCaP cells.**

1.6 Thesis Hypothesis

Exosomes released from NEtD LNCaP cells are involved in cell-to-cell communication in NEPC have the potential to be used as diagnostic biomarkers for NEPC.

2. Chapter 2: Materials and Methods

2.1 Reagents and chemicals

Unless otherwise stated all reagents and chemicals were obtained from Sigma-Aldrich (Gillingham, UK), Thermofisher Scientific (Paisley, UK) or VWR Life Sciences (Leicestershire, UK).

2.2 Cell culture techniques

2.2.1 LNCaP cells

The human prostate adenocarcinoma cell line, LNCaP, was purchased from American Type Culture Collection (ATCC); (CRL-1740).

2.2.2 LNCaP culture conditions

LNCaP cells were maintained as adherent monolayers in T75 tissue culture flasks (Corning, UK) with 10 mL Roswell Park Memorial Institute (RPMI) 1640 cell culture medium (Sigma, UK) supplemented with 10 % FCS (Gibco, UK), 2 mM L-glutamine and 1 % penicillin/streptomycin (complete medium) in a humidified 37°C, 5 % CO₂ culture safe CO₂ precision 190D incubator (LEEC, UK).

2.2.3 Depletion of exosomes from Foetal Calf Serum by differential ultracentrifugation

To deplete foetal calf serum (FCS) of exosomes, differential ultracentrifugation was performed according to protocol by Shelke et al. (2014). FCS and charcoal stripped (CS)-FCS, were differentially centrifuged in 15 mL falcon tubes at 300 x *g* for 10 minutes at 4°C followed by 16,500 x *g* for 20 minutes at 4°C in a centrifuge using a JA14 rotor: (Beckman Coulter, USA). The supernatant was transferred into polycarbonate tubes (#355603; Beckman Coulter, USA) then ultracentrifuged (70.1 Ti rotor; (Beckman Coulter, USA)) at 120,000 x *g* for 18 hours at 4°C. The light clarified layers of FCS/CS-FCS described by Théry et al. (2006) as exosome depleted (dFCS/dCS-FCS) were filter sterilised (22 µm

syringe filter; Star Lab, UK), then stored at -20°C, prior to supplementation into cell culture medium.

2.2.4 Androgen deprivation of LNCaP cells

For androgen deprivation (AD), 10 % CS-FCS (Sigma, UK), 2 mM L-glutamine and 1 % penicillin/streptomycin was supplemented into phenol-red free RPMI 1640 culture medium (CS-complete). AD LNCaP cells were seeded at 1×10^6 in 10 mL of complete culture medium in a T75 cell culture flask; control LNCaP cells were seeded at 2.5×10^5 in 10 mL complete medium. LNCaP cells were grown at 37°C, 5 % CO₂ incubator (LEEC, UK). Control and AD LNCaP cells were seeded at different densities to compensate for the increased proliferation of control cells due to presence of androgen in the complete medium. To stimulate AD, after 24 hours, the complete medium was discarded, LNCaP cells were washed with 10 mL 0.9 % NaCl (Baxter, UK) and cultured with CS-complete medium. Complete medium was also renewed for control LNCaP cells. Control and AD LNCaP cells were cultured for 15 days; the culture medium was renewed every 3 to 4 days, LNCaP cells were not passaged during treatment.

2.2.5 Exosome depletion of LNCaP cells

For androgen deprivation with exosome depletion (dAD), LNCaP cells were maintained as above however, CS-complete medium was supplemented with 10 % CS-FCS, pre-depleted of exosomes by ultracentrifugation (section 2.2.2). An exosome depleted control (dC) was produced by using complete medium supplemented with 10 % exosome depleted FCS.

2.2.6 Sub Culturing LNCaP cells

LNCaP cells were passaged once 70-90 % confluence was reached, the culture medium was removed and discarded. LNCaP cells were washed with 10 mL 0.9 % NaCl (Baxter, UK) to remove residual media. To detach LNCaP cells, 2 mL of 1X trypsin (Gibco, UK), prepared from 10X trypsin with 0.9 % NaCl (Baxter, UK) was added to the flask to cover the monolayer of LNCaP cells and incubated

at 37°C for 2-5 minutes. Cell culture flasks were gently tapped to detach the cells, and ensure dissociation from the tissue culture flask. Once detached, 8 mL of complete medium was added to neutralise the trypsin and the LNCaP cell suspension was transferred to a 15 mL falcon tube. LNCaP cells were collected by centrifugation at 148 x g for 5 minutes at 20°C, in a Universal 320R centrifuge (Hettich, Germany). The medium was discarded and the cell pellet, which was resuspended by flicking of the tube and pipetting up and down in 10 mL fresh media. LNCaP cells were sub-cultured into T75 tissue culture flasks at a ratio of 1:10.

2.2.7 Cryopreservation of LNCaP cells

LNCaP cells were grown to 70-90 % confluence, trypsinised and collected as outlined in section 2.2.6. Cryopreservation solution contained sterile dimethyl sulfoxide (DMSO; Sigma, UK) and FCS (Gibco, UK) at a ratio of 1:4. The media was removed and the pellet was resuspended in a 1:1 ratio of complete medium and cryopreservation solution. The LNCaP cells were transferred in 500 µL aliquots to 1.8 mL cryovial tubes (Simport, Canada) and placed into an isopropanol freezing module – Mr Frosty™ (Nalgene; Thermofisher Scientific, UK), and stored at -80°C for at least 24 hours before cryovials were transferred to liquid nitrogen (-196°C) for long term storage.

2.2.8 Reviving LNCaP cells

To revive LNCaP cells from liquid nitrogen, the cells were resuspended by gentle pipetting of 10 mL warmed (37°C) complete medium. Once thawed, cells were transferred into a 15 mL falcon tube and collected by centrifugation at 145 x g for 5 minutes at room temperature in a Universal 320R centrifuge (Hettich, Germany). The cells were resuspended by gentle flicking and 10 mL of complete medium was added, the resuspended LNCaP cells were then transferred to a T75 culture flask. The LNCaP cells were incubated at 37°C in 5 % CO₂ and left to adhere to the flask for three days, the medium was replaced every 3-4 days until LNCaP cells were attached and confluent.

2.2.9 Counting LNCaP cells

LNCaP cells were counted after passage (section 2.2.6) to ascertain the number of cells in the T75 flask. A glass coverslip was placed on the haemocytometer (Weber Scientific, USA), 10 μ L of cell suspension was pipetted into each chamber of the haemocytometer. Cells were visualised under a Zeiss Primovert light microscope (Zeiss, UK) at 100X magnification and cells, in the central square of the haemocytometer grid were counted. The mean count across both chambers was representative of 1×10^4 cells per millilitre and was used to calculate the total number of cells in the 10 mL suspension.

2.2.10 LNCaP morphology/microscopy

Brightfield microscopy (Primovert; Zeiss, UK) images were taken of control, exosome depleted control, AD and exosome depleted AD LNCaP cells at regular intervals. Images were taken at 100X, 200X and 400X magnification and saved as Jpeg files.

2.2.11 Harvesting cells

LNCaP cells were harvested on ice, the medium was collected and cleared as per section 2.2.2 for downstream isolation of exosomes (section 2.3.1). Cells were washed once with 10 mL of ice-cold phosphate buffered saline (PBS; 5 PBS tablets dissolved in 1 L of dH₂O; Sigma, UK). The PBS was removed, discarded and 1 mL of fresh PBS was added to the flask. Using a cell scraper (Corning, UK) LNCaP cells were scraped into 1 mL of PBS, transferred into a 1.5 mL microcentrifuge tube (Eppendorf, Germany) before centrifugation in 5415R refrigerated centrifuge (Eppendorf, Germany) at 145 x g for 5 minutes at 4°C to pellet cells. The PBS was aspirated, and cell pellets were stored at -80°C for future experiments.

2.3 Assessing exosomes

2.3.1 Exosome isolation from conditioned culture medium

To isolate exosomes from culture medium the Exo-spin™ exosome purification kit (Cell Guidance Systems, UK) for cell culture media and other low-protein biological fluids was used per manufacturer's instructions. Medium was collected from exosome depleted control and exosome depleted androgen deprived LNCaP cells. Clarified media was either stored at -80°C or used immediately to isolate exosomes.

To precipitate exosomes, approximately 19 mL of exosome depleted control medium or exosome depleted AD medium was transferred to polycarbonate centrifuge tubes and 50 % of Exo-spin™ buffer (Cell Guidance Systems, UK) was added. Tubes were mixed by inversion then incubated at 4°C overnight. The next day, media with Exo-spin™ buffer was centrifuged at 16,000 x *g* for 1 hour at 4°C in an ultracentrifuge using a type 70.1 Ti rotor (Beckman Coulter, USA). The supernatant was removed and exosome pellets were resuspended in 100 µL of PBS using sterile plastic Pasteur pipettes.

Exo-Spin™ columns (EX01) were prepared prior to application of sample by removing the outlet plug and placed into the collection tube. Preservative buffer was aspirated from the column and discarded. To equilibrate the column, 200 µL of PBS was added to the column bed and the column was centrifuged at 50 x *g* for 10 seconds at 4°C. The flow through was discarded and the column was placed into a 1.5 mL microcentrifuge tube. The 100 µL of PBS containing resuspended exosomes was applied to the top of the column. The column was centrifuged at 50 x *g* for 60 seconds at 4°C, the eluate was collected and stored at -80°C until subsequent identification of exosomes. The column was placed into a new microcentrifuge tube and 200 µL of PBS applied to the top of the column. This was centrifuged at 50 x *g* for 60 seconds at 4°C to collect the purified exosomes. The resulting 200 µL eluate of purified exosomes was aliquoted for analysis and stored at -80°C.

2.3.2 Assessing exosomes via Dynamic Light Scattering

The particle size of exosome samples was analysed by dynamic light scattering (DLS), using a Zetasizer Nano-ZS (Malvern, UK). Exosome samples were prepared 1:100 in sterile PBS and transferred to 40 μ L cuvettes (ZEN0040; Malvern, UK). Standard settings were applied (Refractive Index = 1.331, Viscosity = 0.89 and Temperature = 25°C) for 3 x 10 measurement runs. After the runs were completed an output was provided and analysed using Dispersion Technology Software (DTS; V7.01) supplied by Malvern, UK. DTS generated a graph labelled “Intensity PSD (M)”, providing information on the mean diameter (nm), mean width (nm) and percentage of isolated particles in the sample as an average of the 3 runs.

2.3.3 Exosome Lysis

Exosomes suspended in PBS were lysed 1:1 with 1X radioimmunoassay precipitation (RIPA) buffer (150 mM, 5 mM EDTA pH 8, 50 mM Tris pH 8, 1% (w/v) NP-40, 0.5% (w/v) sodium deoxycholate, 0.1% (w/v) SDS containing 1% (w/v) halt protease inhibitor (Thermofisher Scientific, UK)) or 1:5 with 5X RIPA buffer (750 mM NaCl, 25nM EDTA pH 8, 250 mM Tris pH 8, 5% (w/v) NP-40, 2.5% (w/v) sodium deoxycholate, 0.5% (w/v) SDS containing 1% (w/v) halt protease inhibitor). Exosomes were incubated on ice for 30 minutes then sonicated in a sonicating water bath for 3 x 5 seconds at 37°C. Lysates were centrifuged at 15,700 x g for 5 minutes at 4°C in a 5415R refrigerated centrifuge (Eppendorf, Germany). The supernatant containing soluble protein was transferred into a sterile, pre-chilled 1.5 mL micro-centrifuge tube and protein concentration was determined by Bradford assay (section 2.6.2) or stored at -80°C.

2.4 Synthetic inhibition and induction of exosome release

2.4.1 Stock solutions

A stock solution (2.2 mM) of sphingomyelinase inhibitor (Ludwig *et al.*, 2019), GW4869 (hydrochloride chlorate); (Cayman Chemicals, USA) was produced by

dissolving GW4869 in DMSO. The solution was vortexed, aliquoted and stored at -80°C. Monensin sodium salt (Cayman Chemicals, USA) stock solution (25 mM) was generated by dissolving in molecular grade ethanol (EtOH) the solution was aliquoted and stored at -80°C until use.

2.4.2 Treating LNCaP cells with GW4869 or Monensin

LNCaP cells were seeded at 4×10^6 in 10 mL of complete medium in T75 flasks and incubated at 37°C 5% CO₂ for 24 hours. The next day media was removed, and cells were washed with 10 mL 0.9 % NaCl (Baxter, UK) and replenished with 10 mL of exosome depleted control medium or exosome depleted AD medium and cultured for 3 days. On day 4, post seeding, cells were treated with either 25 μM GW4869, or 2 μM Monensin or the corresponding drug vehicle control: 1 % (v/v) DMSO or 0.01 % (v/v) EtOH. After 24 hours the conditioned culture medium was collected, and cells harvested (section 2.2.11).

2.5 MTT assay

To assess cell metabolic activity the MTT assay was performed using methods from Mosmann (1983), LNCaP cells were seeded at 8×10^3 cells per well in 96-well plates in 100 μL of complete medium and cultured at 37°C 5% CO₂. After 24 hours medium was removed and replaced with exosome depleted control or exosome depleted AD medium and cultured for a further 3 days. On day 4, GW4869 (100, 50, 25, 10, 5, 1 and 0.5 μM) or Monensin (20, 10, 5, 2, 1, 0.2, 0.1 μM) were added and incubated for 24 hours. LNCaP cells were also treated with EtOH and DMSO as vehicle controls respectively.

The next day, the media was removed and replaced with 100 μL of fresh media and 10 μL of 5 mg/mL MTT stock solution for a final concentration of 0.5 mg/mL MTT. Wells containing media and MTT only or MTT, media and cells were included as controls. Media containing 2 % v/v Triton-X (Sigma, UK) was used as a positive control for cell death. To mix the MTT and media the plate was gently tapped, covered with foil to protect from the light, then returned to the

incubator at 37°C, 5 % CO₂. After 2.5 hours media was removed and 100 µL of isopropanol was added to dissolve the formazan. The plate was shaken gently to ensure crystals were dissolved. Absorbance was analysed at 550 nm using a LT-5000MS plate reader with Manta software (LabTech, UK). Raw data were analysed by subtracting the absorbance of MTT and media only from all readings. Absorbance of untreated control cells were taken to be 100% viable and all readings were expressed as a percentage of this.

2.6 Protein analysis

2.6.1 Cell lysis

Cells were lysed in approximately 3 x the pellet volume of lysis buffer (50 mM Tris pH 8, 150 mM NaCl, 1mM EDTA pH 8, 1% NP-40 containing 1% Halt protease inhibitor) on ice for 30 minutes. Lysates were centrifuged at 3000 x g for 5 minutes at 4°C in a 5415R refrigerated centrifuge (Eppendorf, Germany). Supernatant, containing soluble protein was transferred into a sterile, pre-chilled 1.5 mL micro-centrifuge tube and protein concentration was determined by Bradford assay or stored at -80°C.

2.6.2 Protein quantification by Bradford analysis

Bradford reagent was prepared by dissolving 50 mg of Coomassie Blue G250 in 50 mL methanol, prior to adding 100 mL of 85 % phosphoric acid, then was made up to 1 L with dH₂O. This was filtered through a sterile 22 µm syringe filter (Star Lab, UK), to remove any precipitate, stored at 4°C and covered with foil to protect from light.

A stock of 10 mg/mL bovine serum albumin (BSA) solution was prepared in dH₂O. known BSA concentrations were created by diluting the stock to 2, 1, 0.5, 0.25, 0.125 and 0.0625 mg/mL in dH₂O. BSA standards were stored at 4°C until use.

The protein concentration of lysates generated in section 2.6.1 were analysed by adding 200 µL of Bradford reagent to each well of a 96 well plate (Corning, UK),

1 μL of each BSA standard was added to the Bradford reagent. Protein samples were diluted 1:5 in dH_2O , then 1 μL of this was added in triplicate to the wells and mixed. The “blank well” contained Bradford reagent only. Samples were incubated at room temperature for 10 minutes before absorbance at 595 nm was measured using a LT-5000MS plate reader with Manta software (LabTech, UK). The blank background absorbance was subtracted from all samples. Sample concentrations were generated from the BSA standard curve using the equation of the line ($y=mx+c$). Protein concentration was multiplied by the dilution factor to obtain final protein concentration.

2.6.3 Preparation of protein for immunoblotting

Due to conditions required for downstream immunoblotting (section 2.6.5) samples were prepared in either native or reduced/denatured conditions. For denaturing/reducing conditions, samples were diluted with 4X loading sample buffer (LSB) (20 % (w/v) glycerol, 200 mM Tris pH 6.8, 4 % (w/v) SDS, 10 mM EDTA, 1 % bromophenol blue, supplemented with 100 mM of the reducing agent dithiothreitol (DTT)) to a final concentration of 1 $\mu\text{g}/\text{mL}$. Samples were denatured for 5 minutes at 100°C in a heat block. For native conditions, samples were prepared without reducing agents or denaturation and diluted with 4X LSB (20 % glycerol, 200 mM Tris pH 6.8, 4 % SDS, 10 mM EDTA, 1 % bromophenol blue) to a final concentration of 1 $\mu\text{g}/\text{mL}$. Samples were used immediately or stored at -20°C.

2.6.4 Sodium Dodecyl Sulphate – Polyacrylamide Gel Electrophoresis (SDS-PAGE)

Proteins were resolved by SDS-PAGE based on methods by Laemmli (1970). The resolving gels contained either 8, 10 or 12 % (w/v) acrylamide (30 % w/v stock acrylamide; Thermofisher Scientific, UK, 375 mM Tris pH 8.85, 0.1 % (w/v) SDS and 0.08% (w/v) ammonium peroxodisulphate (AmPs). To polymerise the mixture 0.005 % (w/v) N,N,N',N'-Tetramethylethylenediamine (TEMED); (Sigma- Aldrich, Germany) was added. The resolving gel was pipetted into the glass plates assembled within a casting chamber, 200 μL of isopropanol was applied to the

top of the resolving gel to remove air bubbles. Once polymerisation had occurred, isopropanol was removed, and the gel rinsed with water. Stacking gel was prepared (5 % (w/v) polyacrylamide, 130 mM Tris pH 6.8, 0.1 % SDS, and 0.12 % (w/v) AmPs) followed by the addition of 0.01 % (w/v) TEMED to promote polymerisation and the well comb was added immediately.

Gels were removed from their casting chambers and placed into an electrophoresis tank (BioRad, USA) and submerged in 1X running buffer (25 mM Tris- HCL, 192 mM Glycine, 35 mM SDS). A pre-stained broad range protein marker (PageRuler™ Pre-stained Protein Ladder, 10 to 250 kDa; ThermoFisher Scientific, UK; 5 µL) was used to determine the size of the proteins of interest. The gels were electrophoresed at 185 V for approximately 50 minutes or until the blue loading buffer dye front reached the bottom of the SDS gel.

2.6.5 Immunoblotting

Immunoblotting was performed based on methods by Towbin et al. (1979). Following protein separation *via* SDS-PAGE, immunoblots were prepared by submerging a cassette in 1X transfer buffer (25 mM Tris pH 8.5, 0.2 M Glycine and 20 % (w/v) methanol). The cassette was layered with a sponge, 2 x 3 MM paper, gel, nitrocellulose membrane (0.2 µm, Optiran BA-S 83), 2 x 3 MM paper and a sponge and compressed to remove air bubbles. The cassette was inserted into an electrophoresis tank and submerged with 1X transfer buffer. Proteins were electrophoretically transferred onto the nitrocellulose membrane at 100 V for 1 hour. Once transfer was complete, the nitrocellulose was rinsed with PBS with 1% tween (PBS-T) and stained with Ponceau S solution (0.1 % Ponceau S, 5 % acetic acid) to ensure equal transfer of proteins. It was washed three times in 1% PBS-T and blocked with 5 % (w/v) non-fat milk (Marvel) for 1 hour at room temperature with agitation on a shaker plate.

Primary antibodies were prepared by dilution in 5% (w/v) non-fat milk in PBS-T as indicated in Table 2.1 and incubated on the nitrocellulose membrane overnight at 4°C. The membrane was washed three times in PBS-T before probing with the appropriate secondary antibody (Table 2.2) in 5 % (w/v) non-fat milk containing

0.01 % SDS for 45 minutes at room temperature. The membrane was then washed three times with PBS-T. Membranes were analysed by LI-COR Odyssey image system (Odyssey-3074, LI-COR, 51 Cambridge, UK) and Odyssey Image Studio v2.0 software (ThermoFisher Scientific, UK). Images were downloaded from the software and saved as Tiff files.

Table 2.1: Primary antibodies used within this study for immunoblotting

Target Protein	Host Species	Working Dilution	Source and Catalogue Number
ALIX (1A12)	Mouse Monoclonal	1:500	Santa Cruz Biotechnology (sc-53540)
AR (441)	Rabbit Polyclonal	1:1000	Santa Cruz Biotechnology (sc-7305)
β -actin (C4)	Goat Polyclonal	1:1000	Santa Cruz Biotechnology (sc-47778)
CD9	Mouse Monoclonal	1:1000	Cell Guidance Systems (EX201)
CrgA	Mouse Monoclonal	1:1000	Thermofisher Scientific (LK2H10)
hASH1	Rabbit Polyclonal	1:1000	Abcam (ab74065)
Hsp70	Rabbit Monoclonal	1:1000	Abcam (ab181606)
NSE	Rabbit Monoclonal	1:1000	Abcam (10H7L13)
PSA (A67-B/E3)	Goat Polyclonal	1:500	Santa Cruz Biotechnology (sc-7316)

Table 2.2: Secondary antibodies used within this study for immunoblotting

Name	Species Reactivity	Dilution	Source and Catalogue Number
IRDye 680LT	Goat anti-rabbit	1:5000-1:10000	LI-COR (926-68021)
IRDye 680LT	Donkey anti-goat	1:10000	LI-COR (926-68024)
IRDye 800CW	Goat anti-mouse	1:5000-1:10000	LI-COR (926-32210)
IRDye 800CW	Goat anti-rabbit	1:10000	LI-COR (926-32211)

2.7 RNA extraction, quantification and reverse transcription

2.7.1 Preparing DEPC treated water

To produce nuclease-free water, distilled water was treated with diethylpyrocarbonate (DEPC); (Sigma, UK) to a final concentration of 0.1 %. The solution was mixed by vigorous shaking and incubated overnight at room temperature, then autoclaved for 1 hour at 121°C and 15 psi to inactivate DEPC. The DEPC water was cooled to room temperature before use.

2.7.2 RNA extraction

TRIsure (Bioline, UK) was used to extract total RNA from LNCaP cell pellets according to manufacturer's instructions. The cell pellets (section 2.2.11) were retrieved from -80°C, and 1 mL of TRIsure was added to the cell pellet. To disrupt the cell membrane, the solution was pipetted up and down. Samples were incubated at room temperature for 5 minutes before 200 µL of chloroform was added. Samples were shaken vigorously for 15 seconds by hand, then incubated for 3 minutes at room temperature for phase separation. Samples were centrifuged at 13,000 x g for 15 minutes at 4°C in a 5415R refrigerated centrifuge (Eppendorf, Germany). The upper translucent phase containing RNA was

transferred to a fresh autoclaved microcentrifuge tube, and 500 μ L of chilled isopropanol was added to precipitate the RNA. Samples were incubated on ice for 10 minutes followed by centrifugation of 12,000 x g for 10 minutes at 4°C in a 5415R refrigerated centrifuge. The RNA pellet was washed with 1 mL chilled 75 % ethanol in DEPC water by vortexing and centrifuged at 10,000 x g for 5 minutes at 4°C in a 5415R refrigerated centrifuge. The supernatant was removed, and RNA pellet allowed to dry for 45 minutes to 1 hour at room temperature. RNA pellet was then resuspended in 30 μ L of DEPC water and incubated in a heat block at 60°C for 10 minutes, RNA was stored at -80°C.

2.7.3 RNA quantification by Nanodrop 2000 (Spectrophotometer)

RNA concentration and purity were analysed by spectrophotometry using the Nanodrop 2000 (ThermoFisher Scientific, UK). The Nanodrop provided an approximate concentration of total RNA, for use in downstream Bioanalyzer analysis (section 2.8.4). The instrument was blanked with 1 μ L of DEPC water and the absorbance of RNA samples at 260 nm was analysed. The ratio of the absorbance at the 260nm and 280nm was used to assess RNA purity, a ratio of ~2.0 was considered to be pure, a reduction in the ratio is indicative of contamination from protein or phenol or other contaminants, which absorb strongly at 280nm (Desjardins and Conklin, 2010). The 260/230 ratio is the secondary measure of RNA purity, expected values are ~2.0-2.2, a considerably lower ratio may indicate the presence of contaminants that absorb at 230 nm such as, ethanol and phenol (Desjardins and Conklin, 2010).

2.7.4 Microfluidic analysis of RNA by Bioanalyzer 2100

For quantification of RNA integrity and an accurate concentration of intact RNA samples, microfluidic analysis was performed with the bioanalyzer 2100 (Agilent Technologies, UK) and Agilent RNA 6000 nano kit (Agilent Technologies, UK) as per manufacturer's instructions.

The 100 bp RNA 6000 NanoLadder was prepared by heat denaturing at 70°C for 2 minutes then chilled on ice, aliquots of prepared ladder were stored at -80°C. Nano gel matrix was prepared by filtering 550 µL of gel through a spin filter column at 10,000 x *g* for 10 minutes at room temperature. The filtered gel matrix was used immediately or stored at 4°C for up to 4 weeks. RNA 6000 NanoDye concentrate was vortexed for 10 seconds and pulse centrifuged for 5 seconds in a 5418 centrifuge (Eppendorf, Germany). One microlitre of dye was added to 65 µL of gel. The gel-dye mix was centrifuged at 13,000 x *g* for 10 minutes at room temperature in a 5418 centrifuge (Eppendorf, Germany).

RNA Samples were diluted to approximately 250 ng/µL, within the optimal range (25-500 ng/µL) with DEPC water and heat denatured in a heat block at 70°C for 2 minutes. The RNA 6000 Nano chip was added to chip priming station, to which 9 µL of gel-dye mix was added. The gel was dispersed throughout the chip by applying gentle pressure to the 1 mL syringe plunger on the chip priming station, until the syringe was held under the clip. The plunger was depressed for 30 seconds, then the clip was released, after 5 seconds the syringe plunger was carefully pulled to the 1 mL position. A further 9 µL of gel-dye mix was then added. Five microliters of RNA 6000 Nano marker were added to the ladder and sample wells, followed by 1 µL of RNA ladder to the ladder well and 1 µL of RNA sample to each sample well. One microlitre of marker was added to the wells, which did not contain sample. The chip was vortexed for 60 seconds at 2400 RPM using an IKA vortex mixer (Agilent Technologies, UK). Chip was analysed using Bioanalyzer 2100 via Agilent 2100 expert software, which generates microfluidic gel images, electropherograms and RNA integrity numbers (RIN), which were downloaded.

2.7.5 Reverse transcription of RNA

To reverse transcribe total RNA for the synthesis of complementary (c)DNA, the High Capacity RNA to cDNA™ Kit (Applied Biosystems, USA) was used per manufacturer's instructions. The reactions contained 2 µg of RNA in a final volume of 20 µL, containing 1 X RT buffer, 1X RT enzyme mix and DEPC water

in 0.2 mL thin-walled reaction tubes. A control negative reverse transcriptase was prepared, where 1X RT enzyme mix was replaced with DEPC water. Reactions were incubated at 37°C for 60 minutes, then heat inactivated at 95°C for 5 minutes in a thermal cycler (2720 Thermal Cycler Applied Biosystems, UK). It was assumed that the cDNA synthesis reaction was 100 % efficient producing 2 µg of cDNA for each 20 µL reaction therefore, a final concentration of 0.1 ng/µL. cDNA was diluted to 5 ng/µL using DEPC water before use in quantitative reverse transcriptase polymerase chain reaction (qRT-PCR) experiments or stored at -20°C.

2.8 Quantification of gene expression

2.8.1 Oligonucleotide design and preparation

Oligonucleotides, targeting mRNA transcripts of interest were designed to span exon boundaries to avoid genomic DNA amplification, with annealing temperatures between 58-60°C, 16-25 bp in length, 40-60 % guanine and cytosine content and amplicon size of 100-200 bp. Annealing temperatures were calculated using OligoCalc (JustBio, <https://www.justbio.com/index.php?page=oligocalc>); (Kibbe, 2007) and *in silico* analysis to evaluate oligonucleotide self-complementarity and specificity was performed using the nucleotide basic local alignment tool (BLAST; <https://blast.ncbi.nlm.nih.gov/Blast.cgi>) hosted by the National Centre for Biotechnology Information (NCBI; Altschul *et al.*, 1990). Alignment of transcript variants was performed using, Aligner (JustBio, <https://www.justbio.com/index.php?page=aligner>). All oligonucleotides shown in Table 2.3 were purchased from MWG Eurofins (Ebersberg, Germany), diluted to a stock concentration of 100 µM in DEPC water and stored at -20°C.

2.8.2 qPCR

qRT-PCR experiments contained 25 ng of cDNA, 200 nM of forward and reverse oligonucleotides (MWG Eurofins, Germany) and 1X PrecisionPLUS qRT-PCR mastermix (PrimerDesign, UK) in a final volume of 20 µL. Reactions were prepared in BrightWhite 96-well plates (Primer Design, UK) in triplicate.

Transcripts were amplified and quantified using StepOnePlus qRT-PCR system (Applied Biosystems, UK) using SYBR green detection chemistry with the instrument settings: 95°C for 10 minutes followed by 40 cycles of; 95°C for 15 seconds and 58-60°C annealing temperatures for 1 minute. Negative controls included negative reverse transcription and a no template control (NTC), where RNA samples were substituted with an equal volume of DEPC water in the qRT-PCR experiment. Specific amplification was determined via melt curve analysis (Taylor *et al.*, 2010). The melt curves were generated by heating the final PCR product from 60°C to 95°C in 0.3°C increments followed by a final 15 second hold. Melt curves and test samples were compared to NTC to differentiate between the desired product and unwanted primer oligomers or potential genomic DNA contamination.

2.8.3 Identification of reference genes

To analyse candidate reference genes, geNorm oligonucleotide kit (Primer Design, UK) and qBase+ software (Biogazelle, Belgium) were used. A panel of 6 candidate reference genes (ACTB, GAPDH, EIF4A2, RPL13A SDHA and YWHAZ) were screened against LNCaP cells in duplicate using the reaction set up outlined in section 2.8.2. The reference genes, with the most consistent expression across all treatments were ACTB, GAPDH and RPL13A.

Table: 2.3 Oligonucleotides used for qRT-PCR analysis in this study

Target Gene	Accession Number	Sequence 5' – 3'
<i>ALIX</i>	NM_013374.6	F: CCTTAAGTCGAGAGCCGACC
		R: TGGGGAGAGTATCTTTGTATTGACA
<i>AR</i>	NM_000044.4	F: ACTGCTACTCTTCAGCATTATTCC
		R: GCTATTGCGAGAGAGCTGCAT
<i>ASCL1</i>	NM_004316.3	F: AAGCAGGGTGATCGCAAAC
		R: ATGCCTCGCTTAGTTGGGG
<i>CD9</i>	NM_001769.4	F: TGGGACTGTTCTTCGGCTTC
		R: CAGCCAAACCACAGCAGTTC
<i>EN02</i>	NM_001975.2	F: TATCCTGTGGTCTCCATTGAGG
		R: TTGCACGCTTGGATGGCTTC
<i>KLK3</i>	NM_001648.2	F: ATTGAACCAGAGGAGTTCTTGAC
		R: AGCACACAGCATGAACTTGGTC
<i>PTOV1</i>	NM_017432.4	F: AACCTGGAGACCGACCAGTG
		R: TCTCTGTTGGTGAAGTGGAAGT
<i>RAB27A</i>	NM_004580.5	F: GGGCAGGAGAGGTTTCGTAG
		R: TCTGCGAGTGCTATGGCTTC
<i>REST</i>	NM_005612.4	F: ATATGCGTACTCATTGAGGTGAG
		R: AATTGAACTGCCGTGGGTTCCAC
<i>SYP</i>	NM_003179.2	F: TGTAGTCTGGTCAGTGAAGCC
		R: CTAGGTGCCAGTCTTGAGT
<i>TSG101</i>	NM_006292.4	F: TATCCGCCATACCAGGCAAC
		R: GATGAGAGAGGCTCGGATGG
<i>VAMP7</i>	NM_005638.6	F: GAGCACAGACAGCACTTCCAT
		R: CTCCTCGCTGAGCTACCAGA

2.8.4 Quantification of fold change in gene expression

The average cycle threshold (C_T) value of ACTB, GAPDH and RPL13A were used in the cube root to calculate the geometric mean and used as an internal control. The expression of unknown target genes was then analysed relative to the reference genes ACTB, GAPDH and RPL13A. The fold change in gene expression was calculated using the $2^{(\Delta\Delta-Ct)}$ method (Livak and Schmittgen, 2001). Fold change values were calculated using Excel for Mac (Microsoft) and plotted as graphs using GraphPad Prism v8 (GraphPad Software Inc). Results shown as the mean of three independent experiments \pm standard error of the mean (SEM).

2.9 Statistical analysis

Statistical analysis was carried out using GraphPad Prism v.8 (GraphPad Software Inc). Results are shown as the mean \pm standard error of the mean (SEM) where $n=3$ or as the mean \pm standard deviation (SD) where $n=2$. For fold change in gene expression data the significance was determined by using a one-way ANOVA with Geisser-Greenhouse correction and Tukey's multiple comparisons where * $p < 0.05$, ** $p < 0.01$, *** $p < 0.001$, **** $p < 0.0001$.

3. Chapter 3: Establishing a model for the analysis of exosomes derived from NEtD LNCaP cells

3.1 Introduction

In the tumour microenvironment, NE-like cells may communicate with epithelial prostate cells by releasing exosomes (Lin *et al.*, 2017). Exosomes potentially drive the progression of PCa and shift the epithelial cell population to resistant NE-like cells and trigger aggressive neuroendocrine prostate cancer (NEPC) formation (Lin *et al.*, 2017). The role, if any, of exosomes within the NEtD process and PCa progression is unclear, therefore, investigating exosomes released from NEtD prostate cancer cells *in vitro* may clarify this.

LNCaP cells are androgen sensitive human PCa epithelial cells, which are an established *in vitro* model central to investigating PCa (Sampson *et al.*, 2013). When deprived of androgens, LNCaP cells undergo neuroendocrine trans-differentiation (NEtD); (Yuan *et al.*, 2006). Charcoal stripping of FCS (CS-FCS) is the most common and well established method of androgen deprivation (AD) *in vitro* (Shen *et al.*, 1997; Fraser *et al.*, 2019) and it reduces the androgen content of FCS by approximately 86% (Cao *et al.*, 2009). Phenol red is also omitted from culture medium as it is a weak oestrogen, thus, preventing stimulation of AR and interference with NEtD of LNCaP cells (Sikora *et al.*, 2016).

CS-FCS is commercially available however, exosome depleted CS-FCS is not, therefore, exosome depleted CS-FCS was created by ultracentrifugation (Théry *et al.*, 2006). However, ultracentrifugation may extract factors such as albumin (Caradec *et al.*, 2014), which is associated with androgen binding (Sedelaar and Isaacs, 2009), growth factors or androgen binding proteins (Ludwig *et al.*, 2019); (Figure 3.1). It has not been reported whether ultracentrifugation of FCS or CS-FCS affects LNCaP cell culture and NEtD. Therefore, it is possible that the culture medium of exosome depleted control (dC) LNCaP cells may be partially androgen deprived and reduced growth factors, which may interfere with cellular function (Figure 3.1A). Exosome depletion of LNCaP cells grown in AD conditions may

induce a further effect of AD, cellular functions and NEtD of LNCaP cells (Figure 3.1B). In order to investigate the potential impact of exosome depletion of FCS, LNCaP cells were grown in culture medium supplemented with either FCS, exosome depleted FCS, CS-FCS or exosome depleted CS-FCS. The differing conditions allowed analysis of the impact of exosome depletion on LNCaP cells and AD-induced NEtD of LNCaP cells.

Exosomes have been isolated from PCa cell lines, including LNCaP cells, cultured in exosome depleted medium, (Corcoran *et al.*, 2012; Mizutani *et al.*, 2014; Lin *et al.*, 2017). However, those investigating exosomes released from LNCaP cells fail to acknowledge how exosome depletion of FCS may affect LNCaP cell function. FCS-derived exosomes are taken up by cardiac progenitor cells, and can influence cellular functions such as proliferation and migration (Angelini *et al.*, 2016), therefore, it is necessary to ascertain the effects of exosome depletion on LNCaP cells.

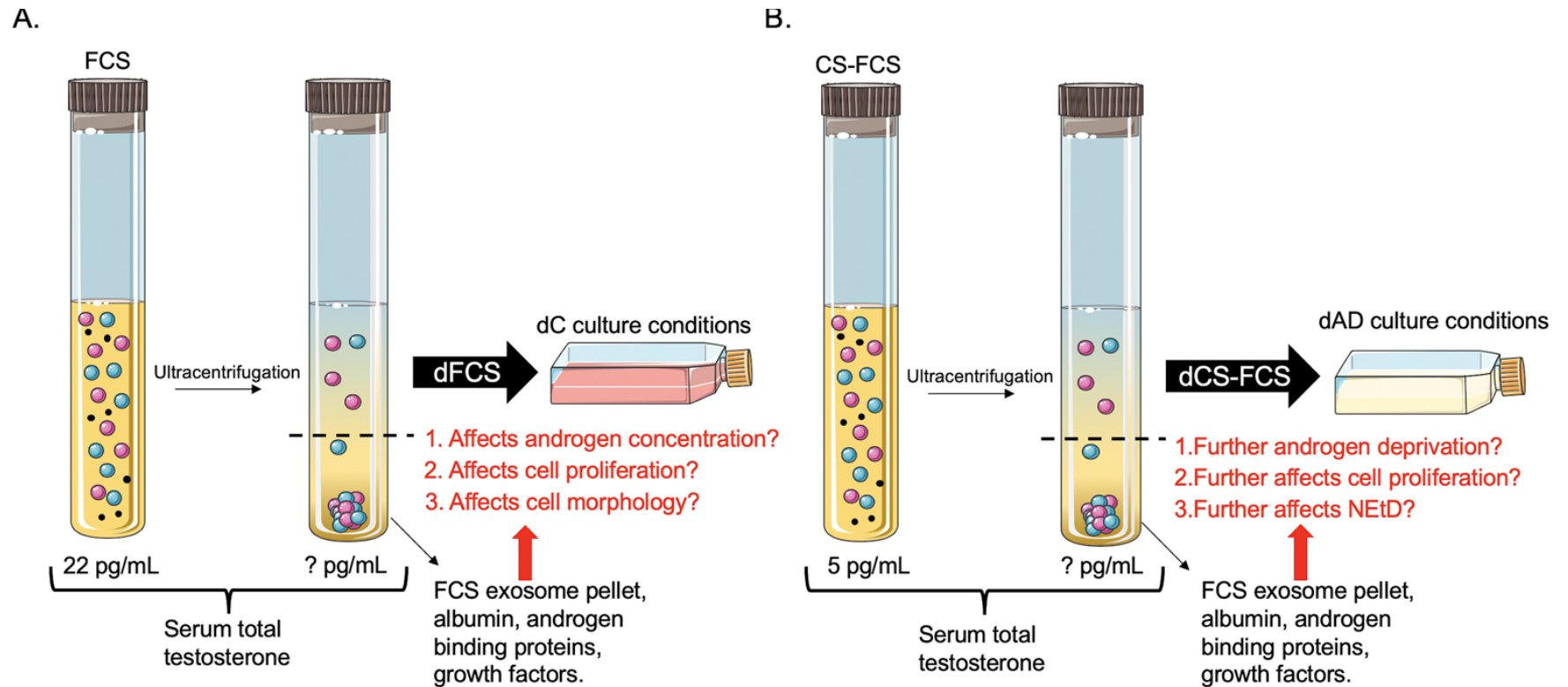


Figure 3.1 Schematic highlighting the potential effects of exosome depletion of serum on culture of LNCaP cells. Exosome depletion of FCS and CS-FCS by ultracentrifugation causes loss of albumin, androgen binding proteins and growth factors, it is unknown how this may affect LNCaP cells in culture. **A.** It is possible that the androgen concentration, cell proliferation and morphology of LNCaP cells may be affected when grown in the presence of exosome depleted FCS (dFCS). **B.** Exosome depletion of CS-FCS (dCS-FCS) may cause further androgen deprivation, further affect cell proliferation and neuroendocrine transdifferentiation (NETD) of LNCaP cells. Created using Servier Medical Art by Servier.

3.2 Study aims and research questions

3.2.1 Overall aim:

To establish a robust *in vitro* model to investigate exosome release from AD-induced NEtD LNCaP cells.

3.2.2 Objectives

1. Develop a protocol, which removes exosomes from CS-FCS.
2. Analyse the effect of exosome depletion on morphological and molecular characteristics of AD-induced NEtD LNCaP cells.

3.2.3 Research questions:

1. Do LNCaP cells still undergo NEtD in exosome depleted CS-FCS media?
2. Does exosome depletion affect the NEtD morphology of LNCaP cells?
3. Does exosome depletion alter the expression of key markers of androgen signalling and NEtD in LNCaP cells?

3.3 Results

3.3.1 Analysing the effect of exosome depletion on NEtD of LNCaP model – cell morphology analysis

LNCaP cells were grown for 15 days in control (C), exosome depleted control (dC), AD and exosome depleted (d)AD culture conditions and morphology was analysed using brightfield microscopy to assess evidence of NEtD at regular intervals (Figure 3.2). At day 0, LNCaP cells grown in each of the four conditions display characteristic epithelial morphology (Horoszewicz *et al.*, 1983; Gaupel *et al.*, 2013). Throughout the 15-day treatment, control LNCaP cells retained their epithelial morphology and resembled cells at 0 days (Figure 3.2, panel I to V). There were no observed differences in size, shape or growth rate of exosome depleted control LNCaP cells compared to control LNCaP cells, showing that exosome depletion did not affect growth or morphology of LNCaP cells.

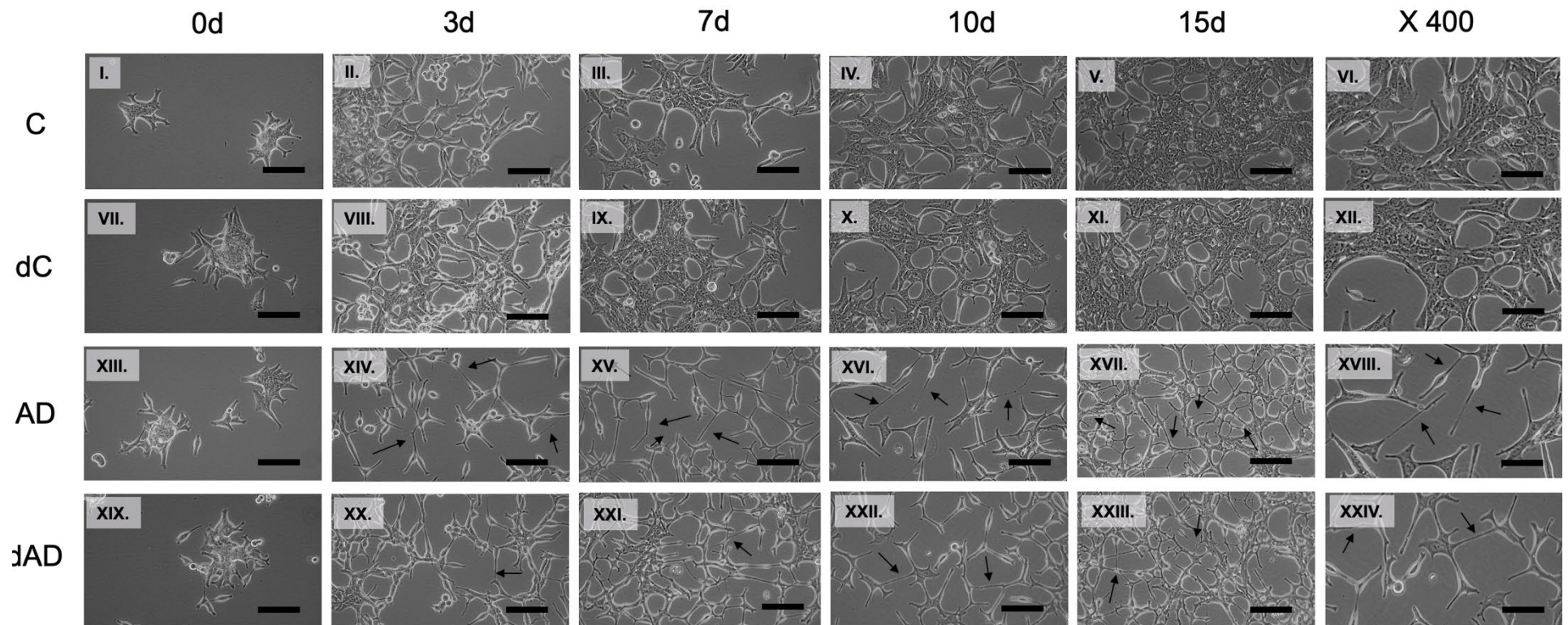


Figure 3.2: Exosome depletion does not affect AD induced NE-transdifferentiation of LNCaP cells. Representative brightfield microscopy images of LNCaP cells cultured for 15 days under control (C), exosome depleted control (dC), androgen deprived (AD) and exosome depleted AD (dAD) conditions at 0, 3, 7, 10 and 15 days (X 200 magnification); (n=3). Arrows indicate the presence of protrusions at 3, 7, 10 and 15 days and appear neuronal-like by 15 days. Magnification at X 400 is also shown to give an enlarged view of neuronal-like projections at day 10. Scale bars are representative of 1 μ m.

After 3 days in AD conditions LNCaP cells exhibited evidence of NEtD showing an emergence of cytoplasmic protrusions (indicated by arrows Figure 3.2, panel XIV). At days 7 and 10 protrusions became more extensive and more defined (Figure 3.2, panel XV and XVI respectively). By 15 days of AD, neurite-like protrusions identified in AD LNCaP cells increased in complexity showing branching of the protrusions and cells adopted a neuronal-like morphology (Figure 3.2, panel XVII). Indicating, there had been a shift from an epithelial to neuronal-like phenotype of LNCaP cells. Exosome depleted AD LNCaP cells also displayed neuronal-like morphology and resembled AD LNCaP cells throughout (Figure 3.2, panel XIX to XXII), evidencing that exosome depletion does not affect morphological changes associated with AD-induced NEtD.

3.3.2 Analysing the effect of exosome depletion on expression of molecular markers of AD-induced NEtD of LNCaP cells

Next, it was assessed whether exosome depletion of CS-FCS affected AD-induced NEtD of associated protein markers to establish if exosome depletion affected AD-induced NEtD at the protein level.

The AR regulates prostate growth and development (Lonergan and Tindall, 2011). No change in AR expression was observed in LNCaP cells grown in control or exosome depleted control conditions (Figure 3.3A). AR expression in AD and exosome depleted AD conditions was also comparable to expression in control LNCaP cells. Stability of AR across the different conditions indicates that exosome depletion did not affect the expression of the AR (Figure 3.3A).

Prostate specific antigen (PSA) is a target gene of the AR, when activated by androgen AR induces transcription of PSA (Akbaş *et al.*, 2015). PSA was only detected in control LNCaP cells and was undetectable following AD (Figure 3.3B, lane 3), providing evidence that the AR was not activated and unable to induce AR-target genes, such as PSA. Therefore, the *in vitro* AD model has successfully reduced activation of the AR (Mao *et al.*, 2009). Unfortunately, the PSA antibody was unreliable and failed to consistently detect PSA in known positive samples. Therefore, PSA could not be analysed under exosome depleted conditions.

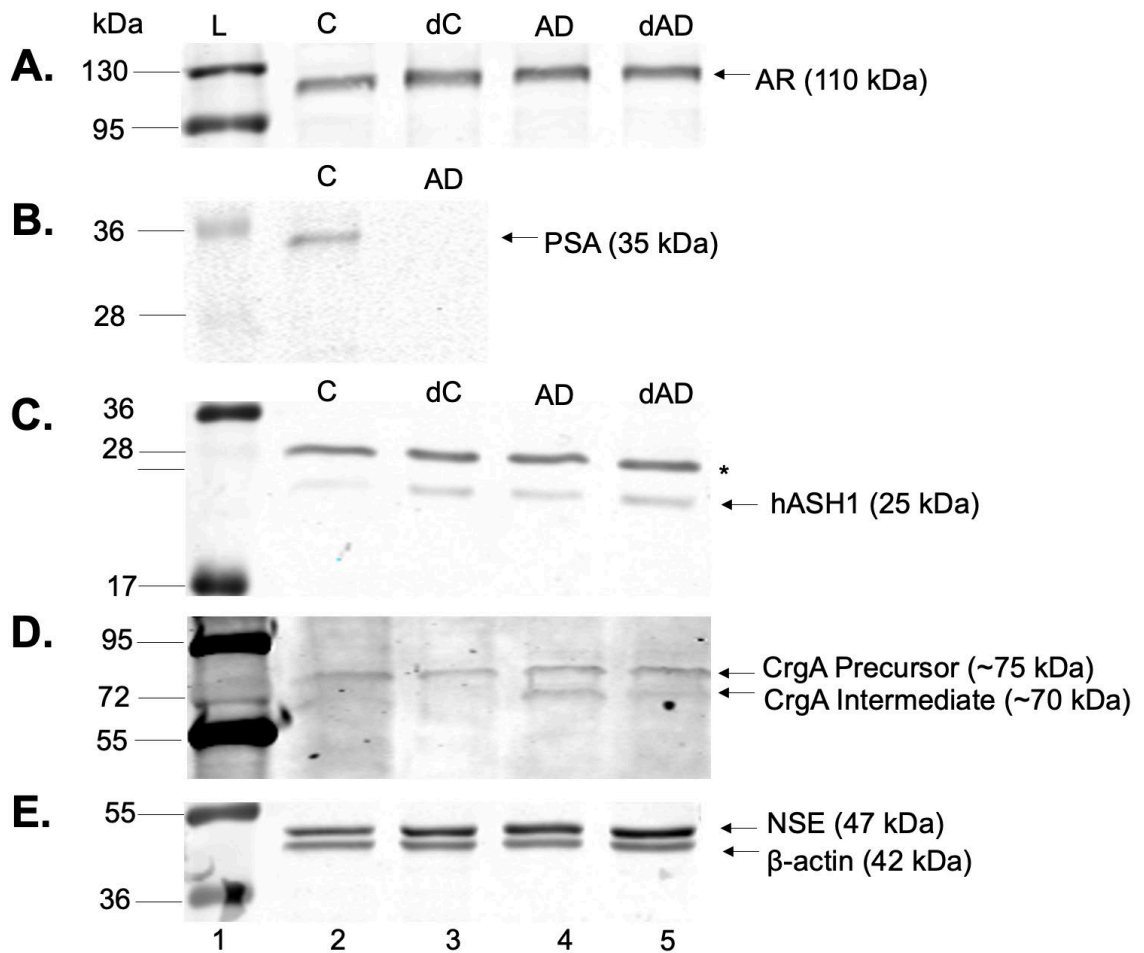


Figure 3.3 Exosome depletion may affect expression of NED-associated markers in LNCaP cells. Representative immunoblot analysis of protein expression in LNCaP cells cultured in control (C), exosome depleted control (dC), androgen deprivation (AD) or exosome depleted androgen deprived (dAD) conditions for 15 days. **A.** Androgen receptor (AR), **B.** Prostate specific antigen (PSA), **C.** Human achaete-scute homolog 1 (hASH1), **D.** Chromogranin A (CrgA). **E.** Neuron specific enolase (NSE) and β -actin. Equal loading was assessed by β -actin, expression of β -actin was analysed on each membrane however, only one representative immunoblot is shown. Molecular weights are indicated and * is representative of non-specific staining of hASH1 antibody (n=2).

hASH1 is a neuronal marker involved in cell commitment and neuronal differentiation (La Rosa *et al.*, 2013), therefore expression of hASH1 is expected to increase with NEtD (Fraser *et al.*, 2019). In control LNCaP cells, a faint band can be identified showing the expression of hASH1. Expression of hASH1 appears to be induced by exosome depletion in control conditions (Figure 3.3C, lane 3) suggesting exosome depletion may affect hASH1 expression. AD LNCaP cells show induced hASH1 expression compared to control LNCaP cells. In exosome depleted AD LNCaP cells hASH1 expression remained evident, and somewhat stronger than AD alone (Figure 3.3C, lane 3). These findings suggest exosome depletion may affect hASH1 expression in control and AD LNCaP cells.

Chromogranin A (CrgA) is a secretory protein that induces generation of secretory granules and is a precursor of several functional peptides (Gong *et al.*, 2007; Gkolfinopoulos *et al.*, 2017). In control cells a protein of ~75 kDa was detected, corresponding to the CrgA precursor protein (Maina *et al.*, 2016; Figure 3.3, lane 4). This was also detected in exosome depleted control cells, suggesting exosome depletion did not affect the expression of the CrgA precursor protein (Figure 3.3, lane 4). Interestingly, following AD, LNCaP cells expressed CrgA proteins at 75 kDa and 70 kDa. The 70 kDa protein corresponds to the presence of an intermediate CrgA (Maina *et al.*, 2016). This suggests that AD-induced NEtD initiates processing of the CrgA precursor protein (Figure 3.3, lane 4). In exosome depleted AD LNCaP cells, precursor and intermediate CrgA can be identified however, the 70 kDa intermediate CrgA protein appears less abundant (Figure 3.3, panel 4). These results suggest exosome depletion combined with AD may suppress processing of the CrgA precursor protein.

NSE is found within cells of neuronal origin and is associated with NE-transdifferentiation (Isgrò *et al.*, 2015). NSE was expressed under control conditions and expression remained comparable in control exosome depleted LNCaP cells (Figure 3.3, lane 5). There was a marginal increase in the expression of NSE under AD compared to control cells, the increase in NSE expression was preserved in exosome depleted AD LNCaP cells (Figure 3.3, lane 5).

β -actin was used as a control for equal loading, the expression of β -actin was equal across all conditions (Figure 3.3E, lane 5). Changes in protein expression were not associated with unequal protein loading but the effect of exosome or androgen depletion.

Increased expression of key markers associated with NEtD shows AD-induced NEtD of LNCaP cells. However, exosome depletion of control and AD LNCaP cells affected expression of hASH1 and CrgA. These results suggest that exosome depletion may impact upon the NEtD of LNCaP cells however, further molecular analysis is required.

3.3.3 Identifying stable reference genes for exosome depleted AD-induced NEtD LNCaP model

qRT-PCR was used to assess changes in protein expression were accompanied by changes in gene expression. Before gene analysis could be completed it was crucial to identify appropriate reference genes for normalisation of gene expression data. Exosome depletion of FCS may remove growth factors, cytokines or other non-EV products therefore, it was necessary to check whether this caused global effects on gene expression (Ludwig *et al.*, 2019). Total RNA was extracted from cells grown in control, exosome depleted control, AD, and exosome depleted AD conditions and quantified. There was no change in cell confluence between conditions however, there was a noticeable reduction in total RNA concentration in exosome depleted compared to non-exosome depleted samples by approximately 5X. Analysis of RNA quality via Bioanalyzer confirmed that each RNA sample had appropriate RIN values (>8) and the RNA was of good quality (data not shown); (Fleige and Pfaffl, 2006; Mueller *et al.*, 2016). This provided evidence that the reduction in RNA concentration was not caused by degradation but possibly a result of exosome depletion.

Expression of six reference genes: β -actin (ACTB), eukaryotic translation initiation factor 4A2 (EIF4A2), glyceraldehyde 3-phosphate dehydrogenase (GAPDH), ribosomal protein L13a (RPL13A), succinate dehydrogenase complex

subunit A (SDHA) and 14,3,3 protein zeta/delta (YWHAZ) was analysed in control, exosome depleted, AD and exosome depleted AD LNCaP cells by qRT-PCR. Expression of these reference genes is also of importance, as there is no documented data demonstrating the reference genes used when LNCaP cells are grown in exosome depleted conditions.

The cycle threshold (C_T) value is the number of cycles required for the fluorescent signal to cross the threshold by exceeding the background fluorescent signal (Wong and Medrano, 2005). Low C_T values are indicative of a greater abundance of target transcripts and therefore, expression of the target gene (Heid *et al.*, 1996). geNorm identifies the most stable reference genes across all growth conditions. Therefore, the average C_T values from all four growth conditions were plotted to identify which genes were the most stable and could be used as reference genes to normalise future gene expression experiments. ACTB, GAPDH and RPL13A had the lowest C_T values, which were also the most stable as the C_T values for these genes were within a narrow range (between 15-18 C_T ; Figure 3.4A). Whilst EIF4A2 did not have large variability in C_T value, the C_T values were higher than that of ACTB, GAPDH and RPL13A (18-19 C_T ; Figure 3.4A), indicating a reduction in target transcript abundance for EIF4A2. SDHA and YWHAZ showed significant variability in C_T values (9-19 and 9-17 C_T respectively; Figure 3.4A) under control, exosome depleted, AD and exosome depleted AD conditions and, therefore, were not suitable as reference genes.

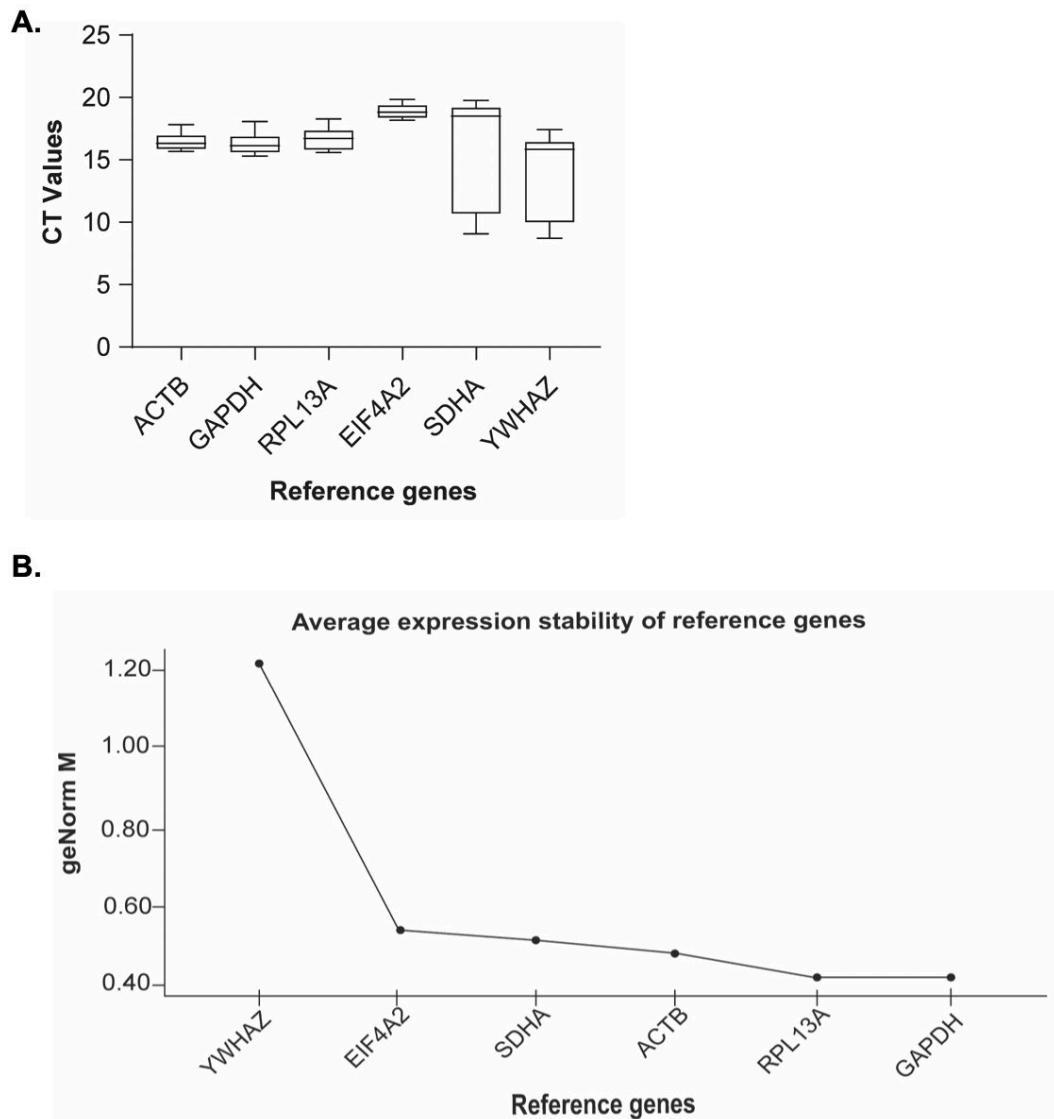


Figure 3.4: Identifying stable reference genes in exosome-depleted model of AD-induced NETd in C, dC, AD and dAD LNCaP cells. **A.** Box and whisker plot of the mean cycle threshold (Ct) values for reference genes β -actin (ACTB), glyceraldehyde 3-phosphate dehydrogenase (GAPDH), ribosomal protein L13A (RPL13A), eukaryotic translation initiation factor 4A2 (EIF4A2), succinate dehydrogenase complex flavoprotein subunit A (SDHA) and 14-3-3 protein zeta/delta (YWHAZ) in control (C), exosome depleted control (dC), androgen deprived (AD) and exosome depleted androgen deprived (dAD) LNCaP cells, Ct values are expressed as mean \pm SEM (n=3). **B.** Average expression stability of reference genes YWHAZ, EIF4A2, SDHA, ACTB, RPL13A and GAPDH based on the Ct values shown in panel A and analysed by qbase⁺ software using their algorithm to generate geNorm M values.

The qbase+ software calculates the M value of the reference targets and reflects their relative stability; the higher the M value, the less stable the reference gene (Le Bail *et al.*, 2013). Figure 3.4B shows the graph produced by qbase+ software demonstrating ACTB, GAPDH and RPL13A had the lowest geNorm M values (>0.5) and, thus were most stable (Figure 3.4B). ACTB and GAPDH have previously been identified as stable reference genes within LNCaP cells (Zhao *et al.*, 2018) therefore, the data are in keeping with that of others. The output obtained from qbase+ stated that use of the three reference genes, ACTB, GAPDH and RPL13A was optimal when used in the geometric mean (cubed root of the average C_T values) to provide rigid analysis, less variation in results and reliable data. Therefore, the geometric mean of ACTB, GAPDH and RPL13A, was used for the normalisation of gene expression data.

3.3.4 Analysing the effect of exosome depletion on the expression of key genes associated with NEtD

It was important to assess if affects to neuronal markers caused by exosome depletion at the protein level were reflected in gene expression data. Expression of androgen signalling markers (AR and kallikrein related peptidase 3 (KLK3), which encodes PSA), neuroendocrine markers (enolase 2 (ENO2), encoding NSE, beta tubulin class III (TUBB3) and synaptophysin (SYP)) and regulators of neurogenesis (human achaete-scute homolog 1 (ASCL1) encoding hASH1, RE-1 silencing transcription factor (REST) and prostate specific gene 1 (PTOV1)) were analysed by qRT-PCR (Figure 3.5).

In line with AR protein data (Figure 3.3A), there was no significant change observed in AR expression in exosome depleted control LNCaP cells when compared to control LNCaP cells (Figure 3.5A). AR expression was significantly induced in AD LNCaP cells versus control LNCaP cells (3.5-fold; $p < 0.0001$), additionally exosome depletion of AD did not affect AR induction when compared to exosome depleted control cells (3.1-fold; $p < 0.0001$); (Figure 3.5A). However, there was significant difference ($p = 0.0262$) in AR expression between AD and

exosome depleted AD LNCaP cells, suggesting AD combined with exosome depletion affects AR expression.

Depletion of exosomes did not affect KLK3 expression, however, KLK3 expression was significantly downregulated (47-fold; $p < 0.0001$) by AD, which suggests loss of androgen signalling and activation, in line with the observed loss of PSA protein expression (Figure 3.3A). Downregulation of KLK3 expression in exosome depleted AD when compared to exosome depleted control LNCaP cells was not as dramatic as that observed in AD cells, but it was significant demonstrating interruption of AR signalling (7.5-fold; $p = 0.0001$; Figure 3.5A). The significant difference in KLK3 gene expression between AD and exosome depleted AD LNCaP cells ($p = 0.0022$) suggests exosome depletion in combination with AD affects KLK3 expression.

ENO2 (encoding NSE) is a marker of neuronal cells (Isgrò *et al.*, 2015) and is associated with neuroendocrine tissues (Wiedenmann *et al.*, 1986). As expected, ENO2 expression was unaffected by exosome depletion in control LNCaP cells ($p = 0.2375$; Figure 3.5B). After AD, there was a 4.3-fold increase of ENO2 expression, which was mirrored by exosome depleted AD LNCaP cells by a comparative 4.8-fold increase ($p = 0.0012$ and $p < 0.0001$ respectively; Figure 3.5B). Induction of ENO2 correlates with increased NSE protein expression (Figure 3.3D).

Unfortunately, chromogranin A (CHGA) was not included in qRT-PCR analysis, as the repetitive sequences of bases within the CHGA sequences prevented the design of specific oligonucleotides. Therefore, the neuron specific marker, TUBB3 was included. TUBB3 was increased as progenitor cells differentiate into neurons (Nierode *et al.*, 2019), therefore, it was anticipated that expression would increase with AD. TUBB3 expression was unaffected in exosome depleted control compared to control LNCaP cells (Figure 3.5B). Following AD, TUBB3 expression was significantly increased (6-fold; $p < 0.0001$), this trend was also reflected by exosome depleted AD LNCaP cells (7-fold; $p < 0.0001$; Figure 3.5B).

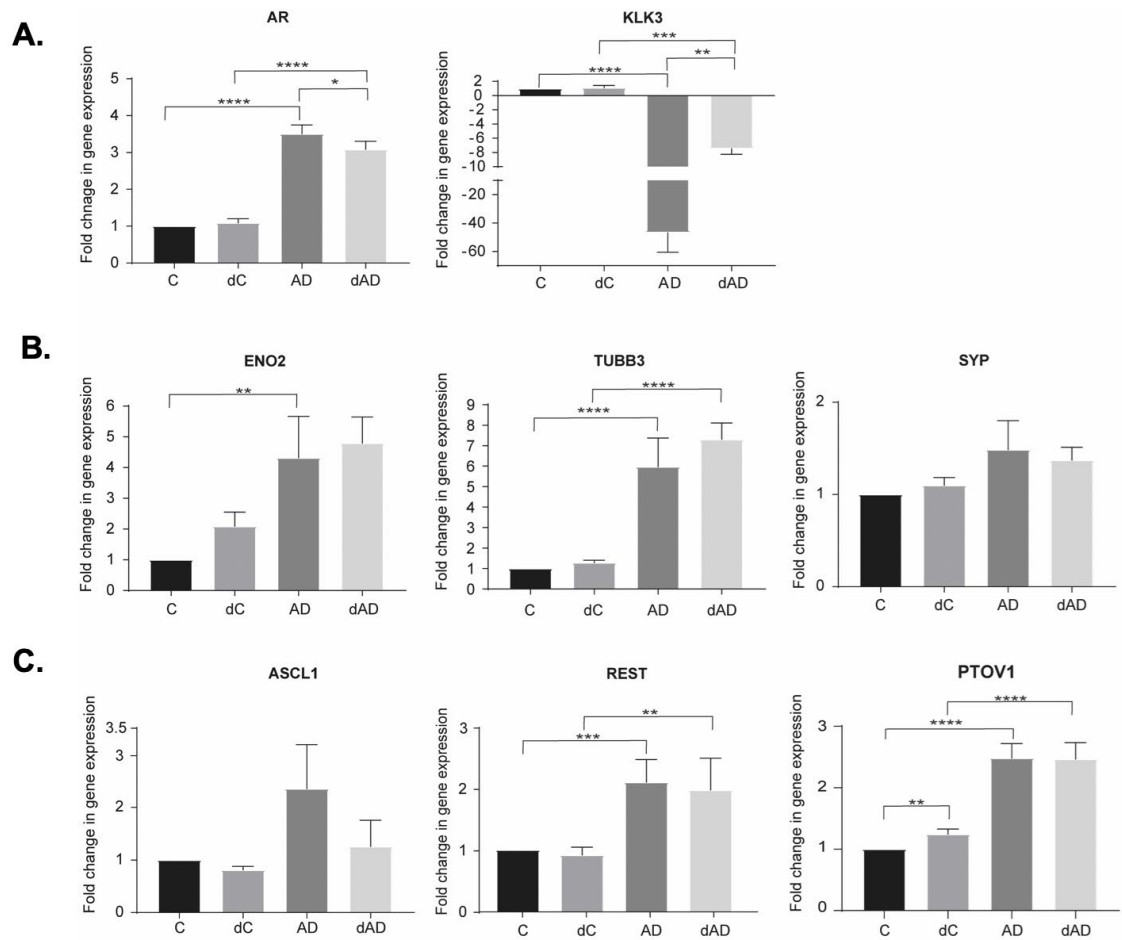


Figure 3.5: Assessing the effect of exosome depletion on NETd LNCaP cells.

Cells were grown in control (C), exosome depleted control (dC), androgen deprived (AD) or exosome depleted androgen deprived (dAD) for 15 days, RNA was extracted, and relative gene expression was assessed by qRT-PCR. **A.** Androgen receptor (AR) and kallikrein-3 (KLK3). **B.** Enolase 2 (ENO2), class III β -tubulin (TUBB3) and synaptophysin (SYP). **C.** Achaete-scute homolog 1 (ASCL1), RE-1 silencing transcription factor (REST), and prostate tumour over expressed gene 1 (PTOV1). Data were analysed by $\Delta\Delta$ Ct (Livak and Schmittgen, 2001) and normalised to the geometric mean of ACTB, GAPDH and RPL13A to obtain the fold change in gene expression. Data are expressed as the mean fold change \pm SEM (n=3). Data were analysed by one-way ANOVA and Tukey's post hoc analysis; *p<0.05, **p<0.01, ***p<0.001 **** p<0.0001.

Expression of SYP, a broad spectrum neuroendocrine marker (Wiedenmann *et al.*, 1986), was unchanged in exosome depleted control conditions compared to control LNCaP cells (Figure 3.5B). SYP expression increased slightly in AD LNCaP cells (1.5-fold; $p=0.0928$) compared to control (Figure 3.5B). Increased SYP expression was mirrored in exosome depleted AD cells (1.5-fold $p=0.00792$); (Figure 3.5B), showing exosome depletion did not affect SYP expression in control or AD LNCaP cells.

ASCL1, a driver of neurogenesis (Raposo *et al.*, 2015) was unaffected by exosome depletion in control cells and marginally increased in AD cells (1.25-fold, not significant); (Figure 3.5C). These results contrast with induced hASH1 protein expression of exosome depleted control and exosome depleted AD LNCaP cells (Figure 3.3C). This suggests that exosome depletion may impact on the expression of ASCL1.

REST is the master repressor of neurogenesis (Mozzi *et al.*, 2017), REST expression was unchanged in exosome depleted control cells (Figure 3.5C). Conversely, AD LNCaP cells exhibited a 2-fold; $p=0.0002$ increase in the expression of REST (Figure 3.5C), which was replicated in exosome depleted AD cells ($p=0.0048$). Indicating exosome depletion did not affect REST expression.

PTOV1, is overexpressed in early and late stage prostate cancer (Benedict *et al.*, 2001). PTOV1 expression was significantly increased in exosome depleted control cells (1.24-fold; $p=0.0022$). AD cells show induced PTOV1 expression with a 2.5-fold increase $p=0.0001$, this result is replicated by exosome depleted androgen deprived cells, indicating exosome depletion affects PTOV1 in control cells and not AD cells (Figure 3.5C).

3.3.5 Conclusions

The data shows exosome depletion did not affect control LNCaP cell morphology nor the morphological changes associated with AD-induced NEtD. Additionally, exosome depletion of CS-FCS did not appear to alter the ability of LNCaP cells to undergo NEtD and the extent of NEtD was unchanged. However, assessment

of protein and gene expression markers revealed that exosome depletion affected the expression of AR, KLK3, hASH1/ASCL1, PTOV1 and CrgA while all other markers remained unchanged.

3.4 Discussion

Neuroendocrine prostate cancer (NEPC) is the most lethal form of PCa (Lin *et al.*, 2017). Release of neuropeptides by neuroendocrine (NE) cells in the tumour microenvironment (Abrahamsson, 1999) is thought to be the driver of neuroendocrine transdifferentiation (NEtD) of epithelial prostate cells to NE-like cells (Soundararajan *et al.*, 2018). Recently, exosomes were proposed to play a role in NEPC progression (Lin *et al.*, 2017). The isolation of exosomes from AD-induced NEtD LNCaP cells provided an opportunity to study their potential role in NEPC. However, exosomes are not only released by LNCaP cells but are also found in FCS (Datta *et al.*, 2018). Therefore, LNCaP cells grown in the presence of FCS are exposed to FCS exosomes, which may affect LNCaP cellular function, the NEtD process during AD and also interfere with LNCaP exosome isolation and analysis (Eitan *et al.*, 2015; Szatanek *et al.*, 2015; Angelini *et al.*, 2016). The aim of this research was to create an *in vitro* model to evidence the involvement of exosomes in AD-induced NEtD of LNCaP cells.

3.4.1 Establishing a model to assess exosomes released from NEtD LNCaP cells

Creating a model to analyse and characterise exosomes derived from AD-induced NEtD LNCaP cells was critical due to the presence of exosomes in FCS, a component of cell culture medium (Datta *et al.*, 2018). FCS exosomes may interfere with analysis of exosomes released by NEtD LNCaP cells (Jeppesen *et al.*, 2014). Nanoparticle tracking analysis (NTA) of freshly prepared culture medium, confirmed there was a significant population of EVs prior to the addition of cells (Szatanek *et al.*, 2015), emphasising the importance of depleting FCS associated EVs, which could otherwise skew downstream exosome isolation results (Shelke *et al.*, 2014).

FCS associated RNA can be co-isolated with extracellular RNA from cells, which interferes with downstream analysis of EV RNA (Wei *et al.*, 2016). miR-1246 encodes one of the most abundantly expressed miRNAs in FCS and is only present within four species, bovine, human, orangutan and chimpanzee (Wei *et al.*, 2016). Intriguingly, although there are no sequences homologous to hsa-miR-1246 in the mouse genome, mature miR-1246 was consistently found in all mouse cell lines, when cultured in the presence of 10% FCS (Wei *et al.*, 2016). This underscores the internal impact FCS exosomes can have on cells in culture and in turn influence downstream analysis and results from exosomes of interest. In addition to the co-isolation of RNA, proteomic and flow cytometry-based analysis of isolated exosomes suggested, isolated exosomal fractions often contain FCS exosomes and the extent of co-isolation depends on the method of isolation used (Gardiner *et al.*, 2016). Soluble proteins frequently co-isolated with exosomes are albumin, immunoglobulins and matrix metalloproteases, which are abundant in serum (Caradec *et al.*, 2014; Ludwig *et al.*, 2019). There is a need to discriminate the true exosome content versus contaminating nucleic acids or proteins coating the surface of exosomes to prevent the presentation of false data due to the masking of true exosomes with FCS exosomes.

FCS exosomes can be removed by ultracentrifugation, ultrafiltration, exosome precipitation kits, microfluidic techniques or by using commercially available pre-depleted serum (Li *et al.*, 2017). In this model, exosomes were depleted from FCS by ultracentrifugation, an established, cost effective and universally preferred method of exosome depletion (Soares Martins *et al.*, 2018). Ultracentrifugation does not remove 100% of exosomes from FCS, analysis revealed FCS exosomes were reduced by 70 % (Lehrich *et al.*, 2018). The 70% reduction of FCS exosomes ensures a reduced basal concentration of interfering exosomes, which can affect cellular function and also downstream analysis of exosomes of interest. Standardisation of exosome depletion has not been agreed, resulting in variations to the ultracentrifugation method including the model of centrifuge, the type of centrifuge rotor, the speed and duration samples are centrifuged (Livshits *et al.*, 2015). These adaptations create divisions between those researching exosomes, contributing to a larger problem, as the field is no closer to reaching a standardised protocol.

Quantifying the success of exosome depletion, appears to have been somewhat overlooked by those researching exosomes and using exosome depleted FCS in cell culture conditions. Few acknowledge the extent of exosome depletion and also, what other factors may be depleted alongside FCS exosomes. Measuring depletion success is an important consideration as in different cellular models, cells may exhibit different effects due to the change in their culturing conditions. Previously Lehrich et al. (2018) used nanoparticle tracking analysis (NTA) to quantify the number of exosomes in FCS prior and following exosome depletion, to determine the percentage depletion. In the *in vitro* AD-induced NEtD model combined with exosome depletion, the extent of exosome depletion is not known and could suggest why there was no change in cell size, growth or confluence of LNCaP cells when morphology was observed. Thus, in future work the success of exosome depletion should be quantified. Performing dynamic light scattering (DLS) prior to and following exosome depletion, would allow quantification of the number of particles, which represent the exosome population. These data could then be used to identify the percentage of exosome depletion and the success of the process. It would be accepted that batch to batch variation may occur when performing exosome depletion of FCS. To ensure reproducible and consistent results a cut-off point for the percentage of depletion should be considered. Based on findings from Lehrich et al. (2018) a cut-off of 70% +/- 5% depletion should be considered when 18 hour ultracentrifugation is used for exosome depletion of FCS.

As well as assessing the percentage of depletion, assessing proteins associated with FCS exosomes before and after exosome depletion of FCS may indicate the extent of depletion. Assessment of markers of exosome machinery such as ALG-2 interacting protein X (Alix; (Szatanek *et al.*, 2017) via immunoblotting from non-exosome depleted and exosome depleted FCS may reveal a change in expression. It would be expected that Alix expression would be reduced in exosome depleted FCS.

Commercially pre-depleted FCS may minimise variations in the ultracentrifugation method for exosome depletion however, it is costly. It was shown that pre-depleted FCS had a reduction of 75% in exosome content and

was able to support standard cell growth and diminished bovine miRNAs (Chen *et al.*, 2013). A shortcoming of pre-depleted FCS is that manufacturers who produce pre-depleted FCS do not state the method of exosome depletion used. It is also unknown in what proportions other factors found in FCS are removed as this has not been quantified. Pre-depleted FCS could not be applied to the AD-induced NEtD model as exosome depleted charcoal stripped FCS (CS-FCS) is not a commercially available product. CS-FCS is essential for androgen deprivation and induction of NEtD, which is central to the model used (Fraser *et al.*, 2019). Therefore, if commercially available pre-depleted FCS was utilised, appropriate comparisons could not be drawn between exosome depleted control and exosome depleted AD conditions, further supporting the use of ultracentrifugation to produce exosome depleted CS-FCS.

3.4.2 The consequence of exosome depletion of FCS

FCS is fundamental to provide additional nutrients like fatty acids, cholesterol, endocrine factors, such as androgens, insulin, epidermal growth factor and cell attachment proteins like fetuin to cells in culture (Sedelaar and Isaacs, 2009). Whether exosome depletion of serum enhances or reduces the effects of LNCaP AD-induced NEtD cell morphology is unknown. However, Eitan *et al.* (2015) previously showed exosomes from FCS are internalised by cells and interact with lysosomes. Therefore, FCS exosomes may serve as carriers of signals or nutrients, promoting normal cell growth (Eitan *et al.*, 2015). It was important to ascertain whether the potential loss of other essential supplements from FCS did not affect LNCaP cell growth under different experimental conditions. This would demonstrate whether the proposed model was appropriate for the study of exosomes isolated from NEtD LNCaP cells.

FCS-derived exosomes in culture medium can have a significant influence on cellular function. Angelini *et al.* (2016) showed FCS-derived exosomes supported cell growth and migration of human cardiac progenitor cells. The size, yield and extracellular matrix production were affected when exosomes were depleted from FCS (Angelini *et al.*, 2016), demonstrating the influence of FCS exosomes on cells in culture. Proliferation of cardiac progenitor cells increased, when FCS

exosomes were supplemented back into exosome depleted medium, in a dose dependent manner. Interestingly, when morphology was assessed no significant changes in the appearance of the cardiac progenitor cells were identified Angelini et al. (2016). Further, Shelke et al. (2014) revealed cell migration was reduced in airway epithelial cancer (A549) cells grown in culture medium containing exosome depleted FCS. FCS exosomes were added to exosome depleted medium, inducing transmigration. The FCS exosomes were labelled with PKH67, a fluorescent membrane dye and live cell imaging performed, the results displayed uptake of the FCS exosomes by A549 cells. Indicating that exosomes, which originate from FCS have a direct migratory effect on A549 cells (Shelke *et al.*, 2014). These data indicate, that although morphological changes were not observed in LNCaP cells cultured in exosome depleted medium, if proliferation (MTT assay) and migration (scratch assay) assays were performed, such analysis may provide further data to elucidate the effect of exosome depletion on LNCaP cells.

3.4.3 Androgen deprivation and exosome depletion

Charcoal stripping of FCS reduces the androgen content by approximately 86%, and reduces the total serum testosterone concentration from 22.0 +/- 6.1 pg/mL to 5.0 +/- 0.49 pg/mL (Sedelaar and Isaacs, 2009). In healthy males, the normal range of total serum testosterone is 3-10 ng/mL, conversely in chemically castrated PCa patients, total serum testosterone concentrations are reduced to <0.5 ng/mL (Sedelaar and Isaacs, 2009). LNCaP cells are routinely cultured with normal FCS prior to culture with CS-FCS, resulting in residual androgens in culture, as well as low concentrations of androgens in CS-FCS, which could potentially activate the AR (Davey and Grossmann, 2016). There are no data to indicate if the androgen concentration is affected by exosome depletion therefore, a change in the androgen concentration of culture conditions could impact AD and subsequent NED.

In addition to reducing androgens, charcoal stripping of FCS also reduces vitamins, electrolytes and certain metabolites however, albumin was unaffected by charcoal stripping (Cao *et al.*, 2009). Stability of albumin following charcoal

stripping is important, as albumin plays a role in binding free testosterone in serum. Sex hormone binding globulin (SHBG) and albumin are abundant within serum (Tan *et al.*, 2015). Approximately 60% of testosterone and dihydrotestosterone (DHT) are bound to SHBG and the remaining 40% is bound to albumin (Heinlein and Chang, 2002). Albumin has a low affinity for androgens, therefore, continuously releases and rebinds serum testosterone, whereas SHBG replenishes free testosterone, which is lost via diffusion to stabilise total serum testosterone (Sedelaar and Isaacs, 2009). Therefore, albumin plays a critical role in regulating androgens and a reduction in the albumin concentration during exosome depletion of FCS may impact the androgen concentration in culture conditions.

Albumin is frequently co-sedimented with exosomes during ultracentrifugation (Van Deun *et al.*, 2014); indeed, albumin is a common contaminant of exosome pellets (Caradec *et al.*, 2014; Lehrich *et al.*, 2018). Therefore, androgen bound to albumin may also be co-sedimented in the ultracentrifugation process. Reduction in albumin content of FCS following ultracentrifugation may also reduce binding of free androgen to albumin in culture medium. This could reduce the androgen concentration in exosome depleted FCS therefore, cell culture medium containing exosome depleted FCS or CS-FCS is likely to have a reduced androgen content compared to non-exosome depleted culture medium. Moreover, in CS-FCS, where the concentration of androgens is already substantially reduced, androgens could be further diminished. If exosome depleted control medium was deprived of androgen it may be expected that exosome depleted cells display potential NEtD. Curiously, when morphology of exosome depleted control LNCaP cells was analysed, these cells did not exhibit NEtD and morphology reflected that of control LNCaP cells (Figure 3.2). Fraser *et al.* 2019 showed upon reintroduction of the synthetic androgen R1881, NEtD NE-like LNCaP cells lost their neurite-like extensions and 15 days post AD NE-like cells resembled control cells. However neuronal markers, NSE and hASH1 remained elevated, demonstrating the potential of morphology to mask many changes at a molecular level (Fraser *et al.*, 2019).

While NEtD may not have been morphologically evident, protein expression data revealed increased hASH1 expression in exosome depleted conditions when compared to their non-exosome depleted counterpart (Figure 3.3C). hASH1 is involved in the regulation of cell fate and commitment (Raposo *et al.*, 2015), increased expression of hASH1 could suggest that cells cultured in exosome depleted conditions may influence NEtD through increased reduction of androgens in culture medium. Additionally, PTOV1, a marker of prostate cancer progression (Benedict *et al.*, 2001) was upregulated in exosome depleted conditions versus control (Figure 3.5C), suggesting reduced androgens in exosome depleted control medium may promote NEtD. These data suggest that exosome depleted control growth medium has a reduced androgen concentration compared to control growth medium.

The concentration of androgens in FCS prior to and following exosome depletion was not measured. Assessing protein concentration of factors such as albumin by radioimmunoassay (RIA) in FCS pre and post ultracentrifugation, may reveal whether exosome depletion affects the concentration of albumin and androgens to provide knowledge of the culture medium composition following exosome depletion. It would be suggested that androgen concentration in exosome depleted conditions should be reflective of their control (22 +/- 6.1 pg/mL) or AD (5 +/- 0.49 pg/mL) counterpart (Sedelaar and Isaacs, 2009). However, it is important that the concentrations are consistent within experiments to ensure reliability and reproducibility of results.

3.4.4 Exosome depletion of FCS may cause reduction in total RNA concentration

The total RNA yield was reduced in LNCaP cells grown in exosome depleted cell culture medium however, microfluidic assay of RNA integrity did not provide any evidence to account for the reduced yield, as the RNA was fully intact. FCS-derived RNA is enclosed in EVs however, there are other macromolecules, such as ribonucleoproteins (RNPs) and lipoprotein particles associated with FCS RNA that co-sediment with exosomes (Mateescu *et al.*, 2017). The overlap in size and density of RNP and lipoproteins with exosomes accounts for the unavoidable co-sedimentation of FCS-derived RNA (Driedonks *et al.*, 2018). Here, FCS-derived RNA present in culture medium, is removed due to ultracentrifugation of FCS prior to the addition of cells, therefore, there is a reduced basal concentration of RNA. Co-sedimentation of FCS-derived RNA may account for the reduced total RNA yield from LNCaP cells grown in exosome depleted conditions compared to LNCaP cells grown in the presence of FCS.

3.5 Conclusions and future work

This study aimed to identify an appropriate model for the study of exosomes released from NE-like LNCaP cells by using exosome depletion of serum. The impact of exosome depletion on LNCaP cells has not been documented, therefore, morphological and molecular analysis of LNCaP cells grown in exosome depleted conditions was performed. No changes in cell morphology considering growth and appearance of the cell was observed. Exosome depleted control cells retained the epithelial morphology and exosome depleted AD cells showed neuronal-like protrusions associated with a shift in phenotype from epithelial to neuronal-like LNCaP cells. This suggests exosome depletion does not affect LNCaP cell growth or NEtD. However, protein and gene expression markers of androgen signalling, NE cells and neurogenesis (AR, KLK3, hASH1/ASCL1, PTOV1 and CrgA) were shown to be affected. More work may be required to ensure that the model is appropriate to study NE-like exosomes released from LNCaP cells.

To link protein and gene expression data, validation of chromogranin A gene (CHGA) would be beneficial. CHGA is a marker used in the clinic for the diagnosis of NEPC alongside other markers such as NSE (Gkolfinopoulos *et al.*, 2017). These data would add to the evidence collected here and also provide links between *in vivo* NEPC and the *in vitro* AD-induced NEtD model by using a more clinically relevant marker of NEPC (D'amico *et al.*, 2014). Performing end-point PCR of control, exosome depleted control, AD and exosome depleted AD LNCaP cell samples, may elucidate if the multiple bands corresponding to precursor and intermediate CrgA protein and identified in CrgA protein expression (Figure 3.3D) are also identified in gene expression analysis. Also, including multiple time points of AD exosome depletion, may identify when expression of CHGA is greatest, providing a more accurate representation of when LNCaP cells are most neuronal-like.

4. Chapter 4: Isolation and characterisation of exosomes from AD-induced neuroendocrine transdifferentiated LNCaP cells

4.1 Introduction

4.1.1 Exosomes and PCa/ NEtD

Exosomes are involved in cellular communications by inducing signals directly through surface molecules or by transfer of their cargo to recipient cells (Patel *et al.*, 2019). PCa cells, including LNCaP cells release exosomes, which can be isolated and characterised (Vlaeminck-Guillem, 2018). exosomes released from androgen sensitive (LNCaP) and androgen independent (PC3 and DU145) PCa cell lines can increase cellular proliferation of other PCa (Soekmadji *et al.*, 2017), transfer cell specific cargo (Read *et al.*, 2017) and initiate formation of the pre-metastatic niche (Itoh *et al.*, 2012). These data illustrate the ability of exosomes to manipulate PCa cells *in vitro* (Vlaeminck-Guillem, 2018).

In the prostate adenocarcinoma microenvironment, neuroendocrine (NE) cells are thought to release potent neuropeptides to induce neuroendocrine transdifferentiation (NEtD) of neighbouring epithelial prostate cells to NE-like cells (Soundararajan *et al.*, 2018). Exosomes may also mediate NEtD via crosstalk of exosomes released in the tumour microenvironment (Lin *et al.*, 2017). In this chapter an *in vitro* model of androgen deprivation (AD) that transdifferentiated control, epithelial LNCaP cells to NE-like LNCaP cells was applied. It is possible that exosomes released from epithelial and NE-like cancer cells drive cancer growth. However, whether exosome release drives different aspects of tumour growth or tumour types remains, as yet, unknown. Isolating and characterising exosomes released from these two different lineages of PCa cells created an opportunity to assess the profile of exosomes and to examine the potential differences in exosome number, size and content.

4.1.2 Isolation and characterisation of exosomes released from NEtD LNCaP cells

Typically, exosome isolation methods do not exclusively isolate exosomes as there is a biochemical overlap between exosomes and other EVs such as microvesicles (Li *et al.*, 2017). Exosomes can be isolated by various methods, including differential ultracentrifugation, exosome precipitation, size exclusion chromatography, ultrafiltration and density gradients (Witwer *et al.*, 2013). The most widely applied method of exosome isolation is differential ultracentrifugation where exosomes and EVs are separated by particle density, size and shape (Jeppesen *et al.*, 2014).

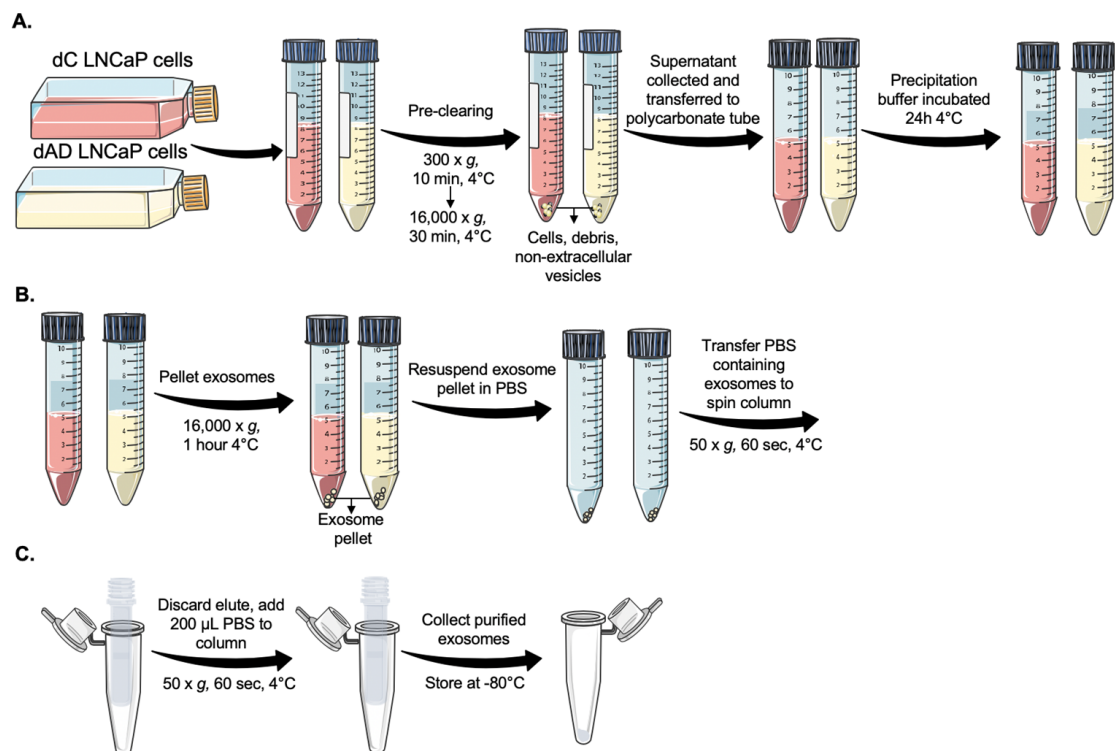


Figure 4.1: Exosome isolation, precipitation and purification. **A.** Conditioned medium is collected and pre-cleared of cells, cellular debris and non-extracellular vesicles via differential ultracentrifugation at increasing speeds and durations. Supernatant is incubated with precipitation buffer overnight. **B.** To pellet exosomes the medium and buffer mixture is ultracentrifuged. **C.** The exosome pellet is then purified via size exclusion chromatography columns. Created using Servier Medical Art by Servier.

In this research, a commercially available precipitation kit was used to isolate exosomes from cleared medium via polyethylene glycol (PEG; Figure 4.1A). Precipitated Exosomes can then be collected by centrifugation (Figure 4.1B) and purified by column chromatography (Figure 4.1C; Gurunathan *et al.*, 2019). Dynamic light scattering (DLS) was employed to provide physical characterisation and immunostaining for biochemical analysis of exosomes isolated from AD-induced NEtD LNCaP cells. DLS analyses fluctuations of scattering intensity of particles in Brownian motion to estimate particle size and concentration (Lane *et al.*, 2015). Multiple proteins such as cytosolic proteins (ALIX and Hsp70) and a transmembrane protein (CD9) were used in combination for immunoblotting to provide robust results (Théry *et al.*, 2018).

4.2 Study aim and research questions

4.2.1 Overall aim:

To isolate and characterise exosomes released from AD-induced NEtD LNCaP cells.

4.2.2 Objective:

To characterise and investigate the profile of exosomes released from control versus AD-induced NEtD LNCaP cells.

4.2.3 Research Questions:

1. Does exosome depletion of FCS/CS-FCS alter the expression of key markers of the exosomal machinery in LNCaP cells?
2. Does AD-induced NEtD of LNCaP cells alter the expression of the exosome machinery?
3. Does AD-induced NEtD of LNCaP cells increase the number of exosomes released?
4. Does the profile of exosomes released from control and AD-induced LNCaP cells differ?

4.3 Results

4.3.1 Identification of exosomal associated markers in androgen deprived LNCaP cell model

It was important to assess if exosome depletion of control and AD LNCaP cell culture conditions affected the expression of exosomal machinery markers. LNCaP cells were cultured in control (C), exosome depleted control (dC), AD or exosome depleted AD (dAD) conditions for 15 days and gene expression of exosomal machinery markers (ALIX, TSG101, RAB27A, VAMP7, and CD9) were assessed by qRT-PCR (Figure 4.2).

Expression of ALIX and TSG101, associated with sorting and packaging of cargo into intraluminal vesicles (Hessvik and Llorente, 2018), RAB27A, involved in the multivesicular body docking (Bebelmann *et al.*, 2018) and the transmembrane protein, CD9 (Witwer *et al.*, 2013) were unaffected by exosome depletion in control LNCaP cells. Expression was comparable to that in LNCaP cells grown in non-depleted control conditions (Figure 4.2A-C), suggesting that exosome depletion did not affect exosome machinery markers.

Curiously, expression of VAMP7, which induces fusion of MVBs with the plasma membrane (Mcgough and Vincent, 2016) was increased 3-fold ($p=0.4813$; not significant) in exosome depleted control conditions compared to non-depleted control conditions. There was considerable variability in VAMP7 expression in exosome depleted control LNCaP cells therefore, it is not certain induction of VAMP7 was the result of exosome depletion (Figure 4.2B).

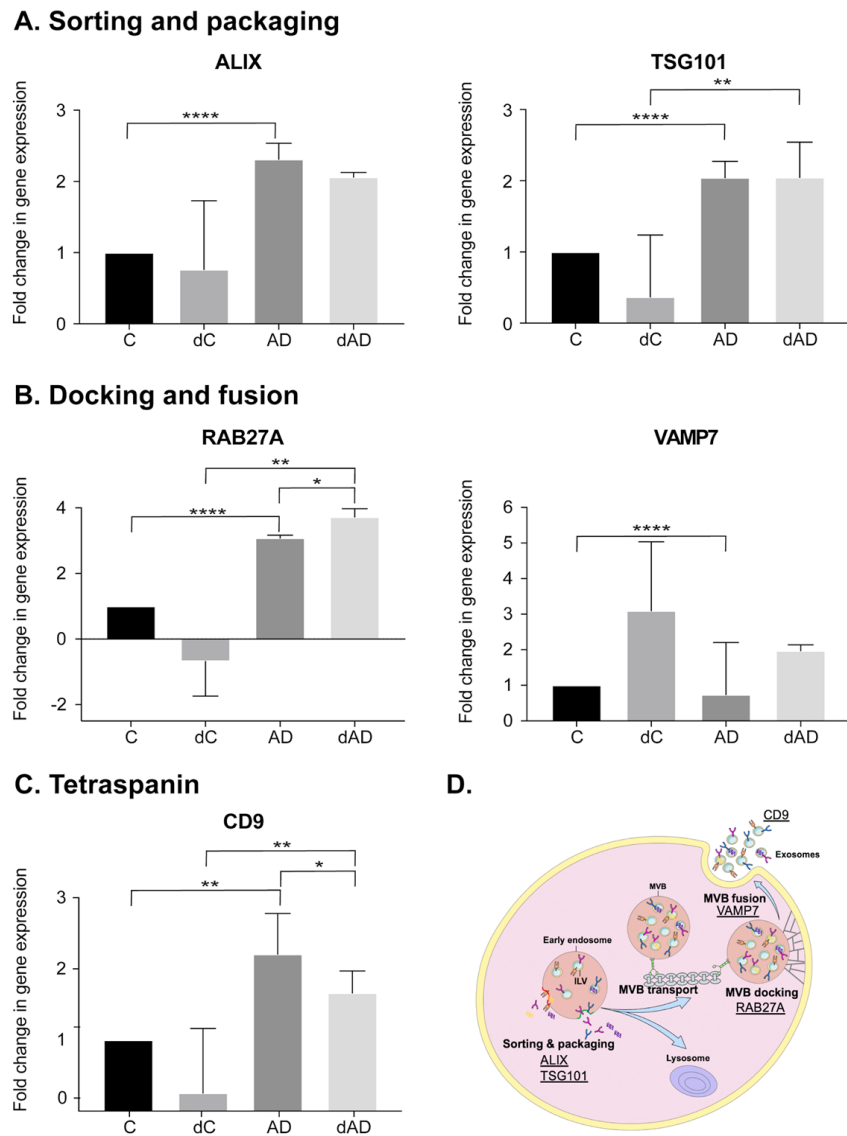


Figure 4.2: Assessing the effect of exosome depletion on expression of exosomal markers in NEtD LNCaP cells. Cells were grown in control (C), exosome depleted control (dC), androgen deprived (AD) or exosome depleted androgen deprived (dAD) conditions for 15 days, RNA was extracted and relative expression of **A.** Markers of sorting and packaging (ALG-2-interacting protein X (ALIX) and tumour susceptibility gene 101 (TSG101)). **B.** Markers of docking and fusion (Ras-associated binding protein 27A (RAB27A) and MVB vesicle associated protein 7 (VAMP7)). **C.** Tetraspanin, CD9 were assessed by qRT-PCR. Data were analysed by Ct and normalised to the geometric mean of ACTB, GAPDH and RPL13A to obtain the fold change in gene expression. Data are expressed as the mean \pm SEM (n=3) and were analysed by one-way ANOVA and Tukey's *post hoc analysis*; * $p < 0.05$, ** $p < 0.01$, **** $p < 0.0001$. **D.** Schematic diagram highlighting the location of exosomal genes in exosome biogenesis.

By contrast, ALIX (2.31-fold; $p < 0.0001$), TSG101 (2.04-fold; $p < 0.0001$), RAB27A (3.08-fold; $p < 0.0001$), VAMP7 expression (1.62-fold; $p < 0.0001$) and CD9 (2.2-fold; $p = 0.0032$); were significantly increased in AD LNCaP cells compared to control LNCaP cells (Figure 4.2A-C), suggesting AD conditions induce the expression of the exosomal machinery in LNCaP cells.

Gene expression was analysed in exosome depleted AD LNCaP cells. Like control conditions, exosome depletion of AD medium had little effect on the expression of the exosomal machinery as expression was comparable to exosome rich AD conditions. Confirmed by gene expression of ALIX (2.06-fold; $p = 0.5203$), TSG101 (2.04-fold; $p = 0.9880$) and VAMP7 (1.97-fold; $p = 0.1545$); (Figure 4.2A-B). Interestingly, exosome depletion of AD did alter RAB27A (3.72-fold; $p = 0.0145$) and CD9 (1.66-fold; $p = 0.0158$), suggesting that a combined effect of AD and exosome depletion affects expression of these exosome machinery markers.

Together, this shows that exosome depletion did not alter the expression of exosome machinery. Curiously, LNCaP cells exposed to AD or exosome depleted AD conditions had induced expression of exosome machinery markers. Therefore, induction of exosome machinery may increase exosome production in AD-induced NEtD LNCaP cells. From herein, all samples and analysis were performed on exosome depleted control and exosome depleted AD samples as the depletion process did not affect LNCaP cells.

4.3.2 Identifying the presence of exosomes isolated from AD-induced NEtD LNCaP cells

The impact of AD on the number of exosomes released from AD LNCaP cells was analysed using DLS (Figure 4.3). Control and AD LNCaP cells were grown for 7 days and the conditioned culture medium was collected for the isolation of exosomes. Previously, LNCaP cells were cultivated in AD conditions for 15 days prior to gene expression analysis, here, LNCaP cells were only exposed to AD for 7 days. This time point was used as NEtD is actively in process therefore, exosomes isolated here would be reflective of this time point. DLS analysis shows

control and AD samples contain a heterogeneous population of particles samples (Figure 4.3A). The presence of two peaks suggests two populations of EVs, one at 30-100 nm thought to represent exosomes (Mcgough and Vincent, 2016) and one at 100-1000 nm thought to represent microvesicles (Doyle and Wang, 2019).

The average diameter of exosomes isolated from control LNCaP cells was 42.38 nm and this increased to 66.59 nm in AD LNCaP cells (Figure 4.3B). The average width of exosome isolated from control LNCaP cells was 8.02 nm and increased to 14.38 nm in AD LNCaP cells (Figure 4.3C). Interestingly, the average percentage of exosomes isolated from control cells increased from 13.9 % in exosome depleted cells to 21.63 % in AD cells (Figure 4.3D). These results indicate AD of LNCaP cells increases the size and number of exosomes produced.

Microvesicles isolated from control conditions had an average diameter of 362.2 nm, which increased to 457.25 nm in AD conditions (Figure 4.3E). The average width of microvesicles released from control LNCaP cells was 85.86 nm and increased to 103.62 in AD LNCaP cells (Figure 4.3F). In line with the observed increase in exosomes isolated from AD LNCaP cells, the average percentage of microvesicles decreased to 78% in AD LNCaP cells from 86% from control LNCaP cells (Figure 4.3G). AD conditions marginally increased microvesicle size and microvesicle production was decreased as exosome production increased.

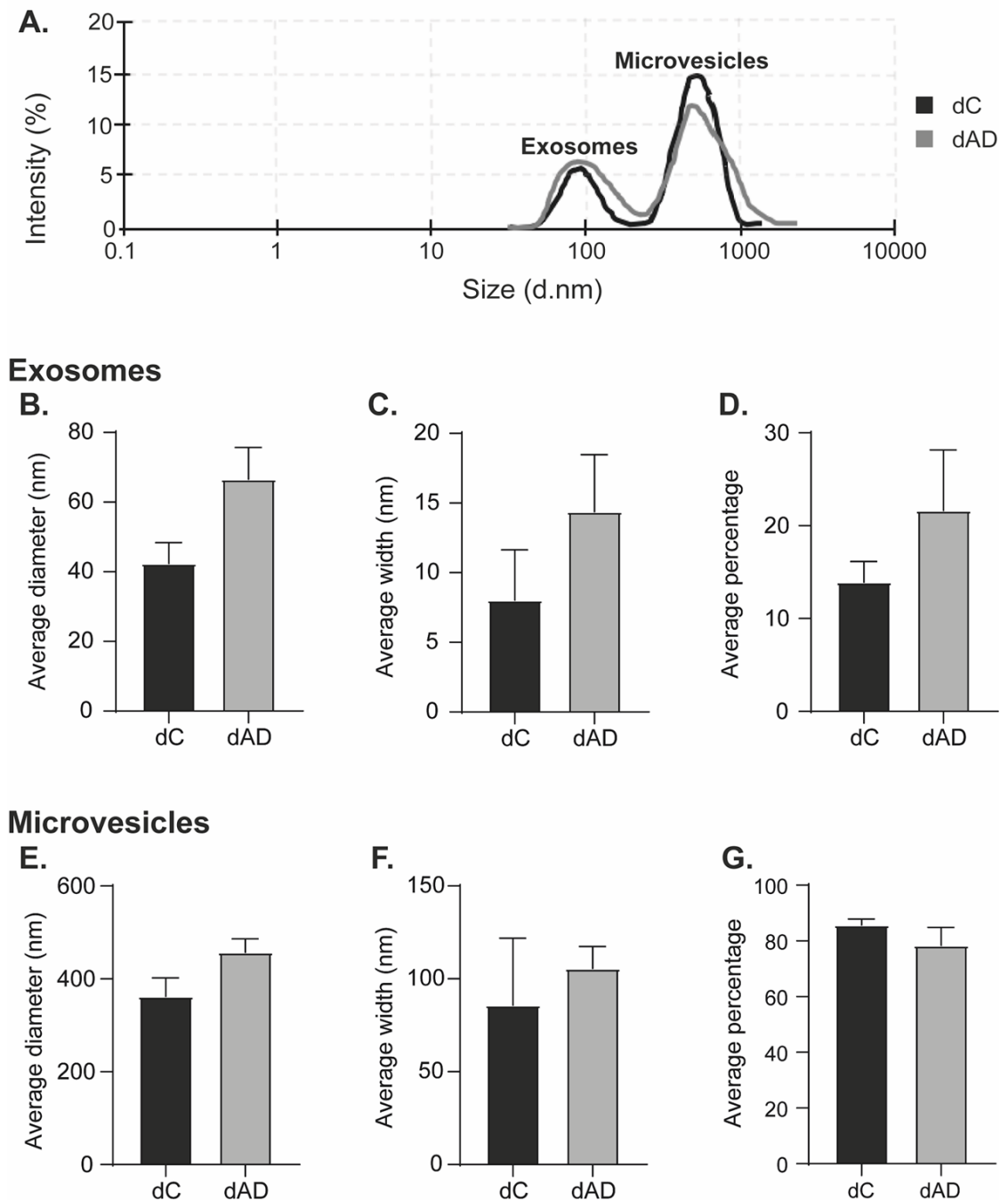


Figure 4.3: Analysing the profile of extracellular vesicle populations secreted by AD LNCaP cells. Conditioned medium from exosome depleted control (dC) and exosome depleted AD (dAD) LNCaP cells was collected after 7 days and exosomes isolated. **A.** Representative example of the profile of populations isolated from dC and dAD LNCaP cells showing peaks corresponding to exosomes and microvesicles. The profile of the vesicles was analysed by DLS assessing the average diameter (**B** and **E**), width (**C** and **F**) and overall percentage (**D** and **G**) of exosomes, (**B-D**) or microvesicles (**E-G**). Data are expressed as the mean \pm SEM (n=3) and were analysed by Welch's t-test.

4.3.3 Analysing exosomes isolated from AD-induced NEtD LNCaP cells

The profile of exosomes isolated from control and AD LNCaP cells were analysed using known exosome markers (ALIX, Hsp70 and CD9) via immunoblotting. Radioimmunoprecipitation assay (RIPA) buffer is the most common method of exosome lysis as it allows identification of the highest number of exosomal proteins (Subedi *et al.*, 2019). LNCaP cells were used as a positive comparator as these were the source of exosomes. Cells were lysed with NP-40 buffer as this was the standard lysis method used here.

In control LNCaP cells two bands corresponding to ALIX were detected, at ~95 kDa and a very faint band at ~90 kDa (Figure 4.4B, lane 2). Expression of both bands was increased in AD LNCaP cells (Figure 4.4B, lane 3), in line with the observed increase in ALIX gene expression in AD LNCaP cells (Figure 4.2A). The 95 kDa ALIX protein was identified in exosomes isolated from control LNCaP cells, however, was undetectable in exosomes isolated from AD LNCaP cells (Figure 4.4B, lane 5). Hsp70 was detected in control LNCaP cells and expression remained consistent in AD LNCaP cells (Figure 4.4C, lane 2 and 3 respectively). Hsp70 was also detected in exosomes isolated from control cells however, expression was very faint in AD LNCaP-derived exosomes (Figure 4.4C, lane 5). To detect CD9, non-reducing and non-denaturing conditions are required as this is a transmembrane protein (Andreu and Yáñez-Mó, 2014). There was a small but noticeable increase in CD9 expression in AD LNCaP cells compared to control LNCaP cells (Figure 4.4D, lane 3), in line with gene expression data (Figure 4.3C). CD9 was identified in exosomes isolated from control cells and expression was comparable to the control cell lysate. Expression of CD9 was not clear in exosomes isolated from AD LNCaP cells as a faint and distorted protein was identified. Low exosomal protein yield limited analysis of the profile of exosomes isolated from cells. These data indicate AD of LNCaP cells induces exosome machinery proteins however, the experiment should be repeated to ensure the loading control supports these findings. These data do, however, show that AD of LNCaP cells induces expression of exosome machinery proteins.

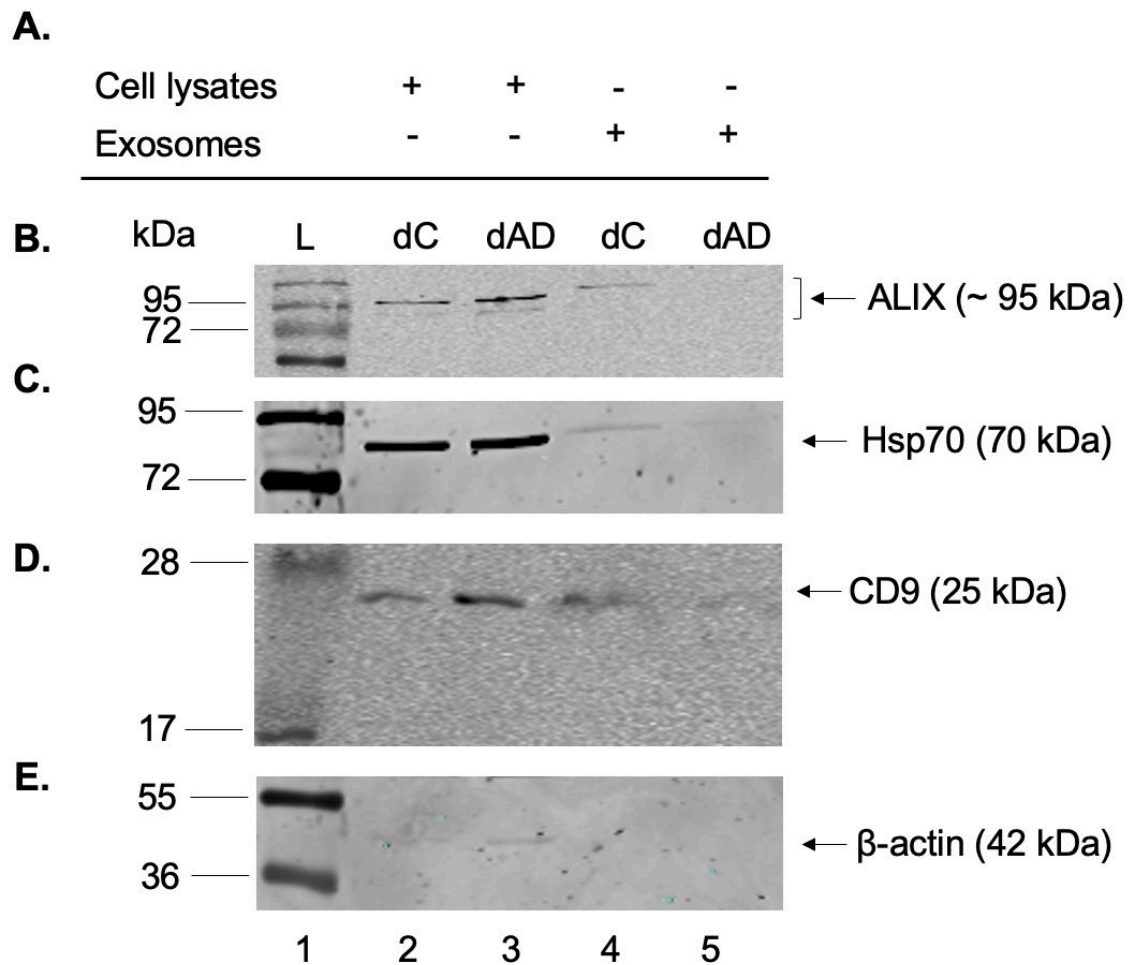


Figure 4.4: Analysing the profile of markers of exosomes isolated from control and AD LNCaP cells. Representative immunoblot analysis (n=3) showing protein expression in exosomes isolated from exosome depleted control (dC) and exosome depleted AD (dAD) after 7 days. dC and dAD cells were grown for 15 days and used as a control. Panel **A** shows a schematic description of the samples present in each lane; the first two samples were prepared with NP-40 lysis buffer whilst the last two lanes were prepared with 1X RIPA lysis buffer. Expression of known markers ALG-2-interacting protein (ALIX; **B**), heat shock protein 70 (Hsp70; **C**) and CD9 (**D**) were analysed by immunoblotting. CD9 analysis was performed in non-denaturing and non-reducing conditions. Molecular weights are indicated, and equal loading was assessed by β -actin (**E**).

4.3.4 Characterising exosomal machinery markers in AD-induced NEtD LNCaP cells

Results obtained from exosomal protein analysis were inconclusive due to the low exosomal protein yield (0.06 $\mu\text{g}/\mu\text{L}$) and subsequent loading of 3.6 μg of exosome protein was insufficient and limited this avenue of research. To overcome this, the profile of exosomal machinery (ALIX, Hsp70, CD9) in control and AD LNCaP cells was analysed via immunoblotting. It was hypothesised that changes in exosome machinery, could reflect changes in the number of exosomes released from LNCaP cells. It was important to optimise lysis conditions first to ensure protein detection therefore, NP-40 and 1X RIPA buffers were used.

Using NP-40 lysis conditions, ALIX expression was increased between control and AD LNCaP (Figure 4.5A, lane 2 and 4 respectively) and expression of Hsp70 increased marginally in AD LNCaP cells compared to control (Figure 4.5B, lane 4 and 2 respectively). Intriguingly, expression of CD9 was considerably increased in AD LNCaP cells compared to control LNCaP cells (Figure 4.5C, lane 4 and 2 respectively). These data are in line with observed increase in gene expression under AD conditions (Figure 4.2), demonstrating that AD conditions induce genes involved in sorting and packaging (ALIX), chaperone (Hsp70) and transmembrane (CD9) exosomal machinery markers.

When LNCaP cells were lysed with RIPA buffer ALIX, Hsp70 and CD9 expression was increased in AD LNCaP cells compared to control LNCaP cells however, detection of ALIX, Hsp70 and CD9 in control and AD LNCaP cells was considerably reduced compared to samples prepared with NP-40 lysis buffer. It was notable that when LNCaP cells were lysed with RIPA buffer the considerable increase of CD9 in AD conditions was not seen, suggesting the lysis condition masked the AD-dependent increase in CD9 expression (Figure 4.4C, lane 4).

Together, these data indicate that AD induced expression of proteins associated with sorting and packaging of exosomal cargo, chaperone proteins and

transmembrane proteins. It is anticipated an increase of these markers in AD LNCaP cells, correlated to induced exosome production, as the exosome profile could not be investigated due to insufficient material.

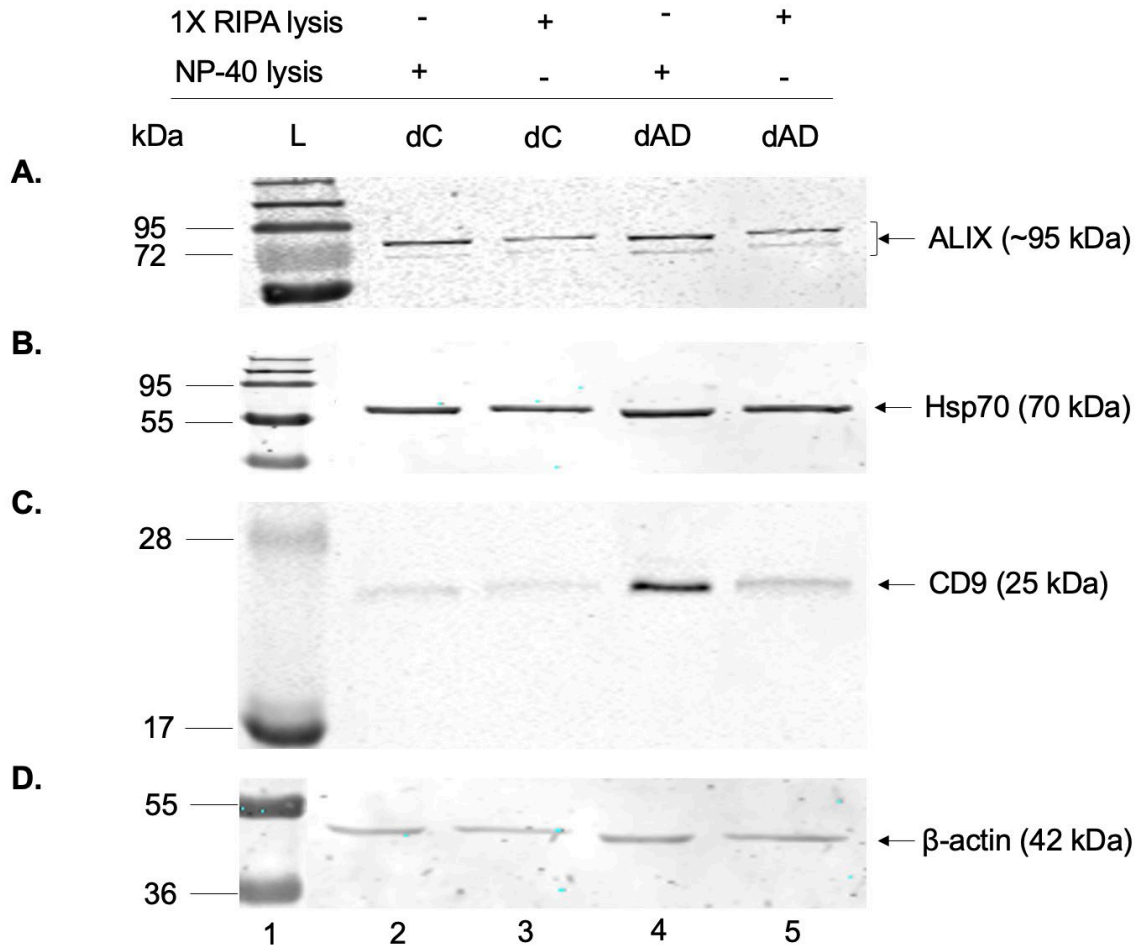


Figure 4.5: Analysing exosome machinery in LNCaP cells. Representative immunoblot analysis (n=2) showing protein expression in LNCaP cells cultured in exosome depleted control (dC) and exosome depleted androgen deprived (dAD) conditions for 15 days. dC and dAD LNCaP cells were lysed in either 1X radioimmunoprecipitation (RIPA) or a NP-40 lysis buffer. Expression of known markers ALG-2-interacting protein (ALIX; **A**), heat shock protein 70 (Hsp70; **B**) and CD9 (**C**) were analysed by immunoblotting. CD9 analysis was performed in non-denaturing and non-reducing conditions. Molecular weights are indicated and equal loading was assessed by β -actin (**D**) or Hsp70 (**B**) for non-denaturing, non-reducing conditions.

4.4 Discussion

The aim of this chapter was to isolate and characterise exosomes from AD-induced NEtD LNCaP cells. Before investigating exosomes released from AD LNCaP cells, it was important to ascertain the effect of exosome depletion on key exosome machinery markers as the effect, if any, was undocumented. Gene expression data revealed exosome depletion did not affect expression of key exosome machinery markers (ALIX, TSG101, RAB27A, VAMP7 and CD9) however, AD conditions induced expression of these markers. Exosomes were successfully isolated and DLS showed that AD increased the size and number of exosomes isolated from LNCaP cells. Microvesicles were also isolated, and AD slightly increased their size however, the number of microvesicles decreased in AD with concurrent increase in exosomes. Together, these data suggest that AD of LNCaP cells induced expression of exosome machinery and this, in turn, increased exosome production.

4.4.1 The potential role of exosomes in PCa and NEtD

Exosomes are involved in cellular communication by either inducing signals directly via surface molecules or transfer of vital proteins and/or nucleic acids to recipient cells (Patel *et al.*, 2019). Exosomes released in PCa have been linked to cellular proliferation (Soekmadji *et al.*, 2017) of treated cell and pre-metastatic niche formation via transfer of cell specific cargo (Itoh *et al.*, 2012). Of particular interest, exosomes are thought to contribute to neuroendocrine transdifferentiation (NEtD); (Lin *et al.*, 2017; Bhagirath *et al.*, 2019).

Exosomes have been shown to have a potential role in NEtD. Treatment of DU145 cells, an androgen independent cell line, with IL6, an alternative treatment to AD induces NEtD via peroxisome proliferator activated receptor gamma and adipocyte differentiation-related protein (Lin *et al.*, 2017). Exosomes isolated from IL6 treated DU145 cells were added to un-treated DU145 cells, increasing the number of adipocyte differentiation-related protein positive cells (Lin *et al.*, 2017). These findings by Lin *et al.* (2017) indicate that proteins associated with AD-induced NEtD in LNCaP cells could be packaged as cargo and transferred to

untreated LNCaP cells to induce NEtD. Treatment of a non-malignant prostate epithelial cell line, RWPE1 with exosomes derived from IL6 treated DU145 cells induced dendrite-like extensions; a feature of NEtD (Lin *et al.*, 2017). This reveals the ability of exosomes to induce NEtD in neighbouring cells in a paracrine manner by the sorting and transfer of adipocyte differentiation-related protein (Lin *et al.*, 2017). This research demonstrates the potential for exosomes to package and transfer NEtD associated cargo to neighbouring PCa cells to drive NEtD, a feature of tumour progression in these cells, providing evidence of the involvement of exosomes in driving neuroendocrine tumour progression.

4.4.2 PCa exosomes and associated cargo

Pro-neuronal transcription factors associated with NEtD of PCa, BRN2 and BRN4, were upregulated in EVs released from CRPC-neuroendocrine xenografts compared to CRPC-adenocarcinoma xenografts (Bhagirath *et al.*, 2019). These data suggest that exosomes released from cells of a different lineage, such as epithelial control and AD LNCaP cells may contain and transfer different cargo to neighbouring cells to propagate NEtD. Enzalutamide, an androgen receptor inhibitor, was used to treat LNCaP cells. Exosomes released from Enzalutamide treated cells were isolated and added to non-treated LNCaP cells, which caused induction of BRN2, BRN4 and neuronal genes chromogranin A and synaptophysin (Bhagirath *et al.*, 2019). This finding demonstrates horizontal transfer of these mRNA to neighbouring cancer cells and dissemination of factors associated with NEtD. Although EVs were isolated from xenografts rather than LNCaP cells, an increased size and number of exosomes were released by CRPC-neuroendocrine xenografts compared to CRPC-adenocarcinoma (Bhagirath *et al.*, 2019). Supporting data in this chapter, which showed increased exosome size and number in AD LNCaP cells compared to control LNCaP cells (Figure 4.3A-D). Enzalutamide resistant LNCaP cells released EVs with significantly increased BRN2 and BRN4 mRNA (Bhagirath *et al.*, 2019), these could act as an adaptive mechanism for PCa cells to survive under selective pressure of AR pathway inhibitors (Bhagirath *et al.*, 2019). Therefore, it is possible that AD induced NEtD LNCaP cells may release exosomes containing

different cargo than epithelial control LNCaP cells, and these exosomes may confer growth and survival advantages to neighbouring PCa cells.

Enrichment of proteins in EVs induced cellular proliferation of PCa cells (Soekmadji *et al.*, 2017). LNCaP cells treated with dihydrotestosterone (DHT), a potent androgen, released CD9 enriched EVs. AD cells were treated with CD9 enriched LNCaP-derived exosomes, which induced cellular proliferation of AD LNCaP cells independent of DHT (Soekmadji *et al.*, 2017). These data are of particular interest as it aligns with the data in this research, which showed that CD9 mRNA (Figure 4.2C) and protein (Figure 4.5C) expression was increased in LNCaP cells grown in AD conditions. Soekmadji *et al.* (2017) showed LNCaP cells grown in AD conditions had an increased EV yield 3-fold concomitant with an ~8 % increase in EV yield in AD conditions in research in this chapter. Interestingly EVs were larger (120 nm) compared to exosomes analysed in this chapter (66.59 nm; Figure 4.3B). However, depending on the isolation method different populations of EVs can be isolated from the same cells (Ludwig *et al.*, 2019). Differential ultracentrifugation was used by Soekmadji *et al.* (2017) whereas, precipitation with size exclusion chromatography was used in this research. Therefore, differences in EV size may be attributed to the isolation method.

Following AD CD9 expression was considerably increased (Figure 4.5C), which may be linked to increased production and release of exosomes. It has been shown that exosomes isolated from patients with advanced and CRPC exhibited higher CD9 expression than those with non-metastatic PCa or healthy volunteers (Mizutani *et al.*, 2014). Thus, the more aggressive the cancer the higher the concentration of exosomes (Mizutani *et al.*, 2014), which is in line with data presented here showing AD LNCaP cells have greater expression of CD9 compared to control LNCaP cells. In the prostate, CD9 may be involved in ligand-independent activity of AR, which when activated, could regulate AR activity (Levina *et al.*, 2015). CD9 is also considered to be a metastasis inhibitory factor (Zöller, 2009) therefore, during AD, where cells are progressing to a NE phenotype, CD9 may be upregulated to prevent metastasis. Data suggests that CD9 is implicated in PCa in various ways and that increased CD9 mRNA and

protein expression in AD LNCaP cells is a means of regulating exosome production, the AR and metastasis.

Significant upregulation of RAB27A, essential for docking of multivesicular bodies at the plasma membrane, was identified in exosome depleted AD conditions (Figure 4.5B), which has not been previously described. Interestingly, overexpression of RAB27A is implicated in promoting cell proliferation, enhancing cell invasion, and increasing chemoresistance of cancer (Hendrix and de Wever, 2013) such as breast cancer (Hendrix *et al.*, 2010), bladder cancer (Ostenfeld *et al.*, 2014), lung adenocarcinoma (Li *et al.*, 2014) and melanoma (Peinado *et al.*, 2012). It could be postulated that exosome depletion in combination with AD upregulates RAB27A expression to promote tumorigenesis.

Exosomes released by LNCaP cells were shown to transfer cargo to cells of a different lineage (Read *et al.*, 2017). This underlines the importance of investigating the profile of epithelial (control) and NE-like (AD) LNCaP cells, to determine if exosomes released from NE-like cells could promote NEtD of epithelial cells in the tumour microenvironment. AR packaged in exosomes released by LNCaP cells was transferred to AR-null PC3 cells (Read *et al.*, 2017). The AR was shown to be functional through translocation to the nucleus and activation of target genes such as prostate specific antigen (PSA), showing functional receptors in EVs can be transported to the nucleus of adjacent cells to modulate expression of responsive genes (Read *et al.*, 2017). This is of importance as such mechanisms may prompt cells of one lineage to engage with another, generating an appropriate microenvironment for tumour growth and survival. Therefore, as there are differences in the number and profile of exosomes released from control and AD LNCaP cells, these exosomes may confer advantages for NEtD and subsequent aggressive tumour expansion.

4.4.3 PCa exosomes and pre-metastatic niche formation

In addition to communication within the tumour microenvironment, it is thought exosomes can promote pre-metastatic niche formation. Prostate tumours are

prone to metastasise to bone and have substantial crosstalk with bone cells in the bone microenvironment (Ibrahim *et al.*, 2010). Exosomes isolated from hormone refractory PCa cells could facilitate osteoblast differentiation (Itoh *et al.*, 2012). Osteoblast differentiation associated transcription factor, Ets1, was highly expressed in PC3 and DU145-derived exosomes and osteoblast differentiation was induced by culture of exosomes containing Ets1 with osteoblasts. Osteoblastic differentiation was also seen in murine pro-osteoblastic MC3T3-E1 cells cultured with PC3 and DU145-derived exosomes (Itoh *et al.*, 2012). This supports the link between exosome release and ability to cause metastatic organotropism to the bone (Roudier *et al.*, 2003). Therefore, exosomes can contribute to the formation of the pre-metastatic niche as oncogenic proteins enclosed in exosomes can spread to adjacent tissues and be taken up by organ specific cells (Pan *et al.*, 2017). These data could suggest that culture of NE-like LNCaP-derived exosomes with osteoblasts could promote metastasis.

4.4.4 PCa exosomes and cellular stress

Cancer cells are frequently exposed to chemotherapy, radiation and the host immune system where cellular stress responses are crucial for their survival (Xu *et al.*, 2018). Rotenone-induced mitochondrial damage increases exosome release from PCa stem cells, it is possible that cellular stress induced by AD may also increase exosome release (Kumar *et al.*, 2014). PCa stem cells were treated with Rotenone, which induced CD9, CD61, CD81 and TSG101 mRNA in exosomes released from these cells (Kumar *et al.*, 2014). However, expression of these exosome machinery markers was only assessed in exosomes released from PCa stem cells and did not include assessment of these markers in the cells. Therefore, increased exosomes in circulation may enhance the potential for greater PCa progression via the exchange of cargo from NE-like cells and promotion of NEtD.

Androgen-mediated autophagy is known to promotes cell growth by augmenting intracellular lipid accumulation, shown to be necessary for PCa cell growth (Shi

et al., 2013). Interestingly, there is an overlap of several proteins, which are associated with exosome biogenesis and autophagy such as components of the ESCRT and SNAREs (Gudbergsson and Johnsen, 2019). Exosome release is also known to be upregulated in PCa patients compared to healthy individuals, which suggests that there is the potential for the AR to influence EV biogenesis (Hessvik and Llorente, 2018).

4.4.5 Exosomes as biomarkers in PCa

Prostate Specific Antigen (PSA) is a clinically useful protein biomarker for diagnosis of PCa, however, PSA has a poor sensitivity and specificity and is known to have a high risk of overdiagnosis and overtreatment (Duijvesz *et al.*, 2013). To prevent unnecessary invasive prostate biopsies, provide patients with optimal treatment and discriminate between benign prostate diseases and the different types of PCa, novel molecular biomarkers are urgently needed (Duijvesz *et al.*, 2013). The first exosome-based cancer diagnostic blood test became commercially available in 2016 for non-small cell lung cancer patients and it is hoped this test can be diversified for other cancers (Sheridan, 2016).

Non-invasive detection of nucleic acids such as miRNAs via liquid biopsy have been shown to be promising biomarkers for PCa to differentiate PCa types, benign prostate hyperplasia and healthy individuals and enhances therapeutic efficiency (Tai *et al.*, 2020). EVs from serum of recurrent PCa patients showed upregulation of miR-141 and miR-375 compared to patients with non-recurrent PCa, providing a potential diagnostic tool to distinguish these PCa types (Bryant *et al.*, 2012). Circulating exosomes isolated from PCa patients undergoing radiotherapy displayed differential expression of miRNAs (miR21 and let-7) induced by radiotherapy (Malla *et al.*, 2018). High expression of exosomal miR-1246 was specifically observed in stage IV metastatic PCa patients as compared to Stage II/III (Bhagirath *et al.*, 2018). More recently, the neuronal transcription factors BRN2 and BRN4 were upregulated in exosomes from PCa patients with neuroendocrine features opposed to PCa patients with adenocarcinoma features (Bhagirath *et al.*, 2018). Thus, investigating exosomes released from AD-induced

NEtD LNCaP cells provides an important avenue to contribute to the use of exosomes as biomarkers for PCa. Further investigation of exosomes released from control and AD LNCaP cells could provide invaluable information regarding the use of exosomes as biomarkers for PCa, identifying the stage of PCa, treatment response or for therapeutic intervention.

4.4.6 The impact of methodology on exosome isolation

This research implemented exosome depletion of cell culturing conditions to ensure low background interference of exosomes from FCS. Gene expression of exosomal machinery markers was analysed to investigate the effect exosome depletion may have on these genes. Exosome depletion of control or AD conditions did not impact the expression of the exosome machinery markers ALIX, TSG101, RAB27A and CD9. There is a notable gap in the literature with regard to the effect of exosome depletion on AD-induced NEtD as researchers do not investigate the impact of culturing conditions upon markers associated with exosome biogenesis and release in exosome source cells. The lack of evidence prompts caution when interpreting data. Primarily research is focused on exosome cargo therefore, there is a distinct lack of analysis performed at a cellular level to make comparisons between the releasing cells and exosomes.

ISEV detailed recommendations in the MISEV18, which cover EV separation, isolation, characterisation and functional studies, encouraging consistency and comparability between research groups (Théry *et al.*, 2018). When characterising exosomes, recommendations outlined by MISEV18 state that quantification methods provide the most valuable information when separation methods with highest expected specificity are used and, therefore, when high recovery low specificity methods are used (e.g. precipitation) more than one quantification method should be employed (Théry *et al.*, 2018). MISEV18 also highlights that including source cell and exosome data is important for robust analysis (Théry *et al.*, 2018). It is possible that exosome depletion can remove essential proteins and growth factors, which may decrease growth-promoting effects and cause cellular stress (Ludwig *et al.*, 2019). Cells exposed to cellular stresses such as

irradiation and hypoxia release an increased number of exosomes and cargo can differ between normal and stress states (Hessvik and Llorente, 2018). Therefore, investigating exosome machinery prior to and following exosome depletion would reveal if the release of exosomes is influenced by potential cellular stress induced by exosome depletion.

In this research, precipitation combined with size exclusion chromatography was used to isolate exosomes from LNCaP cells, which aligned with research by others in the field (Welton *et al.*, 2015; Malla *et al.*, 2018; Wang *et al.*, 2019). Despite successful exosome isolation revealed by DLS, quantification of exosomes by Bradford assay showed exosomal protein yield was very low (0.06 $\mu\text{g}/\mu\text{L}$), resulting in inconclusive characterisation. This was a problem as there was insufficient exosome material for exosome analysis. Others have compared exosome isolation methods to investigate exosome yield and purity (Lane *et al.*, 2015; Soares Martins *et al.*, 2018). A combined method of precipitation and size exclusion chromatography was compared to single methods of precipitation and ultracentrifugation, which showed that combined precipitation and size exclusion chromatography produced the highest exosome yield and purity (Lane *et al.*, 2015; Soares Martins *et al.*, 2018). However, analysis was performed using serum and plasma patient samples as opposed to cell lines and only required 200 μL of starting material. Tang *et al.* (2017) showed that 100 mL of culture medium from A459 cells (lung cancer) was required to produce 50 μg of exosomal protein. The volume of starting material in this research was 20 mL, which produced 3.6 μg of exosomal protein, it is possible that doubling the volume would have increased the amount of protein however, this was not feasible due the high cost of CS-FCS required for culture medium.

Guidance from the manufacturer of the exosome precipitation kit suggested that further elution of the chromatography column would result in co-elution of ribonucleoprotein particles and protein from culture conditions therefore, contaminating the sample. As much as a further elution step may increase yield, it would decrease the purity of the exosome sample therefore, the decision was taken to not include a further elution step. It is also possible that adhesion of

exosomes to polycarbonate bottles may have attributed to low exosome yield as multiple of these were required for the preparation of one sample. The resuspension of exosomes in a small volume (100 μ L) meant it was difficult to ensure all exosomes were collected from the bottles therefore, contributing to a further loss of exosome yield. In future work implementing measures to increase the volume of starting material of exosomes should allow increased exosome yield and better characterisation of exosomes released from control and AD LNCaP cells.

4.4.7 Characterisation of exosomes released from NEtD LNCaP cells

Characterisation of exosomes should be performed by analysing physical and biochemical/compositional properties of exosomes (Doyle and Wang, 2019). Dynamic light scattering (DLS) was used to provide an understanding of exosome size and concentration. However, when there is a heterogeneous mix of particles in the sample, scattered light by smaller particles is harder to detect and can skew data towards larger particles therefore, DLS may underestimate the concentration of exosomes in the sample (Lane *et al.*, 2015). It could mean that the concentration of exosomes was higher than the concentration provided by the DLS. Data obtained from this method of characterisation should, therefore, be used with caution and it should be acknowledged that improvements to analysis may provide more robust results. Recommendations by MISEV18 also suggest that complementary techniques should be used for physical characterisation such as nanoparticle tracking analysis (NTA) and transmission electron microscopy (TEM); (Théry *et al.*, 2018). Like DLS, NTA uses light scattering technologies however, is able to provide more accurate sizing information amongst heterogeneous populations by using antibody mediated fluorophore labelling of exosomes with a fluorescent laser (Théry *et al.*, 2018). Carnell-Morris *et al.*, (2017) detailed a protocol, which used a mouse monoclonal Qdot-conjugated antibody to detect placental EVs, the antibody was specific for the syncytiotrophoblast marker placental alkaline phosphatase. TEM creates an image by electron interference when an electron beam crosses the sample, allowing visualisation and image capture for measurement of isolated particles

(Szatanek *et al.*, 2017). As DLS only provides accurate results for monodisperse populations following recommendations by MISEV18 and implementation of NTA and TEM in future work would ensure robust analysis of the size and concentration of particles isolated from control and AD LNCaP cells (Théry *et al.*, 2018).

4.4.8 Biochemical analysis of exosomes released from NEtD LNCaP cells

Typically, exosome analysis is performed using immunoblotting staining or proteomic analysis (Gurunathan *et al.*, 2019). Wide accessibility and detection of surface and internal exosomal proteins explains why immunoblotting is one of the most commonly used methods of biochemical analysis (Doyle and Wang, 2019). However, immunoblotting comes with its limitations as large amounts of exosomal protein often are required to provide a minimal amount of information (Doyle and Wang, 2019). The results obtained from immunoblotting were inconclusive, due to low exosomal protein yield and therefore, restricted how much protein could be resolved and analysed. The selection of an appropriate buffer for exosome lysis can be challenging as the number of proteins identified varies depending on the cell type and isolation method used (Hosseini-Beheshti *et al.*, 2012). Low protein yield and inconclusive immunoblot results prompted the comparison RIPA and NP-40 buffer for cell lysis of control and AD LNCaP cells. RIPA buffer is the most commonly used method of exosome protein isolation as it allows the identification of the highest number of exosomal proteins (Subedi *et al.*, 2019). However, NP-40 lysis of control and AD LNCaP cells showed more intense protein expression of ALIX, Hsp70 and CD9 compared to RIPA buffer, which appeared to reduce protein recovery of ALIX, Hsp70 and CD9. The chemical composition of RIPA buffer makes this a much stronger detergent that may compromise protein integrity and conformation sites where antibodies would bind, resulting in potential underestimated protein expression or mistaken for a change in expression (Ji, 2010). Therefore, for accurate analysis of protein expression, the lysis condition to best analyse proteins of interest should be considered. It is no-

table that protein analysis was conducted in cell lysates and not exosomes, therefore, to characterise exosomal protein, RIPA lysis buffer is required to disrupt the lipid bilayer (Subedi *et al.*, 2019).

MISEV18 suggests that when immunoblot analysis is performed proteins should be used to demonstrate the presence of exosomes such as transmembrane (CD9) and cytosolic (ALIX and Hsp70); (Théry *et al.*, 2018). In future, the addition of major components of non-EV co-isolated proteins such as albumin should be included in immunoblot analysis to evaluate the degree of purity of the EV preparation. Results obtained demonstrated exosomes were successfully isolated from LNCaP cells and visible differences were identified in exosome and microvesicle populations in control and AD conditions. However, improving methods to increase the yield of exosomes will allow improved characterisation of the profile of exosomes released from control and AD LNCaP cells.

4.5 Conclusion

This research aimed to identify if exosome depletion and AD of culture conditions affected exosomal machinery markers in LNCaP cells. Also, to characterise the profile of exosomes released from control and AD LNCaP cells. It is unknown what role, if any, exosomes play in NEtD of cells in the prostate tumour microenvironment. Exosome depletion, in combination with AD, affected RAB27A and CD9 gene expression however, all other markers were unaffected. Interestingly, gene expression data showed induction of exosomal machinery markers under AD and exosome depleted AD culture conditions. Exosomes were successfully identified by DLS, revealing an increased size and number of exosomes and microvesicles released from exosome depleted AD LNCaP cells. Assessment of protein markers saw induced expression of ALIX, Hsp70 and CD9 under exosome depleted AD conditions. Together these analyses suggest that LNCaP cells exposed to AD induced NEtD have augmented exosomal machinery markers and induced exosome production, suggesting exosomes may be implicated in NEtD of PCa and tumour progression.

5. Chapter 5: Manipulation of exosome release from control and AD-induced neuroendocrine transdifferentiated LNCaP cells

5.1 Introduction

5.1.1 The role of GW4869 in the blockade of exosome release

Exosome biogenesis is driven by ESCRT or ceramide pathways (Zhang *et al.*, 2019). The ceramide pathway is facilitated by neutral sphingomyelinases, a family of enzymes, which convert sphingomyelin into ceramide (Catalano and O'Driscoll, 2020). Sphingomyelinases are predominantly localised on the anti-cytoplasmic leaflets of the plasma membrane. Ceramide molecules spontaneously associate and tightly bind to other ceramide molecules, forming ceramide enriched membrane microdomains (Zhang *et al.*, 2009). The resultant ceramide microdomains can induce the budding and formation of interluminal vesicles into multivesicular bodies, as an early part of the exosome process (Figure 5.1; Catalano and O'Driscoll, 2020). The neutral sphingomyelinase inhibitor, GW4869 is pharmacological compound most commonly used to block the generation of exosomes (Essandoh *et al.*, 2015). GW4869 targets the neutral sphingomyelinase pathway by inhibiting ceramide-mediated inward budding of multivesicular bodies and release of mature exosomes from these multivesicular bodies (Menck *et al.*, 2017); (Figure 5.1). However, GW4869 only inhibits ceramide-mediated exosome release, not ESCRT-mediated exosome release, thus the number of exosomes produced by cells is reduced (Figure 5.1; Essandoh *et al.*, 2015).

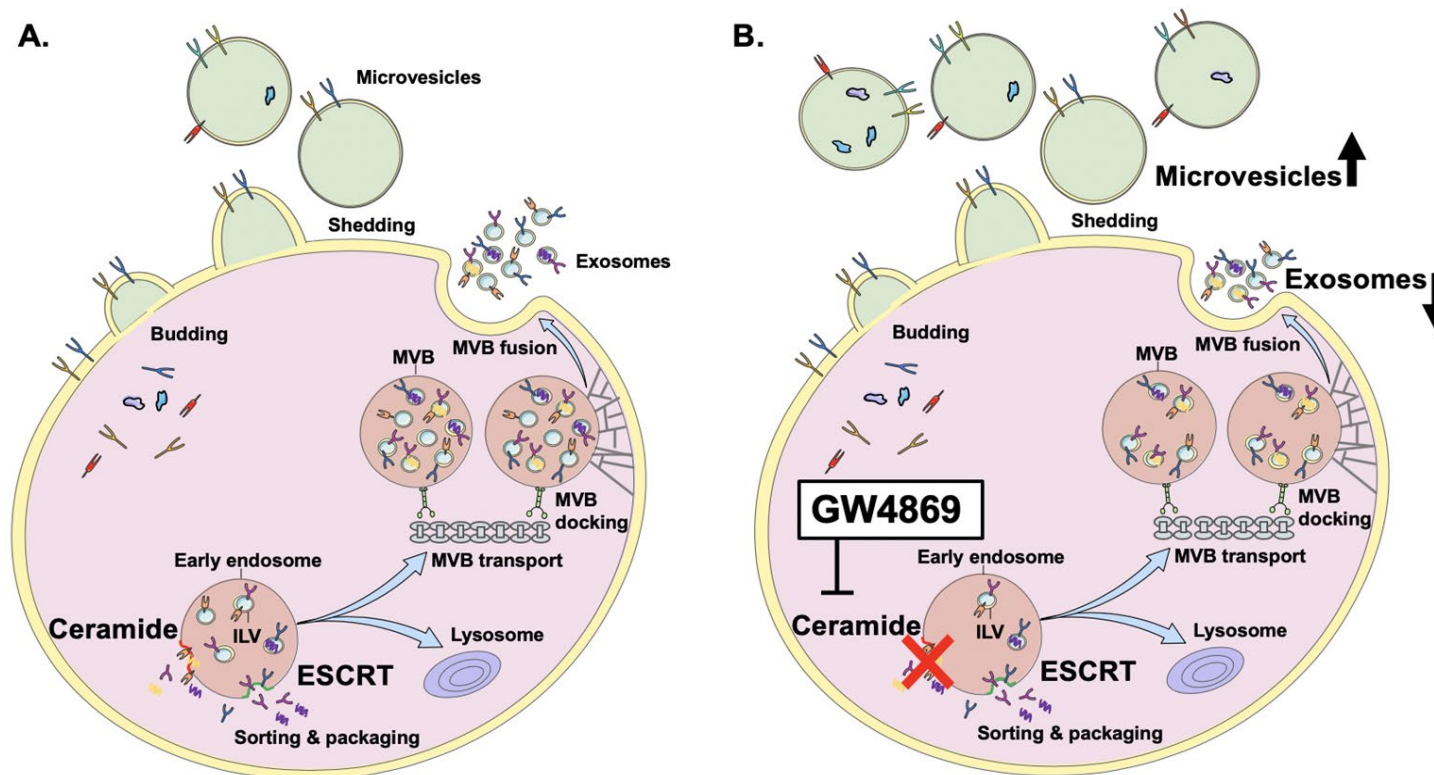


Figure 5.1: Manipulation of extracellular vesicle release via GW4869. (A) Microvesicles are formed via the budding and shedding from the plasma membrane. Exosome biogenesis occurs via ceramide and endosomal sorting complex required for transport (ESCRT) pathways, cargo is loaded in intraluminal vesicles (ILV) contained in multivesicular bodies (MVB), which are transported to and fused with the plasma membrane for exosome release. (B) The sphingomyelinase pathway inhibitor GW4869 blocks the formation and subsequent release of exosomes via the ceramide mediated exosome biogenesis pathway, which reduces exosome release and also increases microvesicle release. Created using Servier Medical Art by Servier.

In contrast to exosomes, microvesicles are generated by outward budding and fission of the plasma membrane (Menck *et al.*, 2017). While exosomes and microvesicles are released by different modes of biogenesis there are similarities in their appearance, they can overlap in size and often have a common composition, which can contribute to the challenge to ascertain their origin when isolated (Van Neil *et al.*, 2018). Interestingly, the activity of neutral sphingomyelinase is not specific to exosome biogenesis and has been linked to the increased shedding of microvesicles from the plasma membrane however, the mechanism is not yet understood but altered membrane fluidity is thought to contribute to this process (Menck *et al.*, 2017).

5.1.2 The role of Monensin in the induction of exosome release

Ionophores are a class of compounds that form complexes with cations to facilitate their transport across lipophilic membranes (Aowicki and Huczynski, 2013). The most widely studied ionophore is Monensin, a polyether antibiotic isolated from *Streptomyces cinnamonensis* (Kim *et al.*, 2016). Monensin is employed in veterinary medicine for treatment of poultry feed to control the protozoa coccidiosis or to improve food metabolism in ruminants (Aowicki and Huczynski, 2013). Treatment of coccidia with Monensin disrupts the normal transport of Na⁺ and K⁺ ions, directly affecting asexual and sexual development of coccidia (Novilla, 2011). Failure of ion transport due to disruption in cellular K⁺ and H⁺ also occurs in bacteria as cell energy is exhausted by trying to maintain homeostasis causing bacteria it to swell, lyse and die (Novilla, 2011).

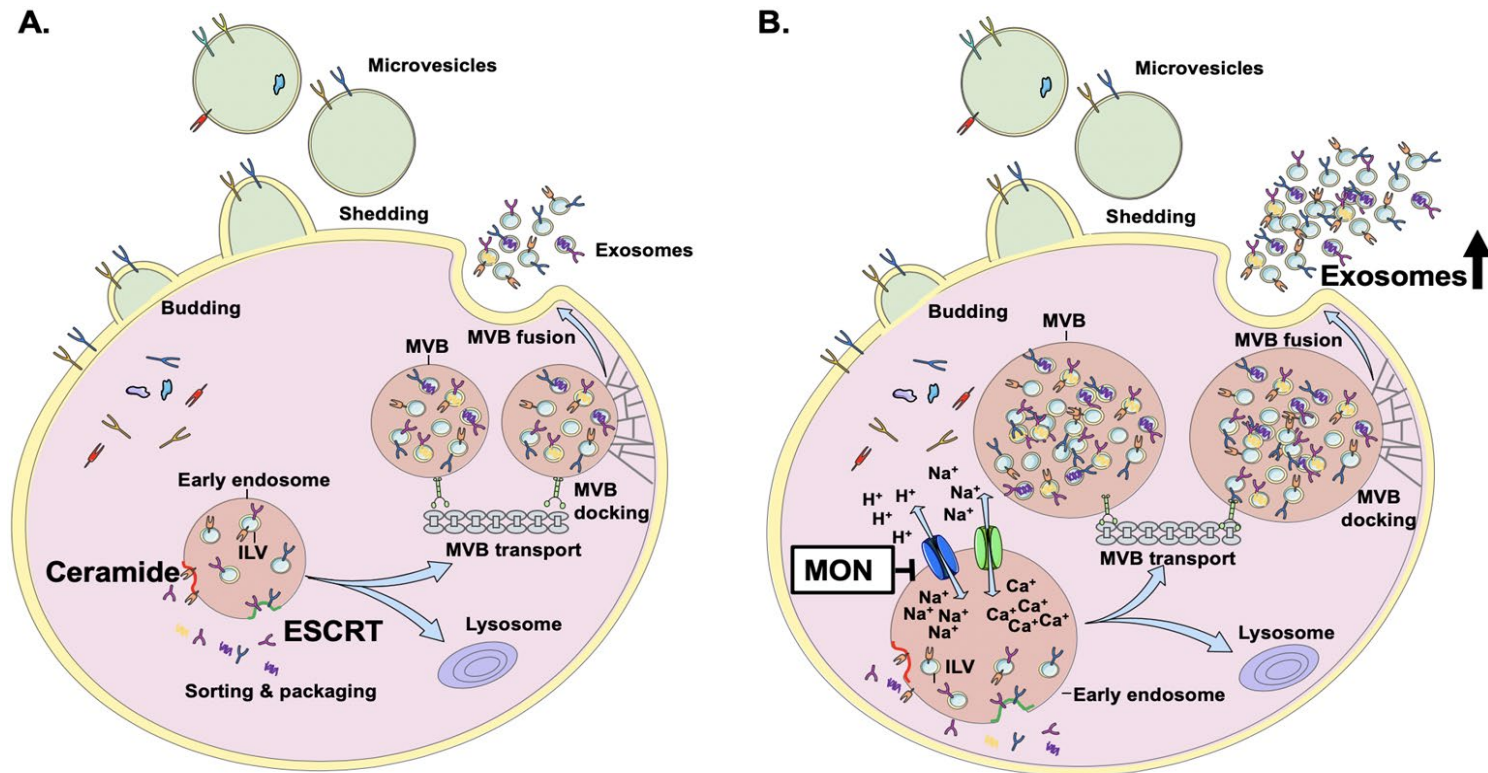


Figure 5.2: Manipulation of exosome release via Monensin. (A) Microvesicles are formed via the budding and shedding from the plasma membrane. Exosome biogenesis occurs via ceramide and endosomal sorting complex required for transport (ESCRT) pathways, cargo is loaded in intraluminal vesicles (ILV) contained in multivesicular bodies (MVB), which are transported to and fused with the plasma membrane for exosome release. **(B)** Monensin acts on the Na⁺ antiporter on endosomes, increasing the intravesicular Na⁺ and subsequent influx of Ca²⁺, causing enlargement of the MVB and increased secretion of mature exosomes from the cell. Created using Servier Medical Art by Servier.

Exosome release can be manipulated *in vitro* via the use of Monensin, treatment of cells with Monensin induces exosome release by acting on the Na⁺/H⁺ antiporter on acidic organelles such as endosomes, causing swelling of these vesicles (Savina *et al.*, 2003). Monensin also induces a Ca²⁺ influx via activity of the Na⁺/Ca²⁺ antiporter (Figure 5.2B; Dömötör *et al.*, 1999). A rise in intracellular Ca²⁺ concentration is a universal intracellular signal necessary to induce regulated secretion in most cell types (Savina *et al.*, 2003). Treatment of cells *in vitro* with Monensin causes the formation of enlarged multivesicular bodies subsequently leading to the increased release of exosomes from these multivesicular bodies (Figure 5.2B); (Savina *et al.*, 2005).

Monensin has been shown to have potential uses in human medicine as an anti-cancer therapeutic based on its' ability to induce apoptosis in a variety of cancer cells such as lung cancer cells (Choi *et al.*, 2013), ovarian cancer cells (Deng *et al.*, 2015) and pancreatic cancer cells (Wang *et al.*, 2018). Monensin was also repositioned as a potential anti-cancer drug for prostate cancer (Kim *et al.*, 2016). The exact mechanism of action Monensin uses to induce apoptosis in cancer cells is not yet known however, it may involve Ca²⁺ dependant apoptosis and reactive oxygen species (Kim *et al.*, 2016).

5.1.3 Employing GW4869 and Monensin to manipulate exosomes release in disease

GW4869 and Monensin have been implemented in various *in vitro* cell models to explore exosomes and their potential role in disease. GW4869 was used to identify the role exosomes may play in sepsis-induced inflammatory response and cardiac dysfunction (Essandoh *et al.*, 2015). Blockade of exosome release by GW4869 diminished sepsis-induced cardiac inflammation, attenuated myocardial depression and prolonged survival, suggesting a role for exosome communication within the immune system and sepsis (Essandoh *et al.*, 2015).

GW4869 and Monensin were used to investigate if exosomes were involved in the dissemination of prions (Guo *et al.*, 2016). Treatment of MoRK13 (mouse

kidney) cells with GW4869, to inhibit exosome release, showed a decrease in intercellular prion transmission. Conversely, Monensin stimulated exosome release, corresponding to an increase in intercellular transfer of prion infectivity (Guo *et al.*, 2016). This demonstrated that manipulation of the exosome biogenesis pathway can highlight the role of exosome communication in prion disease.

5.1.4 Employing GW4869 and Monensin to manipulate exosome release in PCa

GW4869 has been previously used in PCa cell lines for the investigation of exosome communication in PCa. For example, Panigrahi *et al.* (2018) used GW4869 to limit hypoxia-induced exosome release from LNCaP cells (Panigrahi *et al.*, 2018). Whilst Bhagirath *et al.* (2019) used GW4869 to limit exosome release from LNCaP and explore the role of exosome communication in PCa (Bhagirath *et al.*, 2019). Reduction in exosomes affected the neural transcription factors BRN2 and BRN4, cellular levels of BRN2 were increased and decreased exosome associated BRN2. BRN4 was increased in exosomes following AD, treatment with GW4869 attenuated this increase (Bhagirath *et al.*, 2019). The impact of increasing exosome release via Monensin in PCa has not been investigated.

The role exosomes play in NEtD in PCa is not fully understood; to examine their potential role, GW4869 and Monensin were used to manipulate the release of exosomes and microvesicles. As exosomes have been implicated in NEtD and communication (Lin *et al.*, 2017; Bhagirath *et al.*, 2018), impeding or enhancing exosome release may reduce or increase NEtD formation and subsequent aggressive tumour formation. It was also hypothesised that increasing the number of exosomes released by control and AD LNCaP cells, would increase the exosomal starting material to allow better characterisation of exosomes released from control and AD LNCaP cells.

5.2 Study aims and research questions

5.2.2 Overall aim:

To dissect whether exosomes play a role in NEtD AD LNCaP cells.

5.2.3 Objectives:

1. To determine the appropriate concentrations of GW4869 and Monensin to treat control and AD-induced NEtD LNCaP cells.
2. To examine the impact of GW4869 and Monensin on NEtD of LNCaP cells following AD.
3. To examine the impact of GW4869 and Monensin release from LNCaP cells.

5.2.4 Research Questions:

1. Does manipulation of exosome release enhance or impede NEtD of LNCaP cells following AD?
2. Is the expression of the AR signalling, markers of NEtD and the exosomal machinery in control and AD-induced NEtD LNCaP cells altered by GW4869 and Monensin treatment?
3. Does GW4869 or Monensin treatment of control and AD-induced NEtD LNCaP cells alter the profile of exosomes?

5.3 Results

5.3.2 Effect on cell viability after treatment of control and AD-induced NEtD LNCaP cells with different concentrations of GW4869 and Monensin

The effects of GW4869 or Monensin on cell viability of control and AD LNCaP cells were analysed by MTT assay, assessing a range of concentrations derived from the literature (Figure 5.3A; Savina *et al.*, 2003; Wilson *et al.*, 2014; Guo *et al.*, 2016; Panigrahi *et al.*, 2018; Bhagirath *et al.*, 2019).

Analysis of increasing concentrations of the exosome inhibitor GW4869 (Essandoh *et al.*, 2015), showed cell growth was inhibited in a dose dependent manner in control and AD LNCaP cells (Figure 5.3B). At higher concentrations control and AD LNCaP cells showed similar sensitivity to GW4869 (86% +/- 18 % and 86% +/- 16 % respectively at 50 μ M GW4869). However, as the concentration decreased control cells appeared to be more sensitive to GW4869 treatment than AD LNCaP cells (107 % +/- 9 % and 126 % +/- 13 % respectively at 10 μ M GW4869). The concentration, which produced the greatest cell viability at the highest concentration of GW4869 for control and AD LNCaP cells was 25 μ M GW4869 (108 % +/- 9 % and 115 % +/- 16 % respectively; Figure 5.3B). Comparable concentrations were used by others to limit exosome release from LNCaP cells (Panigrahi *et al.*, 2018; Bhagirath *et al.*, 2019).

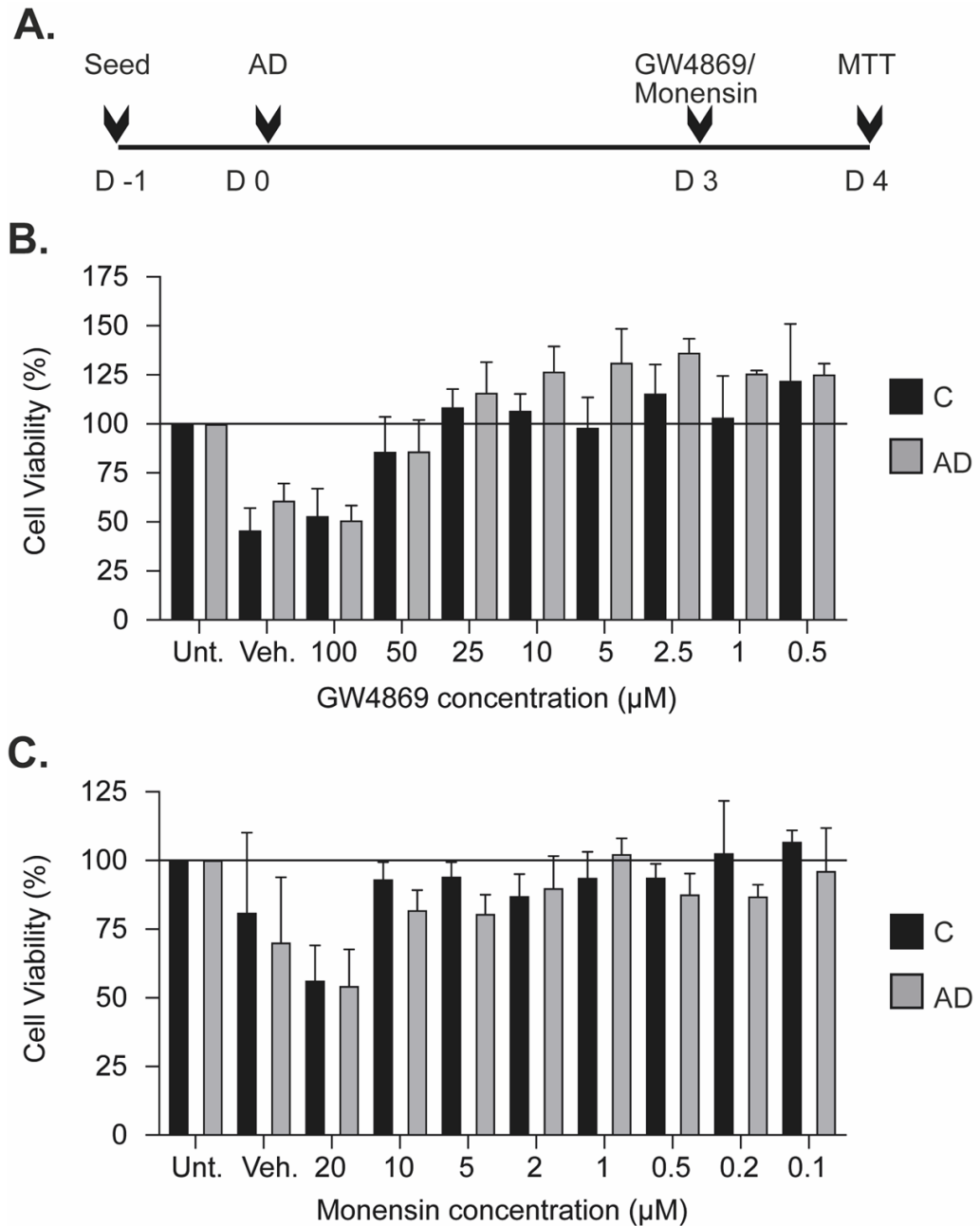


Figure 5.3: Analysing the effect of GW4869 and Monensin on LNCaP cell viability. **A.** LNCaP cells were seeded in control medium, after 24 hours for androgen deprivation (AD) medium was replaced with AD medium, control (C) medium was also replaced. On day 3, C and AD LNCaP cells were exposed to increasing concentrations of GW4869 (**B**) or Monensin (**C**) or their respective vehicle (Veh.) 4.5 % DMSO (**B**) or 0.1 % ethanol (**C**) for 24 hours. Cell viability was assessed via MTT assay, measuring the absorbance at 550 nm. Untreated (Unt.) C or AD cell viability was taken to be 100%, viability of treatments was expressed as a percentage of untreated control or untreated AD cells and presented as mean \pm SEM (n=3). Solid line indicates 100 % cell viability.

To avoid potential cytotoxic effects of DMSO the concentration should be 0.1 % or below (Sumida *et al.*, 2011). A miscalculation of the GW4869 stock concentration resulted in a higher than desired concentration of DMSO in GW4869 working concentrations. Therefore, the highest DMSO concentration of 4.6 % found in 100 μ M GW4869 was used as the vehicle control. As expected LNCaP cell viability was considerably affected by 4.6 % DMSO treatment (Figure 5.3B) however, as the concentration of GW4869 decreased the concentration of DMSO also decreased resulting in a range of DMSO concentrations (4.6 %, 2.3 %, 1.15 %, 0.46 % and 0.23 % corresponding to 100, 50, 25, 10 and 5 μ M respectively; all other DMSO concentrations were 0.01%). Therefore, in the 25 μ M GW4869, the DMSO concentration was 1.15 %, higher than the intended concentration but was in keeping with the literature (Panigrahi *et al.*, 2018; Bhagirath *et al.*, 2019).

Monensin, has not previously been used to induce exosome release in PCa. Therefore, a range of concentrations (20 to 0.1 μ M) were used, based upon findings in other cell lines (Savina *et al.*, 2003; Wilson *et al.*, 2014; Guo *et al.*, 2016) to identify an appropriate Monensin dose for use in LNCaP cells. In the presence of Monensin, cell growth was inhibited dose-dependently (Figure 5.2C). Differences in sensitivity to Monensin was minimal between control and AD LNCaP. The concentration of Monensin which produced the highest viability for control and AD LNCaP cells was 2 μ M, (88 % +/- 8 % and 89.9 % +/- 11 % cell viability respectively; Figure 5.2C). This was in line with Wilson *et al.* (2014) who used 2 μ M Monensin to stimulate exosome release in A549 human lung carcinoma cells, (Wilson *et al.*, 2014). Monensin's vehicle control, EtOH was used at a concentration of 0.1% throughout, and had a marginal effect on control and AD cell viability (Figure 5.3B).

5.3.3 Exosomes released from AD LNCaP cells promote NEtD

The effects of GW4869 or Monensin on LNCaP cell morphology have not been documented previously therefore, it was important to assess if manipulation of exosome release via GW4869 or Monensin altered LNCaP cell morphology. LNCaP cells were seeded in control medium, after 24 hours control medium was removed and replaced with either fresh control medium or AD medium. On day 3, 25 μ M GW4869, 2 μ M Monensin and their respective vehicle controls (DMSO and EtOH) were added to control and AD LNCaP cells and incubated for 24 hours. Brightfield microscope images were taken at day 0 and 3 representing control and AD LNCaP cells respectively as well as at 4 days to assess the effects of GW4869 and Monensin (Figure 5.4).

Untreated control LNCaP cells displayed characteristic epithelial morphology (Gaupe *et al.*, 2013) throughout (Figure 5.4, panel II). Control LNCaP cells treated with 25 μ M GW4869 for 24 hours had increased granularity and single cells could not be distinguished as they formed clusters compared to untreated control LNCaP cells (Figure 5.4, panel V). As expected, untreated AD LNCaP cells showed the presence of neuronal-like projections from the cell body, characteristic of NEtD (Yuan *et al.*, 2006), demonstrating a change from epithelial phenotype at day 0 to neuronal-like phenotype at day 3 (Figure 5.4, panel III). On day 4, there was a slight increase in the presence of neuronal-like morphology. Intriguingly, 25 μ M GW4869, increased granularity and clustering of AD LNCaP and reduced appearance of NE-like projections. LNCaP cell bodies resembled a more characteristic epithelial morphology compared to untreated AD LNCaP cells at day 3, suggesting a regression of the NE-like phenotype (Figure 5.4, panel IX). After 24 hours of Monensin treatment, AD LNCaP cells showed an enhanced NE-phenotype as increased complexity demonstrated by increased branching on projections was identified (Figure 5.4, panel XI). This indicates that manipulation of exosome communication may be involved in NEtD of LNCaP cells.

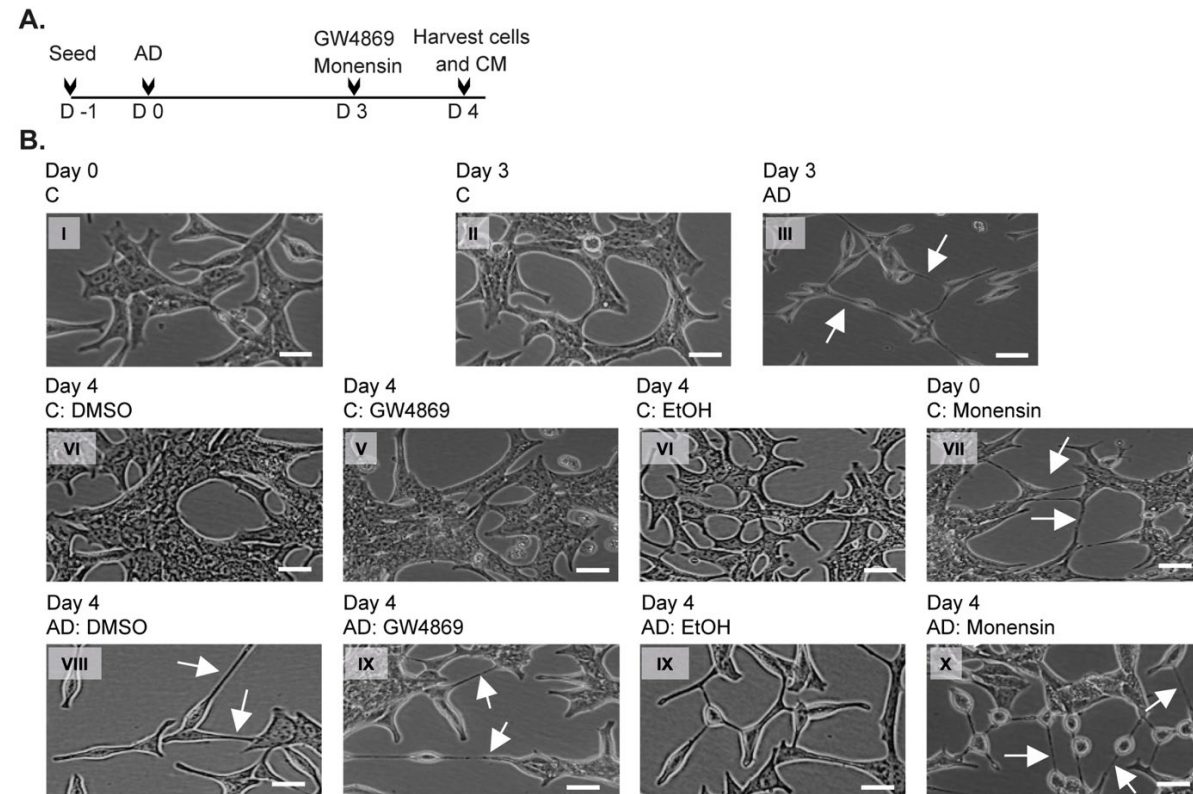


Figure 5.4: Monensin induces a neuroendocrine-like phenotype in control LNCaP cells. **A.** Schematic diagram indicating the treatment timeline of LNCaP cells with GW4869 or Monensin, showing the number of days LNCaP cells were cultured in control (C), androgen deprived (AD) and C or AD plus GW4869 or Monensin. **B.** Representative brightfield microscopy images of C or AD LNCaP cells at days 0, 3 and 4 (X 200 magnification). Cells were treated with 25 μ M GW4869 or 2 μ M Monensin or vehicle controls, 1.15 % DMSO or 0.1 % ethanol (EtOH) for 24 hours (n=2). Arrows indicate the presence of neurite-like protrusions. Scale bars are representative of 1 μ m.

Treatment of control LNCaP cells with Monensin showed extensive granule formation and clustering of the cells (Figure 5.4, panel VII). Curiously, in the presence of Monensin, control LNCaP cells appeared to develop NE-like protrusions and the cells displayed a NE-like phenotype (Figure 5.4, panel VII). Protrusions are a key characteristic of a neuroendocrine-like phenotype (Figure 5.4, panel III), treatment with Monensin and thus, manipulation of exosome communication may independently initiate NEtD in control LNCaP cells.

When treated with DMSO, control LNCaP cells displayed cell bodies which were epithelial in shape, however, they appeared more granular compared to untreated control cells (Figure 5.4, panel IV). EtOH alone did not appear to affect control LNCaP cell morphology and they resembled untreated control epithelial morphology (Figure 5.4, panel VI). The neurite-like projections identified in DMSO and EtOH treated AD LNCaP cells at day 4 were not as evident as untreated AD LNCaP cells at day 3, cells also appeared more granular. This suggests that 1.15 % DMSO and 0.1 % EtOH slightly affects the AD phenotype (Figure 5.4, panel VIII and panel X respectively).

These data suggest exosomes and microvesicles may contribute to induction and maintenance of NEtD in LNCaP cells as the exosome inhibitor GW4869 appeared to reduce the NE-like morphology in AD LNCaP cells compared to untreated AD LNCaP cells. Monensin treatment induces a NE-like phenotype in control LNCaP cells and increased projections and branching of AD LNCaP cells, suggesting increased exosomes, and/or microvesicles, can drive NEtD of PCa.

5.3.4 Analysing the effect of GW4869 and Monensin treatment on the profile of exosomes released from LNCaP cells

Next the impact of GW4869 or Monensin on the profile of exosomes and microvesicles isolated from control and AD LNCaP cells was analysed via dynamic light scattering (DLS) (Figure 5.5 and Figure 5.6). Control and AD LNCaP cells were grown for 3 days, then exposed to GW4869 and Monensin and their vehicle controls DMSO and EtOH respectively. After 24 hours the conditioned culture medium was collected for the isolation of EVs and DLS used

to assess the profile of isolated vesicles (Figure 5.6A). Previously, LNCaP cells were cultivated in AD conditions for 15 days prior to gene expression analysis. Here, LNCaP cells were only exposed to AD for 4 days. This time point was selected as morphological analysis revealed that transformation of LNCaP cells from an epithelial to NE-like phenotype, and thus the beginning of the NEtD process, is evident at day 3 and therefore, this is an important window into the initiation of this process (Chapter 3, Figure 3.2). This data is preliminary therefore, it is not possible to be overly conclusive, further repeats would be included in future work.

As before, a heterogenous population of particles were isolated from untreated control and AD LNCaP cells as seen by the presence of 2 peaks corresponding to exosomes (5 nm – 30 nm) and microvesicles (100 nm – 1000 nm); (Figure 5.5). In keeping with previous findings (Chapter 4, Figure 4.3A), AD conditions increased the number of exosomes released from LNCaP cells compared to control cells with little effect on microvesicles; seen as the rightward shift in the peak corresponding to exosomes in AD LNCaP cells (Figure 5.5). Exosome size was also increased from 9.3 nm to 11.9 nm whilst microvesicle size remained unchanged at approximately 400 nm (Figure 5.6B).

By inhibiting ceramide-mediated biogenesis of exosomes, GW4869 is thought to reduce the number of exosomes produced by cells (Essandoh *et al.*, 2015). Treatment with GW4869 decreased the peak corresponding to exosomes and induced a leftward shift in the peak corresponding to microvesicles in control and AD LNCaP cells (Figure 5.5). This was seen here in control and AD LNCaP cells as exosomes were reduced from 79.1 % to 56.3% and 74.6 % to 52.5 % respectively (Figure 5.6C). GW4869 also had a consequential effect on microvesicles, as there was an increase in microvesicle release from 20.9% to 29.9% in control LNCaP cells and from 25.4 % to 37.1% in AD LNCaP cells (Figure 5.6C). As expected, treatment with GW4869 decreased the average diameter of exosomes and microvesicles released from control and AD LNCaP cells from 9.3 nm to 8.7 nm and from 11.9 nm to 8.5 nm respectively (Figure 5.6B). These data demonstrate the ability of GW4869 to manipulate EV release.

Monensin induces an influx of Na⁺ and consequentially Ca²⁺, which is thought to be responsible for increased exosome biogenesis in cells (Savina *et al.*, 2003). The peak corresponding to exosomes showed a slight leftward shift and a substantial leftward shift in the peak corresponding to microvesicles from control LNCaP cells exposed to Monensin treatment (Figure 5.5). LNCaP cells exposed to AD and Monensin showed a marginal increase in the exosome peak while microvesicle peak was reduced considerably (Figure 5.5). As expected, the number of exosomes from AD LNCaP cells increased from 74.6 % to 78.9 %, subsequently decreasing the number of microvesicles from 25.4 % to 21.1 % (Figure 5.6C). Control LNCaP cells did not show an increase as expected and rather showed a decrease from 74.6% to 64.5% and thus an increase in microvesicles from 20.9 % to 31.7 % (Figure 5.6C). Monensin treatment marginally reduced the size of exosomes from control and AD LNCaP cells, the size of microvesicles from control LNCaP cells were reduced and microvesicles from AD LNCaP cells remained unchanged (Figure 5.6B).

DMSO and EtOH vehicle controls increased exosome release from 79% to 82 % and to 89 % respectively and decreased microvesicle release in control LNCaP cells from 20 % to 18 % and 11 % respectively. Whereas, exosome release was decreased from 75% to 64% and 67 % and microvesicle release increased from 25% to 33 % and 32% in AD LNCaP cells (Figure 5.6C). This suggests that vehicle controls may also alter the profile of EVs released from LNCaP cells. The average diameter of exosomes from control LNCaP cells treated with DMSO was unaffected but reduced to 10 nm AD LNCaP exosomes (Figure 5.6B). Microvesicle diameter was 503 nm in control cells and decreased to 231 nm in AD LNCaP cells (Figure 5.6B). EtOH increased control and decreased AD exosomes to 11 nm and 10 nm respectively whereas, control and AD microvesicles were decreased 182 nm and 189 nm respectively (Figure 5.6B), suggesting that DMSO and EtOH may alter EVs diameter from control and AD LNCaP cells.

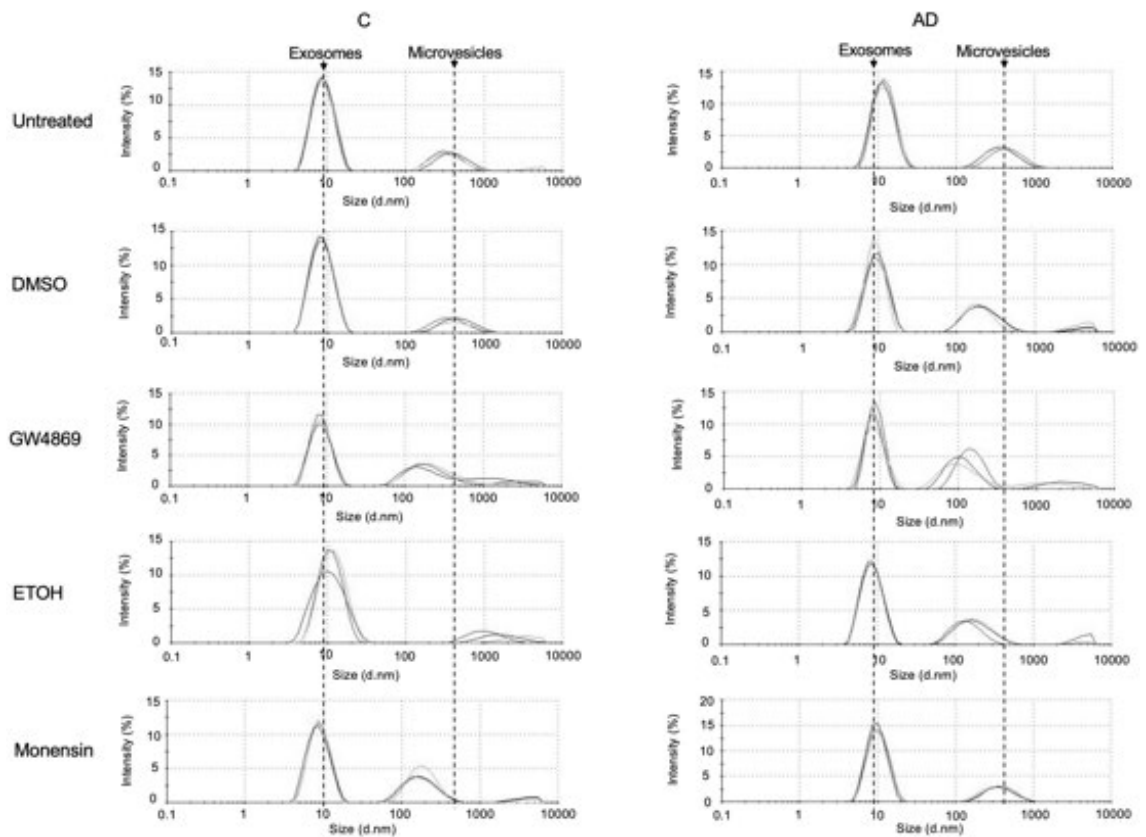


Figure 5.5: Manipulation of exosome release alters the profile of extracellular vesicles isolated from LNCaP cells. Control and AD LNCaP cells were treated with 25 μ M GW4869 or 2 μ M Monensin or their respective vehicle control DMSO (1.15 %) or ethanol (EtOH; 0.1%) for 24 hours. Extracellular vesicles were isolated by precipitation and size exclusion chromatography and analysed via DLS. Exosome and microvesicle profiles from each of the different treatments in control and AD LNCaP cells were aligned to highlight the profile change. The dotted lines indicate the position of the maximum peak of exosomes and microvesicles in control, untreated LNCaP cells.

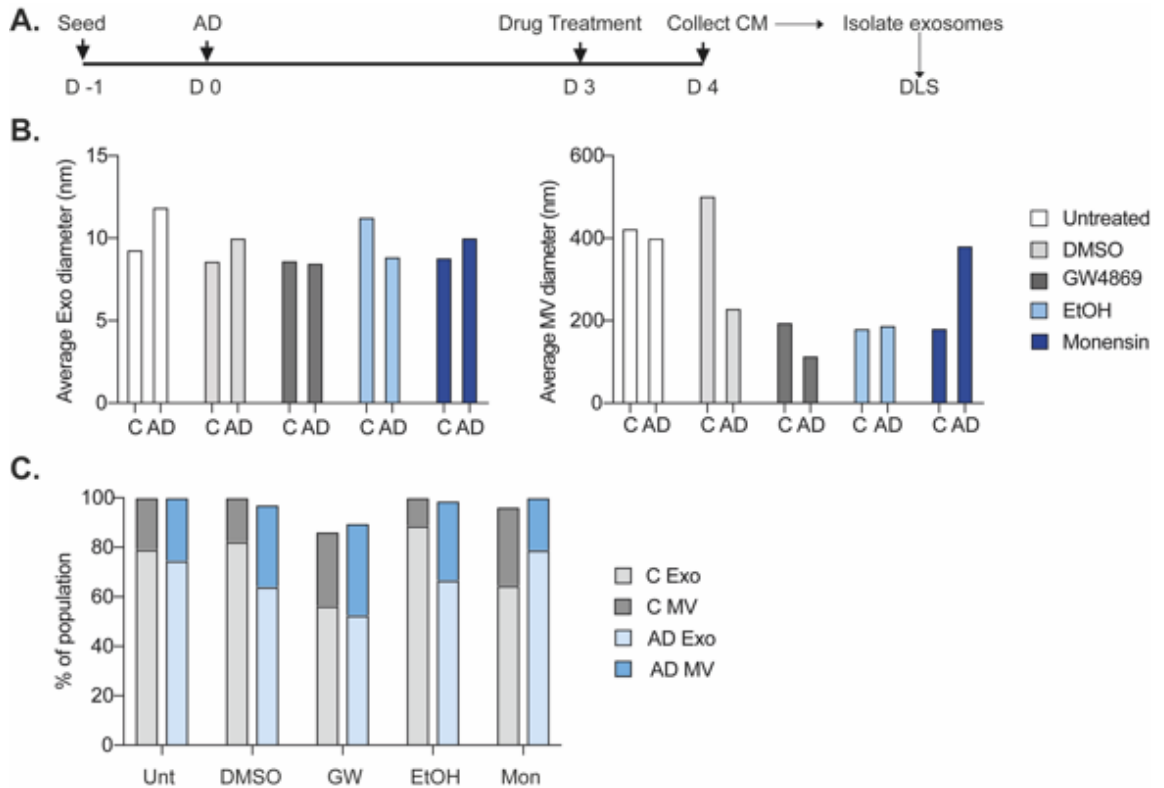


Figure 5.6: Manipulation of exosome release alters the size and number of extracellular vesicles isolated from LNCaP cells. A. Schematic diagram of LNCaP cell treatment timeline. Cells were seeded at day -1, and androgen deprived at day 0. On day 3 cells were treated with 25 μ M GW4869 or 2 μ M Monensin or their respective vehicle controls DMSO or ethanol (EtOH). Conditioned medium (CM) was collected on day 4 subsequently extracellular vesicles were isolated and analysed by DLS. **B.** Assessment of average diameter of exosomes (Exo) and microvesicles (MV) isolated from control (C) and androgen deprived (AD) LNCaP cells. **C.** Graphical representation of the percentage of the population that Exo and MV represent. No statistical analysis was performed as n=1.

These findings demonstrate that GW4869 was successful in the limitation of exosome release from control and AD LNCaP cells and consequential increase of microvesicles release. Monensin induced exosomes from AD LNCaP cells but reduced exosomes from control LNCaP cells. This suggests AD may work synergistically with Monensin to induce exosome release. These data also indicate manipulation of EV release may be useful in elucidating their role in cell-to-cell communication in NEtD of PCa. This data is preliminary therefore, it is not possible to be overly conclusive, to provide robust evidence further repeats would be included in future work.

5.3.5 Analysing the effect of GW4869 and Monensin treatment on the expression of key genes associated with AR signalling and NEtD

To assess the effect of GW4869 or Monensin treatment on key genes associated with AR signalling and NEtD, LNCaP cells were grown in control or AD conditions for 3 days. On day 3, cells were treated with 25 μ M GW4869, 2 μ M Monensin, or their respective vehicle control DMSO or EtOH. After 24 hours cells were harvested, and total RNA was extracted to analyse expression of critical genes via qRT-PCR. Morphological analysis of AD LNCaP cells indicated that inhibition of exosome release could reduce the NE-like phenotype whilst increased exosome release could induce a NE-like phenotype in control LNCaP cells and enhanced NE-like phenotype in AD LNCaP cells. Therefore, it was important to assess whether these results were translated in gene expression.

Work in chapter 3 demonstrated that after 15 days of AD, androgen receptor (AR) expression was increased and kallikrein related peptidase 3 (KLK3; encoding PSA) expression was downregulated (Figure 3.5A). After 4 days AD, AR expression in LNCaP cells was marginally decreased and increased KLK3 expression was observed (Figure 5.7A). This suggests that the gene expression profiles at the earlier 4-day AD time point may differ from fully NE-like LNCaP cells.

GW4869 treatment of AD LNCaP cells triggered a downregulation of AR (-2.7-fold) and KLK3 (-11-fold) expression; in Monensin treated AD LNCaP cells the downregulation of AR (-14-fold) and KLK3 (-9-fold) expression was substantial (Figure 5.7A). DMSO shows comparable effects with GW4869 as expression of AR and KLK3 were reduced in AD LNCaP cells. EtOH also slightly reduced expression of AR and KLK3 expression in AD LNCaP cells, however the effect of EtOH on AR expression is overwhelmed by the effect of Monensin (Figure 5.7A).

AR and KLK3 should be expressed in control LNCaP cells however, AR expression was marginally downregulated (-2-fold) by GW4869 and further downregulated (-4.5-fold) in Monensin treated control LNCaP cells (Figure 5.7A). KLK3 expression was also markedly downregulated by GW4869 (-14-fold) and slightly downregulated in Monensin treated control cells (-1-fold). Of note, expression of AR and KLK3 with DMSO alone replicated the result observed for GW4869, suggesting that DMSO was masking the true effects of GW4869 or there was no effect. EtOH treatment did not affect expression of AR or KLK3 in control LNCaP cells, indicating that Monensin effects are dependent on the presence of the drug. These findings suggest that manipulation of exosome release may alter the expression of androgen signalling markers in LNCaP cells.

In chapter 3, 15 days AD was accompanied by a significant increase in neuronal markers such as neuron specific enolase (ENO2) and class III β -tubulin (TUBB3) and slightly increased synaptophysin (SYP). Here, at 4 days of AD, induction of ENO2, TUBB3 and SYP (Figure 5.7B) was evident but considerably less than 15 days demonstrating the temporal expression of these genes. GW4869 did not alter induction of ENO2 or SYP but increased TUBB3 expression (1.5-fold; Figure 5.7B). It was thought the enhanced NE-like phenotype induced by Monensin (Figure 5.4) would increase neuronal marker expression, however, ENO2 expression was unaffected by Monensin treatment and TUBB3 and SYP expression were notably reduced in AD LNCaP cells (Figure 5.7B), suggesting different temporal expression of NE markers.

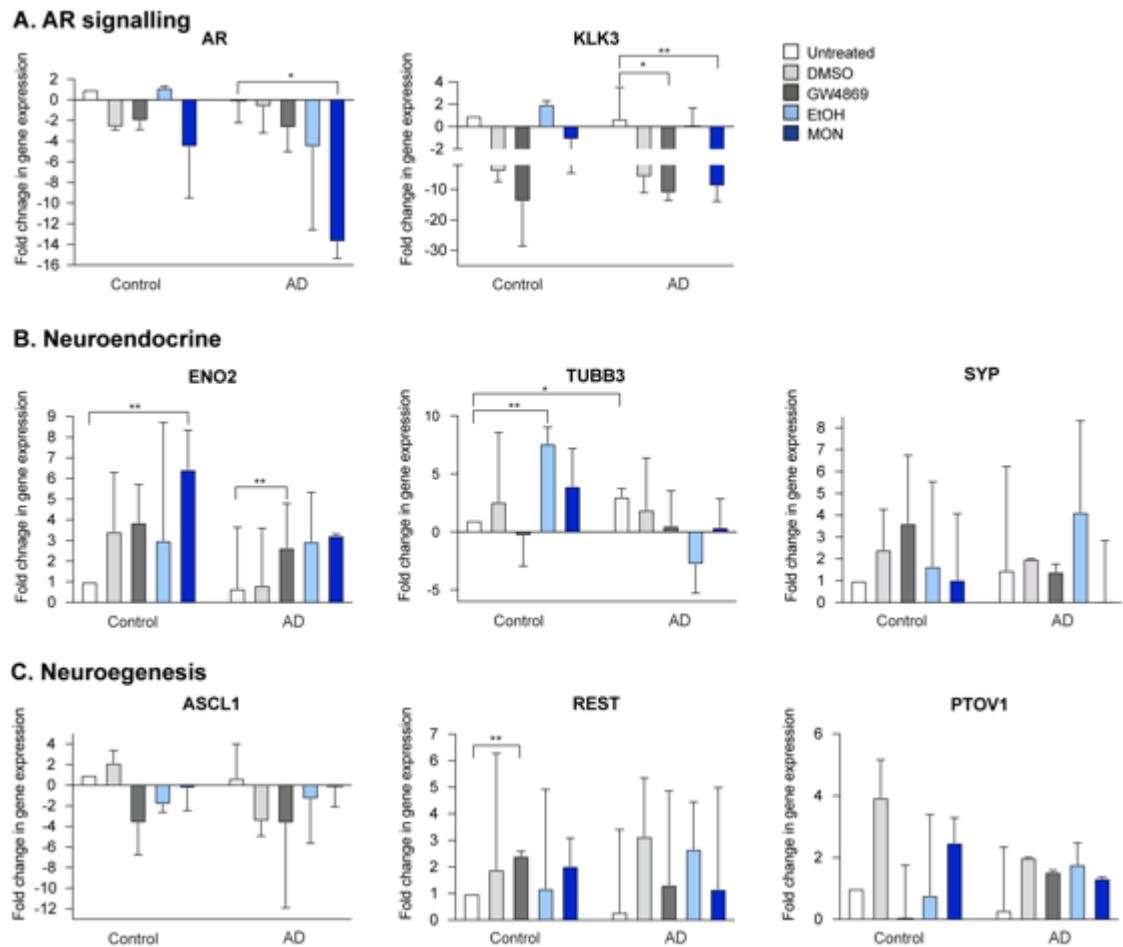


Figure 5.7: Assessing the effect of GW4869 or Monensin treatment on key genes associated with NEtD in LNCaP cells. Cells were grown in control (C), or androgen deprived (AD) conditions for 3 days, cells were then treated with 25 μ M GW4869 or 2 μ M Monensin (MON) or their vehicle controls, DMSO (1.15 %) or ethanol (EtOH; 0.1 %) respectively and incubated for 24 hours. On day 4 RNA was extracted and relative expression of **A.** markers of androgen signalling androgen receptor (AR) and (KLK3) **B.** neuroendocrine markers neuron specific enolase (ENO2), class III β -tubulin (TUBB3), and synaptophysin (SYP) **C.** and markers of neurogenesis (ASCL1), RE-1 silencing transcription factor (REST) and (PTOV1) were assessed by qRT-PCR. Data were analysed by Ct and normalised to the geometric mean of ACTB, GAPDH and RPL13A to obtain the fold change in gene expression. Data is expressed as the mean \pm SD (n=2) and was analysed by one-way ANOVA and Tukey's *post hoc analysis*; *p<0.05, **p<0.01, ****p<0.0001.

Control epithelial LNCaP cells are expected to show little to no expression of neuronal markers yet intriguingly, Monensin treatment increased expression of ENO2, TUBB3 and SYP in LNCaP cells (Figure 5.7B). Aligning with the appearance of a NE-like phenotype after Monensin treatment (Figure 5.4). GW4869 also induced ENO2 and SYP expression in control cells however, TUBB3 was downregulated. Vehicle controls DMSO and EtOH showed slightly increased expression of all neuronal markers (ENO2, TUBB3 and SYP). These data indicate that manipulation of exosome release in control epithelial cells has a dramatic impact on expression of neuronal markers.

Regulators associated with cell fate and neurogenesis were also assessed. Previous findings demonstrated that AD conditions increased expression of human achaete-scute homolog 1 (ASCL1; encoding hASH1), RE-1 silencing transcription factor (REST) and prostate specific gene 1 (PTOV1). GW4869 considerably reduced ASCL1 expression but did not appear to alter REST or PTOV1 expression (Figure 5.7C). Monensin marginally reduced ASCL1 and did not appear to alter REST or PTOV1 expression (Figure 5.7C). Most interestingly, control LNCaP cells showed increased REST and PTOV1 when treated with GW4869 or Monensin (Figure 5.7C). DMSO and EtOH do not appear to affect the expression of ASCL1, REST or PTOV1 (Figure 5.7C.). These results indicate that at an earlier stage in the NEtD process marked expression of neuronal cell fate regulators are not evident. The exact molecular mechanism of NEtD is unknown therefore, the earlier time point of NEtD provides an insight into the temporal changes of gene expression.

5.3.6 Analysing the effect of GW4869 and Monensin treatment on the expression of key genes of exosome machinery

Next the impact of GW4869 and Monensin on expression of the exosomal machinery in control and AD LNCaP cells was analysed. Previous data revealed AD induced expression of exosomal machinery in LNCaP cells after 15 days (Figure 4.2); it was anticipated that the induction would be less marked after 4 days of AD.

ALG-2 interacting protein X (ALIX) and tumour susceptibility gene 101 (TSG101) are associated with cargo sorting and packaging (Zaborowski *et al.*, 2015). ALIX and TSG101 were induced by AD previously (Chapter 4, Figure 4.2), but not here, suggesting that ALIX and TSG101 are induced later in the NEtD process (Figure 5.8). GW4869 or Monensin treatment in combination with AD, showed a slight downregulation of ALIX and more evident downregulation in TSG101 however, the downregulation was not significant due to the variability (Figure 5.8A). Expression of ALIX and TSG101 was slightly more evident in control cells treated with GW4869 or Monensin, suggesting an enhanced effect on control LNCaP cells (Figure 5.8A). In control and AD LNCaP cells the DMSO appeared to induce expression of ALIX and TSG101, whilst EtOH did not appear to alter expression of ALIX or TSG101 in control or AD LNCaP cells (Figure 5.8A).

RAS-associated binding protein 27A (RAB27A) and vesicle associated protein 7 (VAMP7), were induced by AD as previously shown (Figure 4.2), showing that the trends are consistent between 4 days and 15 days AD and that the model is robust and reproducible (Figure 5.8B). Treatment of AD LNCaP cells with GW4869 or Monensin did not further increase expression of RAB27A, suggesting AD may have already altered expression of the exosome machinery (Figure 5.8B). However, treatment of control LNCaP cells with GW4869 and Monensin dramatically induced RAB27A expression (25-fold and 15-fold respectively) to expression levels comparable to AD LNCaP cells (Figure 5.8B). There is possible induction of VAMP7 caused by GW4869 and Monensin treatment of control LNCaP cells however, there was variability in expression (Figure 5.8B). The drug vehicles DMSO and EtOH may have an effect on RAB27A and VAMP7 expression however, they do not mask the effect of the drugs here (Figure 5.8B).

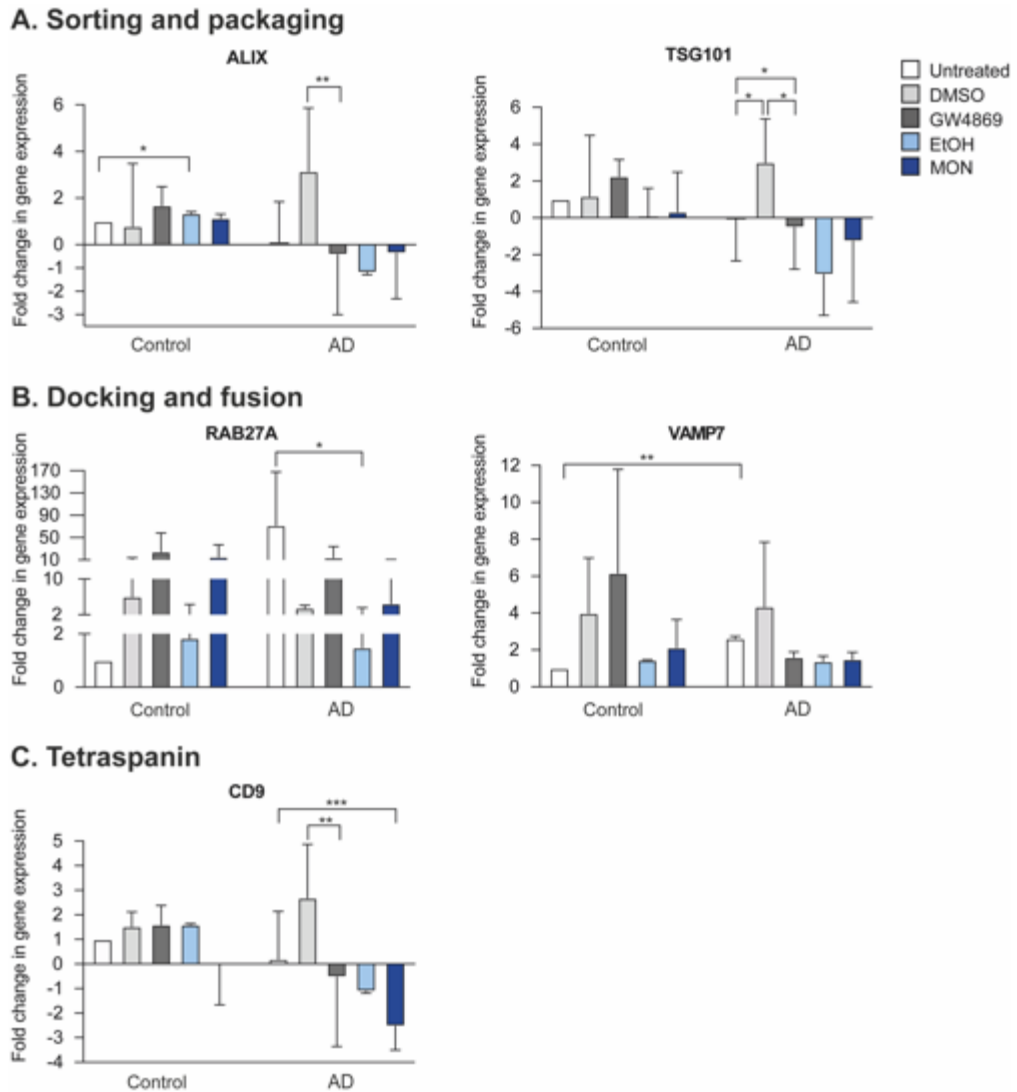


Figure 5.8: Assessing the effect of GW4869 or Monensin treatment on genes associated with exosomes in LNCaP cells. Cells were grown in control (C), or androgen deprived (AD) conditions for 3 days, then cells were treated with 25 μ M GW4869 or 2 μ M Monensin (MON) or their vehicle controls, DMSO or ethanol (EtOH) respectively and incubated for 24 hours. On day 4, RNA was extracted and relative expression of **A.** Markers of sorting and packaging (ALG-2-interacting protein X (ALIX) and tumour susceptibility gene 101 (TSG101)). **B.** Markers of docking and fusion (Ras-associated binding protein 27A (RAB27A) and vesicle associated protein 7 (VAMP7)). **C.** Tetraspanin, CD9 were assessed by qRT-PCR. Data were analysed by Ct and normalised to the geometric mean of ACTB, GAPDH and RPL13A to obtain the fold change in gene expression. Data are expressed as the mean \pm SD (n=2) and was analysed by one-way ANOVA and Tukey's *post hoc analysis*; *p<0.05, **p<0.01, ****p<0.0001.

DMSO and EtOH also increased RAB27A expression in AD and control LNCaP cells however, the extent of expression was less than their corresponding drug treatment (Figure 5.8B). Vesicle associated protein 7 (VAMP7), remained unaffected by treatment with GW4869, Monensin or EtOH in AD LNCaP cells however, DMSO upregulated VAMP7 upregulation (Figure 5.8B). VAMP7 expression was also induced by GW4869 and to a lesser extent DMSO treatment in control LNCaP cells (Figure 5.8B). Monensin or EtOH treatment did not affect VAMP7 expression in control cells (Figure 5.8B). This suggests GW4869 and Monensin treatment may induce docking of multivesicular bodies via RAB27A but not fusion via VAMP7.

Previously CD9 expression was induced after 15 days AD at gene and protein level (Chapter 4, Figure 4.2 And Figure 4.5) however, induction of CD9 was not yet evident at 4 days (Figure 5.8C). GW4869 and Monensin had little effect on CD9 expression in control cells however, expression decreased considerable decrease in AD cells (-0.5-fold and 2.5-fold respectively); (Figure 5.8C). The vehicle controls DMSO and EtOH showed minimal effects on CD9 expression in control LNCaP cells. DMSO upregulated CD9 expression (2.7-fold) in AD LNCaP cells, which may suggest DMSO is masking the effect of GW4869 on CD9 expression (Figure 5.8C). In AD LNCaP cells CD9 expression was marginally decreased by EtOH but did not interfere with effects of Monensin (Figure 5.8C). This suggests that induction of CD9 in NEtD occurs later in the process and provides an insight into the temporal profile of changes occurring in LNCaP cells during NEtD.

5.4 Discussion

The aim of this work was to dissect the potential role of exosomes in the process of neuroendocrine transdifferentiation (NEtD) in control and AD LNCaP cells. GW4869 was used to reduce exosome release while Monensin was used to promote exosome release. It was hypothesised that manipulating exosome biogenesis may indicate the potential role of exosomes in NEtD. Morphological data revealed GW4869 treatment of AD LNCaP cells reduced the neuronal-like

phenotype and appeared more epithelial. Conversely, Monensin enhanced neuronal-like morphology by increasing the complexity through the presence of branching. Most interestingly, control cells not exposed to AD, demonstrated a neuronal-like phenotype as projections appeared from the cell bodies and cells became thin and elongated. Gene expression analysis revealed that control LNCaP cells treated with Monensin had upregulated neuroendocrine and neurogenesis markers. Analysis of the profile of EVs via DLS demonstrated that GW4869 reduced the number of exosomes released and produced a consequential increase in the number of microvesicles from control and AD LNCaP cells. Monensin treatment increased the number and size of exosomes released from AD LNCaP cells however, a decrease was observed in control LNCaP cells. Collectively these results highlight the successful manipulation of the exosome biogenesis pathway in LNCaP cells and the potential role of exosome communication in NEtD of PCa.

5.4.2 GW4869 as an inhibitor of exosome release

The neutral sphingomyelinase (nSMase) inhibitor GW4869 has frequently been used to impede exosome release in multiple diseases such as cardiac dysfunction (Essandoh *et al.*, 2015), neurodegenerative diseases (Guo *et al.*, 2016) and prostate cancer (Panigrahi *et al.*, 2018; Bhagirath *et al.*, 2019). Implementation of GW4869 provides a means of validation for the potential role of exosomes in disease.

To limit exosome release from control and AD LNCaP cells 25 μ M GW4869 was used. As aforementioned a miscalculation of the GW4869 stock concentration resulted in a higher concentration employed to treat LNCaP cells than was initially intended. To validate the release of neural transcription factors in exosomes derived from AD LNCaP cells, 20 μ M GW4869 was used for 48 hours in AD-induced NEtD model (Bhagirath *et al.*, 2019). There were no documented toxic effects to the AD LNCaP cells after treatment of 20 μ M GW4869 and the number of exosomes released by the AD LNCaP cells was reduced (Bhagirath *et al.*, 2019), aligning with the data in this chapter, which demonstrated that control and

LNCaP cell viability was unaffected by the use of 25 μ M GW4869 treatment for 24 hours and successfully limited exosome release.

Hypoxia induced exosome secretion promoted survival of prostate cancer cells (Panigrahi *et al.*, 2018), therefore, limiting exosome release from these prostate cancer cells would indicate whether exosomes provided PCa cells with a survival mechanism (Panigrahi *et al.*, 2018). Treating LNCaP and PC3 cells with 10 μ M or 20 μ M GW4869 for 24 or 48 hours significantly decreased cell viability of LNCaP and PC3 cells, this result was attributed to the decreased cellular exosome release and was suggested that preventing cell-to-cell communication via exosomes reduced the ability to transfer key survival factors for PCa (Panigrahi *et al.*, 2018). LNCaP cells used by Panigrahi *et al.* (2018) were not exposed to AD conditions however, their findings highlight the appropriate use of 25 μ M GW4869 for 24 hours in LNCaP cells.

In a model of sepsis induced inflammatory response and cardiac dysfunction, RAW264.7 macrophages were treated with 10 and 20 μ M GW4869 (Essandoh *et al.*, 2015). Cytotoxic effects were not identified compared to vehicle control (0.005 % DMSO; (Essandoh *et al.*, 2015)) and this, supports the use of 25 μ M GW4869 to treat control and AD LNCaP cells.

5.4.3 Monensin may manipulate exosome release via multiple mechanisms

Monensin is an FDA approved antibiotic used in veterinary medicine as a therapeutic coccidiostat in several target animal species (Novilla, 2011). In poultry farming, feed is treated with Monensin to reduce the proliferation of parasites thus, eliminating attenuation of stock breeding (Aowicki and Huczynski, 2013). Asexual and sexual development of coccidia are affected as Monensin causes Na⁺ and K⁺ transport to fail (Novilla, 2011). Bacteria are affected similarly as they require energy to maintain cellular homeostasis, subsequent treatment with Monensin mediates antiporter activity by exchanging Na⁺ ions with H⁺ ions at the plasma membrane (Markowska *et al.*, 2019). When bacteria have

expended all their energy trying to restore cellular homeostasis the organisms swell, lyse and die (Novilla, 2011). In cattle, Monensin is used to improve the efficiency of food metabolism by reducing energy and waste gas losses associated with formation of volatile fatty acids (Novilla, 2011).

Monensin has also been repositioned in human medicine as an anticancer therapeutic based on its' ability to induce apoptosis in a variety of cancer cells such as lung cancer cells (Choi *et al.*, 2013), ovarian cancer cells (Deng *et al.*, 2015), pancreatic cancer cells (Wang *et al.*, 2018) and most interestingly, prostate cancer cells (Ketola *et al.*, 2010; Kim *et al.*, 2016). It was suggested as a direct effect of Ca^{2+} dysregulation induced by Monensin that regulation of cell cycle and apoptosis associated proteins resulted in, induction of mitochondrial reactive oxygen species- and Ca^{2+} -dependant apoptosis (Kim *et al.*, 2016).

At the cellular level, Monensin facilitates transport of Na^+ ions across the plasma membrane (Novilla, 2011). This triggers the $\text{Na}^+/\text{Ca}^{2+}$ antiporter and subsequent ingress of Ca^{2+} . An increase in intracellular Ca^{2+} is required to induce regulated secretion, thus Monensin can be used to enhance exosome release from cells (Savina *et al.*, 2003). However, Ca^{2+} is an important signalling molecule essential for physiological functions such as cell cycle control, apoptosis, migration and gene expression (Y. F. Chen *et al.*, 2013). Manipulating exosome release via Monensin may also manipulate and differentially affect other Ca^{2+} -dependant mechanisms in LNCaP cells accordingly, care must be taken to identify the correct concentration of Monensin so as not to induce unwanted effects.

5.4.4 The use of Monensin to enhance exosome release

A range of Monensin concentrations are used in the literature to manipulate exosome release from erythroleukemia cells (Savina *et al.*, 2003), lung carcinoma cells (Wilson *et al.*, 2014), mouse kidney and mouse hypothalamic cells (Guo *et al.*, 2016). However, Monensin treatment has not previously been used for manipulation of exosome release in a model of PCa.

Savina *et al.* (2003) showed that treatment of K562 human erythroleukemia cells with 7 μ M Monensin for 7 hours markedly enhanced exosome release. In this chapter LNCaP cells were treated for 24 hours at a lower concentration, it may be notable for future work that different time points of Monensin treatment could be assessed to ensure optimal treatment conditions. In line with the work in this chapter, A459 human lung carcinoma cells were treated with 2 μ M Monensin for 24 hours (Wilson *et al.*, 2014). Monensin was used to demonstrate how the exosome release mechanism is linked to the multifaceted receptor, sortilin by enhancing exosome release (Wilson *et al.*, 2014). There were no documented cytotoxic effects on A459 cells after treatment with 2 μ M Monensin for 24 hours, concomitant with findings here that LNCaP cells had enhanced exosome release and no cytotoxic effects when treated with 2 μ M Monensin. To investigate the relationship between exosome release and intracellular prion dissemination, MoRK13 and GT1-7 cells were stimulated with Monensin, which corresponded to an increase in intracellular transfer of prion infectivity (Guo *et al.*, 2016). MoRK13 cells were treated with 7 μ M Monensin for 48 hours, demonstrating the use of a higher concentration for a longer period of time (Guo *et al.*, 2016). However, GT1-7 cells had increased sensitivity to Monensin and were treated with a considerably lower concentration of 7 nM Monensin for 48 hours (Guo *et al.*, 2016). This highlights the variable sensitivity of different cell lines to Monensin and therefore, conducting cell viability or toxicity assays allows appropriate selection of the Monensin concentration for the chosen cell line. Guo *et al.* (2016) also replaced the culture medium on the day of Monensin treatment, thereby preventing interference of exosomes that were released by cells prior to Monensin treatment. This may provide a more accurate representation of the

exosomes released via treatment with Monensin. Taken together, these works highlight that the concentration and length of treatment is cell dependent and appropriate cytotoxicity assays should be performed before Monensin use. In this chapter LNCaP cells were exposed to AD, Monensin has not previously been used to induce exosome release in this model and consequently may be an additional factor which alters the effect of Monensin on AD LNCaP cells.

5.4.5 Manipulating exosome release alters LNCaP cell morphology

GW4869 treatment regressed the neuronal-like phenotype of AD LNCaP cells suggesting that a reduction of exosome release, may reduce NEtD and restore epithelial morphology in AD LNCaP cells. There is plasticity in NEtD and when AD LNCaP cells are treated with synthetic androgen the cellular morphology reverts back to parental LNCaP epithelial morphology (Shen *et al.*, 1997; Fraser *et al.*, 2019). It is possible, therefore, that exosomes are involved in the maintenance of the NEtD phenotype and when the number of exosomes is reduced, the neuronal-like phenotype cannot be maintained. Preventing the release of exosomes by drugging the exosome pathway may provide a means of preventing PCa progression and formation of NEtD. A similar result was identified in ovarian cancer where it was shown the transfer to and internalisation of CD44 enriched ovarian cancer epithelial cell-derived exosomes by human peritoneal mesothelial cells elevated CD44 and decreased E-cadherin levels in mesothelial cells (Nakamura *et al.*, 2017) This shows that at this stage the ovarian cancer cells are promoting aggressive cancer progression via cell-to-cell communication by exosomes and the associated epithelial mesenchymal transition associated cargo (Nakamura *et al.*, 2017). A change in cellular morphology of mesothelial cells was also observed with ovarian cancer cell-derived exosome uptake, from their characteristic cobblestone-like to elongated spindle-like morphology (Nakamura *et al.*, 2017). When exosome treated mesothelial cells were also treated with GW4869, the cobblestone morphology was restored in a dose dependent manner (Nakamura *et al.*, 2017), showing that ovarian cancer-derived exosomes and their cargo can to drive epithelial mesenchymal transition in ovarian cancer. It is therefore, possible that exosomal cargo may be involved in

driving or maintaining NEtD of PCa and that when exosome release is limited by GW4869 it also limits transfer of exosomal cargo that can drive tumorigenesis.

Morphological analysis revealed that control LNCaP cells, which had not been exposed to AD but were treated with Monensin displayed NE-like protrusions associated with a NE-like phenotype. Effects of Monensin on LNCaP cell morphology however is undocumented, NEtD in PCa arises from distinct range of stress stimuli such as hypoxia (Danza *et al.*, 2012), inflammation (Spiotto and Chung, 2000), irradiation (Suarez *et al.*, 2014) and potent androgen deprivation therapy (Cox *et al.*, 1999). The multiple stressors proposed to drive NEtD indicate that under stress these cells are highly plastic. Thus, it is possible that the appearance of neuronal-like morphology in control LNCaP cells could be caused by Monensin imposing cellular stress and potential induction of NEtD via calcium dysregulation instead of a direct effect of exosomal cargo. There was no morphological evidence of increased apoptosis or autophagy in Monensin treated LNCaP cells. Monensin treatment of PC3 PCa cells reduces expression of B-cell lymphoma 2 (BCL2) and pro-caspase-3 and induces cleavage of the (ADP-ribose) polymerase (PARP) protein contributing to Monensin triggered apoptosis in PC3 cells (Ketola *et al.*, 2010). Further analysis of oxidative stress and apoptosis related genes such as thioredoxin-interacting protein (TXNIP), BCL2 and PARP may provide evidence of stress response to Monensin in AD LNCaP cells (Ketola *et al.*, 2010).

5.4.6 Manipulation of exosome release alters gene expression in LNCaP cells

AD LNCaP cells treated with GW4869, decreased active secretion of mRNA associated with NEtD in PCa into exosomes and increased intracellular mRNA levels (Bhagirath *et al.*, 2019). This suggests that inhibition of exosome release may reduce the ability of PCa to confer survival and progression advantages to neighbouring cells via exosomes. Interestingly, a significant downregulation of AR mRNA in AD LNCaP cells by Monensin treatment was also observed in this research concomitant with previous findings. Treatment of LNCaP cells with Monensin induced a potent reduction in AR mRNA and protein expression

(Ketola *et al.*, 2010) The reduction in AR signalling was enhanced when Monensin treatment coupled with AD (Ketola *et al.*, 2010).

KLK3 mRNA, which is associated with the AR, was also significantly downregulated in AD LNCaP cells treated with Monensin. These data suggest that in PCa, Monensin may alter multiple mechanisms and act on AR signalling as well as exosome release. This may be important in NEtD as NE-like cells are AR and PSA negative and loss of the AR is a mechanism of plasticity employed by PCa to avoid ADT (Hu *et al.*, 2015) providing a link between exosomes released from AD LNCaP cells and their importance in NEtD.

Ketola *et al.* (2010) showed that GW4869 can also reduce expression of exosome protein markers flotillin-1 and TSG101, in agreement with reduced exosome release (Ketola *et al.*, 2010). mRNA analysis demonstrated that under AD conditions, GW4869 may reduce expression of ALIX, TSG101 and CD9, demonstrating the impact of GW4869 in downregulation of exosomal proteins.

This is the first insight into the use of GW4869 and Monensin and their effects on gene expression in control and AD LNCaP cells. There are still many unknowns regarding the use of GW4869 and Monensin and it is unclear whether alterations in morphology and gene expression are a result of potential effects caused by the drugs. It is possible that in manipulating exosome release that the drugs are achieving the same effect and more work will need to be conducted to understand the effect of manipulating exosome release via GW4869 and Monensin at the molecular level.

5.4.7 Manipulating exosome release alters the profile of extracellular vesicles isolated from LNCaP cells

Treatment of the human breast cancer cell line (SKBR3) with GW4869 blocked exosome release but also stimulated budding of microvesicles at the plasma membrane (Menck *et al.*, 2017). In this chapter, exosomes released from GW4869 treated control and AD LNCaP cells were reduced, however, an

increase in the number of microvesicles was observed (Figure 5.7). The data in this research therefore aligns with previous findings to show that in addition to blockade of exosome release, GW4869 enhances microvesicle release. Kosaka *et al.* (2010) identified that GW4869 reduced exosomal protein in a dose dependent manner, however, the exosomal protein composition did not differ from untreated exosomal protein. This indicates GW4869 is an appropriate method of exosome manipulation to investigate the role exosomes may play in AD-induced NEtD LNCaP cells and NEPC.

GW4869 was shown to influence exosome-mediated tumour growth, as the number of lung metastases were reduced in tumour bearing mice (Fabbri *et al.*, 2012). The reduction is thought to result from reduced cell-to-cell exchange of exosomal miRNAs (Fabbri *et al.*, 2012), suggesting that as GW4869 reduced the number of exosomes produced by AD LNCaP cells, there was a reduction in the exchange of exosomal cargo associated with NEtD, reducing the number of cells which undergo NEtD.

Interesting work by Menck *et al.*, (2017) showed treatment of SKBR3, breast cancer cells and murine L cells with GW4869 differentially affected the number of exosomes and microvesicles released. GW4869 treatment successfully reduced exosome release from SKBR3 and murine L cells and surprisingly, increased microvesicle release. These findings, therefore, align with data here, demonstrating that neutral sphingomyelinase inhibition differentially affects subcellular membranes and different EV sub populations.

Treatment with Monensin enhanced the number of exosomes released from AD LNCaP cells, and the phenotype of control LNCaP cells which could suggest that their increased exosome release is associated with cancer progression via NEtD. It has been proposed that disruption of Ca^{2+} homeostasis is caused by enhanced proliferation and metastasis found in various cancers (Messenger *et al.*, 2018). Therefore, the combined effect of increased Ca^{2+} by Monensin may account for the greater increase in exosome release from AD LNCaP cells compared with control LNCaP cells.

Those who have used GW4869 or Monensin to investigate the potential role of exosomes in disease do not provide data of the size or number of EVs, thus there is no evidence that treatment with these drugs alters the EV profile (Guo *et al.*, 2015; Panigrahi *et al.*, 2018; Bhagirath *et al.*, 2019). The conclusion that GW4869 has reduced exosome release is based upon alterations in the cell specific cargo in the EVs and any changes to the size, number or populations identified are not stated.

Cells secrete a wide range of EVs due to limitations in analytical techniques it is unclear what subpopulation of EVs are responsible for any given effect (Van Niel *et al.*, 2018). This can be further complicated by the overlap in the range of sizes of exosomes and microvesicles, similar morphology and variable composition (Van Niel *et al.*, 2018). Cargo from exosomes and microvesicles could differ or deliver different cargo to recipient cells. Future work should include investigation into exosomes and microvesicles to elucidate whether microvesicles may also contribute to NED in PCa.

5.4.8 Limitations of exosome manipulation via GW4869 and Monensin

DMSO is an organic solvent commonly used to dissolve lipophilic compounds, and should be used at 0.1 % or below *in vitro* (Sumida *et al.*, 2011) The DMSO concentration used here was higher than intended, resulting in 1.15 % DMSO in 25 μ M GW4869 however, cell viability was only marginally affected. DMSO can induce adverse effects such as the differentiation of embryonic stem cell at non-cytotoxic concentrations (Adler *et al.*, 2006). Intriguingly, housekeeping genes such as ACTIN, GAPDH and PGK1 are sensitive to exposure to 0.5% (v/v) DMSO and above (Nishimura *et al.*, 2008). In this chapter, ACTIN and GAPDH were included as housekeeping genes however, the C_T values did not appear to be altered by the use of 1.15 % DMSO. These data suggest that DMSO may impact on the expression of genes associated with androgen signalling, NED and exosome machinery and it is possible that the DMSO may have masked effects of GW4869. It is, therefore, possible that GW4869 is having a greater effect than is identified due to interference by DMSO. In future, preparations of the working

GW4869 concentration should contain a concentration of 0.1 % or less DMSO to minimise the potential effects of DMSO on gene expression or exosome and microvesicle profiles.

In previous chapters, gene expression data are representative of three replicate experiments however, time constraints limited gene expression analysis in this chapter to two replicates. The variation between the two replicates may indicate that observed changes in gene expression are not tangible and are instead, a product of variation. In future work a minimum of three replicates should be performed to support more robust analysis and provide a full data set.

When the role of exosomes in PCa adaptation to hypoxia was analysed, Panigrahi et al. (2018) pre-treated PCa cells with GW4869 before exposure to hypoxic conditions (Panigrahi *et al.*, 2018). Here LNCaP cells were treated as NETD/AD was occurring. If LNCaP cells were pre-treated with GW4869 prior to AD it may alter the response of LNCaP cells to AD and provide evidence whether exosomes are involved in driving or maintaining NETD induced by AD.

5.4.9 Alternative methods of exosome manipulation

Dynasore is an alternative drug to GW4869 used to manipulate exosome release. Dynamin2 has been described as an essential mediator of clathrin- and caveolin-mediated endocytosis pathways (Macia *et al.*, 2006). Blocking dynamin2 via dynasore can reduce internalisation of exosomes by cells (Su *et al.*, 2018). Wilson et al. (2014) labelled purified exosomes with PKH67 dye to facilitate visualisation of exosome internalisation into HUVEC cells. Treatment with dynasore also reduced internalisation of fluorescently labelled transferrin, a specific ligand of the clathrin-mediated pathway and the internalisation of exosomes labelled with low density lipoprotein dye (Nanbo *et al.*, 2013). These results indicate clathrin and/or caveolin-mediated endocytosis pathways may be involved in exosome internalisation by the recipient cell. Thus, dynasore should be used in future to reduce internalisation of exosomes released from AD-LNCaP

cells to provide evidence as to whether exosomes play a role in the maintenance of NEtD.

Fluorescent membrane dyes to stain exosomes such as PKH67 or low-density lipoprotein (Dil) dyes should be considered to investigate the fate and potential role of exosomes in recipient cells and tissues (Mulcahy *et al.*, 2014). This could permit tracking and visualisation of exosome uptake via confocal microscopy or flow cytometry. These dyes could be used to confirm exosome uptake by undifferentiated PCa cells or other NEtD PCa and therefore, may be useful to determine the role of exosomes in NEtD in PCa.

Interference of endolysosomal trafficking via the knockdown of two key players in endosomal trafficking N-Myc Downstream Regulated 1 (NDRG1) and Ras-related protein Rab7 also significantly increases the release of exosomes (Ortega *et al.*, 2019). However, these components are not specific to the exosome biogenesis pathway, highlighting the difficulty of dissecting one gene that affects one EV pathway.

5.5 Conclusions

In this work GW4869 and Monensin were used to impede and enhance exosome release from control and AD LNCaP cells respectively. Morphological analysis suggests exosomes are important for maintenance of NEtD as GW4869 appeared to regress the NE-like phenotype in AD LNCaP cells and Monensin enhanced the NE-like phenotype in AD LNCaP cells. Enhanced exosomes also appeared to initiate an NE-like phenotype in control LNCaP cells; this translated in gene expression as there was upregulation of neuroendocrine associated markers suggesting that exosomes released from PCa cells may play a role in cell-to-cell communication. However, there was no conclusive evidence that exosomes specifically play a role in the NEtD of LNCaP cells. Further work will be required to investigate the exosomal cargo released from AD LNCaP to establish the role, if any, of exosomes in driving or maintaining NEtD.

6. Chapter 6: Relevance, research conclusions, and future direction

6.1 Relevance of research

Prostate cancer (PCa) is the most frequently diagnosed cancer in men (Patel *et al.*, 2019) with 48,500 new cases and 11,700 deaths reported annually in the UK (Cancer Research UK, 2017). The shift from androgen dependence to androgen independence is one of the most significant concerns in prostate cancer research, as conventional androgen deprivation therapy is only transiently successful (Cerasuolo *et al.*, 2015). Although most patients receive symptomatic relief from therapeutic intervention by disrupting AR signalling, these treatments do not eradicate all PCa cell populations, resulting in castrate resistant prostate cancer (CRPC); (Terry and Beltran, 2014). A lethal subtype of CRPC, neuroendocrine prostate cancer (NEPC) arises to evade selective pressure of PCa therapies (radiotherapy, ADT, chemotherapy); (Lipianskaya *et al.*, 2014). As a result epithelial PCa cells undergo lineage switching to become NE-like PCa cells (Beltran *et al.*, 2019). NEPC tumours are extremely heterogeneous and lack biomarkers, which contributes to the inability to distinguish CRPC and NEPC to provide targeted and effective therapy (Clermont *et al.*, 2019). NEPC generally represents late-stage PCa with extremely poor prognosis, despite treatment, survival of NEPC patients ranges from 7 months to 2 years (Davies *et al.*, 2018). The high prevalence of PCa and increasing age of the population, make the recognition of alternative treatment methods for NEPC of significant importance (Marcu *et al.*, 2010). Investigation of exosomes and their cargo as potential non-invasive and reproducible biomarkers for NEPC, may provide an opportunity to discriminate between different tumour types, monitor disease progression and provide novel opportunity for future disease targeting for patients with NEPC.

6.1.1 Exosome depletion of FCS is an appropriate *in vitro* model to assess exosomes released from LNCaP and NEtD LNCaP cells

The overall aim of this work was to investigate the potential role of exosomes as a means of intracellular communication, involved in driving or maintaining the process of neuroendocrine transdifferentiation (NEtD) in PCa.

The aim of chapter 3 was to establish a robust *in vitro* model to investigate exosome release from AD-induced NEtD LNCaP cells. Exosomes are released from all cells and biological fluids including FCS (Datta *et al.*, 2018) and can be taken up by and influence recipient cells *in vitro* (Shelke *et al.*, 2014; Angelini *et al.*, 2016). Exosome depleted CS-FCS is not commercially available therefore, differential ultracentrifugation was used to deplete CS-FCS-derived exosomes. The effect exosome depletion may have had on AD-induced NEtD has not previously been documented by those investigating exosomes in AD PCa, thus, the potential effects of exosome depletion on AD-induced NEtD were unknown. CS-FCS exosomes were pelleted to produce clarified CS-FCS with a substantially reduced CS-FCS exosome content. Exosome depletion did not attenuate NEtD of LNCaP cells or alter the growth of NEtD or control cells. Therefore, an *in vitro* model to assess exosome release from LNCaP and NEtD LNCaP cells was successfully generated. This was of vital importance to ensure robust analysis of exosomes of interest.

6.1.2 Androgen deprivation induces exosome machinery markers

In chapter 4, the aim was to isolate and characterise exosomes released from AD-induced NEtD LNCaP cells, that androgen deprivation (AD) induces a neuronal-like phenotype and expression of neuroendocrine associated markers in LNCaP cells (Shen *et al.*, 1997; Terry and Beltran, 2014; Fraser *et al.*, 2019). CD9 may regulate AR activity and consequently, is involved in ligand-independent activity of AR (Levina *et al.*, 2015). However, there has been no further investigation of the AR regulating other aspects of exosome machinery. Androgen-mediated autophagy promotes cell growth by augmenting intracellular lipid accumulation, shown to be necessary for PCa

cell growth (Shi *et al.*, 2013). Autophagy and consequent cell growth are potentiated, in part, by androgen-mediated increases in reactive oxygen species (Shi *et al.*, 2013). Four core autophagy genes (*ULK1*, *ULK2*, *ATG4B*, and *ATG4D*) are transcriptionally regulated by AR in PCa (Blessing *et al.*, 2017). There is a suggested interconnection of autophagy and exosome regulated secretory pathways as several proteins (components of the ESCRT and SNAREs) are involved in the regulation and biogenesis in autophagy and exosomes (Gudbergsson and Johnsen, 2019). Therefore, there is potential for the AR to influence EV biogenesis. EV release is enhanced in patients with CRPC and NEPC so, it is possible that the upregulation of exosomes is associated with autophagy regulated by the AR.

This research is the first to investigate the expression of exosome machinery markers in LNCaP cells. AD has a significant impact on expression of exosome machinery involved in EV cargo packaging and docking and fusion with the plasma membrane therefore, the potential for AD to increase EV release could contribute to NEtD via intracellular communication (Figure 6.1). Exosome release was also enhanced in AD LNCaP cells as shown by Bhagirath *et al.* (2019), demonstrating a link between enhanced EV biogenesis and AD thus, by extension this may occur *in vivo* and in NEPC. The gene expression data presented in chapter 4 is significant, as it provides novel evidence that markers of exosome machinery are upregulated under AD conditions in LNCaP cells (Figure 6.1). Work by others (Bhagirath *et al.*, 2019) has shown that exosomes are important in the transfer of mRNA associated with NEtD, together these findings suggest that exosomes may contribute to NEtD and facilitate the development of a more aggressive PCa phenotype (Figure 6.1).

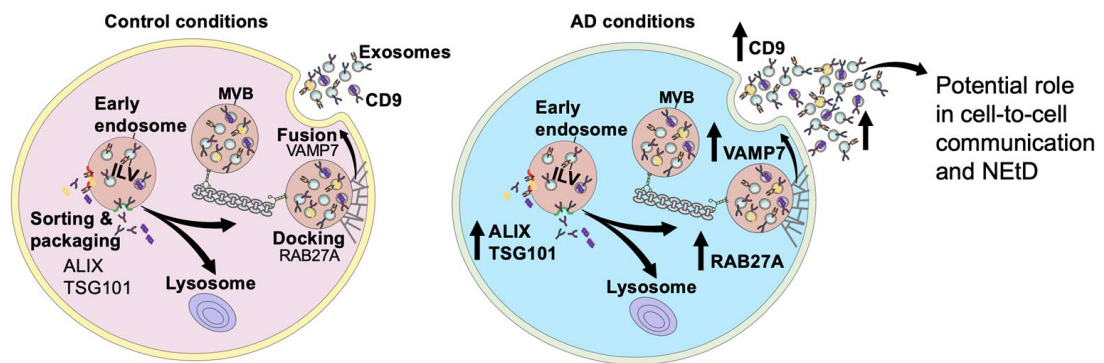


Figure 6.1: Differential expression of exosome machinery genes induced by AD. It was documented that upregulation of ALIX, TSG101, RAB27A, VAMP7 and CD9 by AD-induced NETd of LNCaP cells was concomitant with increased release of exosomes by AD LNCaP cells in comparison to control LNCaP cells. Created using Servier Medical Art by Servier.

6.1.3 Extracellular vesicle manipulation indicates a role for exosomes in NETd in LNCaP cells

In chapter 5, the aim was to manipulate EV release to dissect whether EVs play a role in NETd of AD LNCaP. In order to determine the potential role of EV in NETd of LNCaP cells EV release was manipulated using GW4869, to impede exosome release and Monensin, to enhance exosome release. Inhibition of EV release caused regression of the NETd phenotype in AD LNCaP cells whereas enhanced EV release correlated with an enhanced NETd phenotype in AD LNCaP cells. These findings emphasise the highly plastic nature of NETd and indicate that exosomes may influence the lineage of the disease. The transition from an epithelial to neuronal-like phenotype was observed with augmented expression of neuroendocrine associated markers. These data are of considerable importance, as this is the first time that manipulation of exosome release has been shown to alter the phenotype of control and AD LNCaP cells. These findings support the hypothesis that EVs are implicated in intracellular communication in PCa and disease progression.

6.2 Research limitations

The data collected from this research indicated that exosomes have a potential role of mediating cell-to-cell communication in NEPC however, limitations prevented collection of further evidence. The number of exosomes collected was minimal and resulted in poor protein yield and inconclusive identification of exosome machinery markers. For robust identification of exosome machinery proteins exosome yield would need to be increased. Previous research has documented the need for hundreds of mLs of cell culture medium to provide enough exosomes for protein or gene analysis experiments (Tang *et al.*, 2017). Therefore, future work would need to consider the upscale of cell culture to increase the number of exosomes collected for downstream analysis. A further limitation of this work is the inability to distinguish EV subtypes as there is an overlap in the size range of exosomes and microvesicles, similar morphology and variable composition (Van Niel *et al.*, 2018). It is, therefore, not clear which subtype is responsible for any given outcome thus, further work is needed to improve isolation techniques and identify specific markers for differentiation of EV subpopulations. It is also accepted that the significance of the data may be limited by sample size thus, inclusion of a power calculation in future work would ensure significance. For example, to observe a significant effect of exosome release by GW4869 on LNCaP cells (80% power, 5% significance and two-sided test) 3 replicates would be required based values from Bhagirath *et al.*, (2019).

6.3 Future Directions

6.3.1 Exosomes as biomarkers in AD-induced NEtD LNCaP cells

Exosomal cargo is representative of the parent cell thus, it is hypothesised that the exosome cargo may differ at different stages of the NEtD process. For example, at early stages, cargo may contain factors to drive NEtD, whilst at later stages of NEtD, exosomal cargo may alter to contain factors that maintain NEtD in the tumour microenvironment. Exosomes should be isolated from LNCaP cells throughout AD-induced NEtD and cargo assessed by mass spectrometry to identify if the exosomal cargo protein signature differs throughout NEtD. This

would contribute to the understanding of the role of exosomes in NEtD, as exosomes provide a snapshot of parent cells, NE-derived exosomes could differ from epithelial/adenocarcinoma-derived exosomes so, could be helpful to stratify PCa types. The application of miRNeasy micro kit (Qiagen, UK) to isolate exosomal RNA, followed by the use of TaqMan™ Array Human MicroRNA plates (Applied Biosystems, UK), can detect and accurately quantify 754 human miRNAs, to profile exosomal miRNA. The identification of enhanced exosome production, release and the differing cargo in PCa would be clinically useful for more effective diagnosis of PCa stage, frequent monitoring and provide more accurate treatment options.

There are many known routes and suggested drivers of NEtD in PCa. Exosomes reflect the parent cell however; it is unknown if exosomes generated under different stresses may contain different cargo and thus drivers of NEtD. There is potential to use exosomes and their associated cargo, as biomarkers and by extension the stress state it is potentially under. It would be of interest to perform exosome purification and mass spectrometry to investigate the differential routes of NEtD and the cargo packaged in exosomes released from these cells. If successful, exosomal biomarkers could be used to efficiently diagnose NEtD and distinguish the route of NEtD induction. Knowledge of exosomal biomarkers could provide non-invasive and real-time biomarkers for PCa for a more precise and robust disease diagnosis, allow concurrent disease monitoring of NEPC development and allow stratification of PCa types.

6.3.2 Do exosomes drive NEtD in LNCaP cells?

In chapter 5 inhibition of exosome release via GW4869 caused regression of NEtD of LNCaP cell, suggesting exosomes are involved in maintenance of NEtD in LNCaP cells. To further validate these findings, blockade of exosome uptake by recipient cells should be investigated. The specific inhibitory agent dynasore can be used to block dymanin2, an essential mediator of clathrin- and caveolin-mediated endocytosis pathways (Macia *et al.*, 2006), reducing cellular internalisation of exosomes (Su *et al.*, 2018). It is hypothesised that exosomes

derived from AD induced NEtD LNCaP cells will induce features of NEtD in untransformed, control epithelial cells via transfer of exosomal cargo, therefore exosomes should be isolated and purified from AD-induced NEtD LNCaP cells and added to epithelial LNCaP cells in culture. Morphology would be monitored by brightfield microscopy and changes in gene expression analysed by qRT-PCR. To demonstrate the importance of exosome internalisation and cargo in NEtD, AD exosomes would be applied to epithelial LNCaP cells with or without pre-treatment with dynasore. Exosomes uptake could also be confirmed by labelling with low-density-lipoprotein (Dil) dye, such as PKH67 and confocal microscopy to confirm uptake by epithelial LNCaP cells. This research would add to the current knowledge of exosome communication in PCa and ascertain whether exosomes play an essential role in NEtD of PCa. Identification of specific exosomal biomarkers to intercept the uptake of exosomes in recipient cells could reduce the dissemination of exosomal cargo associated with NEtD and further aggressive disease progression correlated with NEPC.

6.3.3 Do differential time points affect the cargo within AD LNCaP cell exosomes?

In this research differences were found in the temporal expression profile of androgen signalling, neuroendocrine and exosome machinery genes, as expression was substantially less at 4 days than 15 days AD. AD enhances exosome release concomitant with previous research (Soekmadji *et al.*, 2017; Bhagirath *et al.*, 2019). Whether expression of exosome machinery is sequential, parallel or concomitant with AD-induced NEtD is unclear. Therefore, LNCaP cells should be exposed to a time course of 3, 7, 10, 14, 17, 21 days AD to pinpoint at what stage in the NEtD process exosome machinery genes and proteins (ALIX, TSG101, RAB27A, VAMP7, CD9) are induced in AD LNCaP cells. Knowledge of the time point at which, markers of exosome machinery are induced and whether the induction is sustained with relation to AD could provide a detailed and informed timeline of the upregulation of exosome production and how this correlates with NEtD. Using this knowledge, it would be possible to use GW4869 and Monensin at different time points according to when AD influences exosome

machinery and more effective EV manipulation to identify the potential role of EVs in PCa progression and NEtD.

6.3.4 Are drivers of NEtD present in exosomes released from PCa cells?

The presence of EVs in all biological fluids poses an opportunity to identify novel biomarkers for disease that are non-invasive and employed in real-time. Upregulation of several miRNAs (miR-21, miR-145, miR-375) in urinary EVs from PCa patients have been implemented as efficient non-invasive biomarkers to stratify PCa from benign prostate hyperplasia or healthy patients (Foj *et al.*, 2017; Xu *et al.*, 2017). Recently, serum EV containing neural transcription factors, BRN2 and BRN4, were significantly upregulated in CRPC with neuroendocrine characteristics compared to CRPC with adenocarcinoma characteristics (Bhagirath *et al.*, 2019). There are a plethora of suggested drivers of neuroendocrine transdifferentiation, including ASCL1, EZH2, Notch, N-MYC, SOX2 and SRRM4 (Patel *et al.*, 2019). Identifying these genes in EVs would add to our knowledge of NEtD in prostate cancer as a useful tool to distinguish between advanced PCa tumour types and aid tumour stratification. It would also be of interest to detect miRNA capable of inducing NEtD via the ExoCarta database to reveal candidate miRNAs or their apparent targets in EVs (Keerthikumar *et al.*, 2016). This work should first be completed *in vitro* using NCI-H660 cells as they are derived from NEPC, to establish presence of miRNA in these EVs as biomarkers in a cellular model of PCa. Subsequent detection of miRNA within exosomes isolated from PCa patient blood or urine samples should be investigated for the clinical application of exosome biomarkers. The potential to selectively target neuronal factors via siRNA that are capable of inducing NEtD in PCa in EVs presents an increasingly important potential diagnostic tool for the differentiation of tumour type and disease progression. Monitoring and tracking of known NEtD markers via exosomes in blood or urine samples from PCa patients could be employed *in lieu* of invasive procedures such as biopsy.

6.4 Final conclusions

The overall survival of patients diagnosed with NEPC is less than two years, currently there are no biomarkers available to stratify this lethal form of PCa and treatment options are poor. Together, this body of work provides a platform for understanding the potential intracellular communicative role of EVs in NEtD of PCa, advocating their use for identification of novel, non-invasive and real-time biomarkers. These biomarkers could then be used to help stratify NEPC from other PCa types, monitor disease progression and treatment effects and provide more effective treatment options.

References

Abels, E. R. and Breakefield, X. O. (2016) 'Introduction to Extracellular Vesicles: Biogenesis, RNA Cargo Selection, Content, Release, and Uptake', *Cellular and Molecular Neurobiology*. Springer New York LLC, 36, pp. 301–312. doi: 10.1007/s10571-016-0366-z.

Abrahamsson, P.-A. (1999) 'Neuroendocrine cells in tumour growth of the prostate', *Endocrine-Related Cancer*, 6, pp. 503–519.

Adler, S., Pellizzer, C., Paparella, M., Hartung, T. and Bremer, S. (2006) 'The effects of solvents on embryonic stem cell differentiation', *Toxicology in Vitro*. Pergamon, 20(3), pp. 265–271. doi: 10.1016/j.tiv.2005.06.043.

Akbaş, A., Abdulmajed, M. I., Tolga Gülpınar, M. and Sancak, E. B. (2015) 'Is PSA Still the Best Marker in Diagnosis and Monitor-ing of Prostate Cancer?', *European Journal of General Medicine*, 12(2), pp. 187–193. doi: 10.15197/sabad.1.12.40.

Akitake, N., Shiota, M., Obata, H., Takeuchi, A., Kashiwagi, E., Imada, K., Kiyoshima, K., Inokuchi, J., Tatsugami, K. and Eto, M. (2018) 'Neoadjuvant androgen-deprivation therapy with radical prostatectomy for prostate cancer in association with age and serum testosterone', *Prostate International*. Elsevier, 6(3), pp. 104–109. doi: 10.1016/J.PRNIL.2017.10.002.

Al-Nedawi, K., Meehan, B., Micallef, J., Lhotak, V., May, L., Guha, A. and Rak, J. (2008) 'Intercellular transfer of the oncogenic receptor EGFRvIII by microvesicles derived from tumour cells', *Nature Cell Biology*. Nature Publishing Group, 10(5), pp. 619–624. doi: 10.1038/ncb1725.

Altschul, S. F., Gish, W., Miller, W., Myers, E. W. and Lipman, D. J. (1990) 'Basic local alignment search tool', *Journal of Molecular Biology*, 215(3), pp. 403–410. doi: 10.1016/S0022-2836(05)80360-2.

Amorino, G. P. and Parsons, S. J. (2004) 'Neuroendocrine Cells in Prostate Cancer', *Critical Reviews in Eukaryotic Gene Expression*. Begel House Inc., 14(4), pp. 287–300. doi: 10.1615/CritRevEukaryotGeneExpr.v14.i4.40.

Andreu, Z. and Yáñez-Mó, M. (2014) 'Tetraspanins in extracellular vesicle formation and function.', *Frontiers in immunology*. Frontiers Media SA, 5, p. 442. doi: 10.3389/fimmu.2014.00442.

Angelini, F., Ionta, V., Rossi, F., Miraldi, F., Messina, E. and Giacomello, A. (2016) 'Foetal bovine serum-derived exosomes affect yield and phenotype of human cardiac progenitor cell culture.', *BioImpacts : BI*, 6(1), pp. 15–24. doi: 10.15171/bi.2016.03.

Aowicki, D. and Huczynski, A. (2013) 'Structure and Antimicrobial Properties of Monensin A and Its Derivatives: Summary of the Achievements', *BioMed Research International*. Hindawi Publishing Corporation, 2013, pp. 1–14. doi: 10.1155/2013/742149.

Aparicio, A. M., Harzstark, A. L., Corn, P. G., Wen, S., Araujo, J. C., Tu, S. M., Pagliaro, L. C., Kim, J., Millikan, R. E., Ryan, C., Tannir, N. M., Zurita, A. J., Mathew, P., Arap, W., Troncoso, P., Thall, P. F. and Logothetis, C. J. (2013) 'Platinum-based chemotherapy for variant castrate-resistant prostate cancer', *Clinical Cancer Research*. NIH Public Access, 19(13), pp. 3621–3630. doi: 10.1158/1078-0432.CCR-12-3791.

Attard, G., Greystoke, A., Kaye, S. and De Bono, J. (2006) 'Update on tubulin-binding agents', *Pathologie Biologie*. Elsevier Masson SAS, 54(2), pp. 72–84. doi: 10.1016/j.patbio.2005.03.003.

Le Bail, A., Scholz, S. and Kost, B. (2013) 'Evaluation of Reference Genes for RT qPCR Analyses of Structure-Specific and Hormone Regulated Gene Expression in *Physcomitrella patens* Gametophytes', *PLoS ONE*, 8(8), p. e70998. doi: 10.1371/journal.pone.0070998.

Bandu, R., Oh, J. W. and Kim, K. P. (2019) 'Mass spectrometry-based proteome profiling of extracellular vesicles and their roles in cancer biology', *Experimental and Molecular Medicine*. Nature Publishing Group, pp. 1–10. doi: 10.1038/s12276-019-0218-2.

Barrès, C., Blanc, L., Bette-Bobillo, P., André, S., Mamoun, R., Gabius, H. J. and Vidal, M. (2010) 'Galectin-5 is bound onto the surface of rat reticulocyte exosomes and modulates vesicle uptake by macrophages', *Blood*. American Society of Hematology, 115(3), pp. 696–705. doi: 10.1182/blood-2009-07-231449.

Bebelman, M. P., Smit, M. J., Pegtel, D. M. and Baglio, S. R. (2018) 'Biogenesis and function of extracellular vesicles in cancer', *Pharmacology & Therapeutics*. Pergamon, 188, pp. 1–11. doi: 10.1016/J.PHARMTHERA.2018.02.013.

Beltran, H. *et al.* (2019) 'The role of lineage plasticity in prostate cancer therapy resistance', *Clinical Cancer Research*, 25(23), pp. 6916–6924. doi: 10.1158/1078-0432.CCR-19-1423.

Beltran, H., Beer, T. M., Carducci, M. A., De Bono, J., Gleave, M., Hussain, M., Kelly, W. K., Saad, F., Sternberg, C., Tagawa, S. T. and Tannock, I. F. (2011) 'New Therapies for Castration-Resistant Prostate Cancer: Efficacy and Safety', *European Urology*, 60, pp. 279–290. doi: 10.1016/j.eururo.2011.04.038.

Benedit, P., Paciucci, R., Thomson, T. M., Valeri, M., Nadal, M., Càceres, C., de Torres, I., Estivill, X., Lozano, J. J., Morote, J. and Reventós, J. (2001) 'PTOV1, a novel protein overexpressed in prostate cancer containing a new class of protein homology blocks', *Oncogene*. Nature Publishing Group, 20(12), pp. 1455–1464. doi: 10.1038/sj.onc.1204233.

Bhagirath, D., Yang, T. L., Bucay, N., Sekhon, K., Majid, S., Shahryari, V., Dahiya, R., Tanaka, Y. and Saini, S. (2018) 'MicroRNA-1246 is an exosomal biomarker for aggressive prostate cancer', *Cancer Research*, 78(7), pp. 1833–1844. doi: 10.1158/0008-5472.CAN-17-2069.

Bhagirath, D., Yang, T. L., Tabatabai, Z. L., Majid, S., Dahiya, R., Tanaka, Y. and Saini, S. (2019) 'BRN4 is a novel driver of neuroendocrine differentiation in castration-resistant prostate cancer and is selectively released in extracellular vesicles with BRN2', *Clinical Cancer Research*, 25(21), pp. 6532–6545. doi: 10.1158/1078-0432.CCR-19-0498.

Bhome, R., Del Vecchio, F., Lee, G.-H., Bullock, M. D., Primrose, J. N., Sayan, A. E. and Mirnezami, A. H. (2018) 'Exosomal microRNAs (exomiRs): Small molecules with a big role in cancer', *Cancer Letters*. Elsevier, 420, pp. 228–235. doi: 10.1016/J.CANLET.2018.02.002.

Bianco, F., Perrotta, C., Novellino, L., Francolini, M., Riganti, L., Menna, E., Saglietti, L., Schuchman, E. H., Furlan, R., Clementi, E., Matteoli, M. and Verderio, C. (2009) 'Acid sphingomyelinase activity triggers microparticle release from glial cells', *The EMBO Journal*. Nature Publishing Group, 28(8), pp. 1043–1054. doi: 10.1038/emboj.2009.45.

Bill-Axelson, A., Holmberg, L., Garmo, H., Rider, J. R., Taari, K., Busch, C., Nordling, S., Häggman, M., Andersson, S.-O., Spångberg, A., Andrén, O., Palmgren, J., Steineck, G., Adami, H.-O. and Johansson, J.-E. (2014) 'Radical Prostatectomy or Watchful Waiting in Early Prostate Cancer', *New England Journal of Medicine*. Massachusetts Medical Society, 370(10), pp. 932–942. doi: 10.1056/NEJMoa1311593.

Blessing, A. M., Rajapakshe, K., Reddy Bollu, L., Shi, Y., White, M. A., Pham, A. H., Lin, C., Jonsson, P., Cortes, C. J., Cheung, E., La Spada, A. R., Bast, R. C., Merchant, F. A., Coarfa, C. and Frigo, D. E. (2017) 'Transcriptional regulation of core autophagy and lysosomal genes by the androgen receptor promotes prostate cancer progression', *Autophagy*. Taylor and Francis Inc., 13(3), pp. 506–521. doi: 10.1080/15548627.2016.1268300.

Bono, A. V. (2004) 'Overview of Current Treatment Strategies in Prostate Cancer', *European Urology, Supplements*, 3, pp. 2–7. doi: 10.1016/j.eursup.2003.12.002.

Bryant, R. J., Pawlowski, T., Catto, J. W. F., Marsden, G., Vessella, R. L., Rhees, B., Kuslich, C., Visakorpi, T. and Hamdy, F. C. (2012) 'Changes in circulating microRNA levels associated with prostate cancer.', *British journal of cancer*. Nature Publishing Group, 106(4), pp. 768–74. doi: 10.1038/bjc.2011.595.

Cao, Z., West, C., Norton-Wenzel, C. S., Rej, R., Davis, F. B., Davis, P. J. and Rej, R. (2009) 'Effects of Resin or Charcoal Treatment on Fetal Bovine Serum and Bovine Calf Serum', *Endocrine Research*. Taylor & Francis, 34(4), pp. 101–108. doi: 10.3109/07435800903204082.

Caradec, J., Kharmate, G., Hosseini-Beheshti, E., Adomat, H., Gleave, M. and Guns, E. (2014) 'Reproducibility and efficiency of serum-derived exosome extraction methods', *Clinical Biochemistry*. Elsevier, 47(13–14), pp. 1286–1292. doi: 10.1016/J.CLINBIOCHEM.2014.06.011.

Carnell-Morris, P., Tannetta, D., Siupa, A., Hole, P. and Dragovic, R. (2017) 'Analysis of Extracellular Vesicles Using Fluorescence Nanoparticle Tracking Analysis', *Methods in molecular biology*. Humana Press, New York, NY, 1660, pp. 153–173. doi: 10.1007/978-1-4939-7253-1_13.

Catalano, M. and O'Driscoll, L. (2020) 'Inhibiting extracellular vesicles formation and release: a review of EV inhibitors', *Journal of Extracellular Vesicles*. Taylor and Francis Ltd., 9(1), p. 1703244. doi: 10.1080/20013078.2019.1703244.

Cerasuolo, M., Paris, D., Iannotti, F. A., Melck, D., Verde, R., Mazzarella, E., Motta, A. and Ligresti, A. (2015) 'Neuroendocrine Transdifferentiation in Human Prostate Cancer Cells: An Integrated Approach', *Cancer Research*. American Association for Cancer Research, 75(15), pp. 2975–2986. doi: 10.1158/0008-5472.CAN-14-3830.

Chen, L., Wang, Y., Pan, Y., Zhang, L., Shen, C., Qin, G., Ashraf, M., Weintraub, N., Ma, G. and Tang, Y. (2013) 'Cardiac progenitor-derived Exosomes protect ischemic myocardium from acute ischemia/reperfusion injury', *Biochemical and Biophysical Research Communications*, 431(3), pp. 566–571. doi: 10.1161/CIRCULATIONAHA.110.956839.

Chen, Y. F., Chen, Y. T., Chiu, W. T. and Shen, M. R. (2013) 'Remodeling of calcium signaling in tumor progression', *Journal of Biomedical Science*. BioMed Central, 20, p. 23. doi: 10.1186/1423-0127-20-23.

Choi, H. S., Jeong, E. H., Lee, T. G., Kim, S. Y., Kim, H. R. and Kim, C. H. (2013) 'Autophagy inhibition with monensin enhances cell cycle arrest and apoptosis induced by mTOR or epidermal growth factor receptor inhibitors in lung cancer cells', *Tuberculosis and Respiratory Diseases*, 75(1), pp. 9–17. doi: 10.4046/trd.2013.75.1.9.

Clermont, P.-L., Ci, X., Pandha, H., Wang, Y. and Crea, F. (2019) 'Treatment-emergent neuroendocrine prostate cancer: molecularly driven clinical guidelines', *International Journal of Endocrine Oncology*. Future Medicine Ltd, 6(2), p. IJE20. doi: 10.2217/ije-2019-0008.

Corcoran, C., Rani, S., O'Brien, K., O'Neill, A., Prencipe, M., Sheikh, R., Webb, G., McDermott, R., Watson, W., Crown, J. and O'Driscoll, L. (2012) 'Docetaxel-resistance in prostate cancer: evaluating associated phenotypic changes and potential for resistance transfer via exosomes.', *PloS one*. Public Library of Science, 7(12), p. e50999. doi: 10.1371/journal.pone.0050999.

Costa-Silva, B. *et al.* (2015) 'Pancreatic cancer exosomes initiate pre-metastatic niche formation in the liver', *Nat Cell Biol*, 17(6), pp. 816–826. doi: 10.1038/ncb3169.

Cox, M. E., Deeble, P. D., Lakhani, S. and Parsons, S. J. (1999) 'Acquisition of Neuroendocrine Characteristics by Prostate Tumor Cells Is Reversible: Implications for Prostate Cancer Progression 1', *Cancer Research*, 59(15), pp. 3821–3830.

Culig, Z. and Santer, F. R. (2014) 'Androgen receptor signaling in prostate cancer', *Cancer Metastasis Review*, 33, pp. 413–427. doi: 10.1007/s10555-013-9474-0.

D'amico, M. A., Ghinassi, B., Izzicupo, P., Manzoli, L. and Di Baldassarre, A. (2014) 'Biological function and clinical relevance of chromogranin A and derived peptides.', *Endocrine Connections*. Bioscientifica Ltd., 3(2), pp. R45-54. doi: 10.1530/EC-14-0027.

Danza, G., Di Serio, C., Rosati, F., Lonetto, G., Sturli, N., Kacer, D., Pennella, A., Ventimiglia, G., Barucci, R., Piscazzi, A., Prudovsky, I., Landriscina, M., Marchionni, N. and Tarantini, F. (2012) 'Notch signaling modulates hypoxia-induced neuroendocrine differentiation of human prostate cancer cells', *Molecular Cancer Research*. Mol Cancer Res, 10(2), pp. 230–238. doi: 10.1158/1541-7786.MCR-11-0296.

Datta, A., Kim, H., McGee, L., Johnson, A. E., Talwar, S., Marugan, J., Southall, N., Hu, X., Lal, M., Mondal, D., Ferrer, M. and Abdel-Mageed, A. B. (2018) 'High-throughput screening identified selective inhibitors of exosome biogenesis and secretion: A drug repurposing strategy for advanced cancer OPEN', *Scientific Reports*, 8, p. 8161. doi: 10.1038/s41598-018-26411-7.

Davey, R. A. and Grossmann, M. (2016) 'Androgen Receptor Structure, Function and Biology: From Bench to Bedside.', *The Clinical biochemist. Reviews*. The Australian Association of Clinical Biochemists, 37(1), pp. 3–15.

Davies, A. H., Beltran, H. and Zoubeidi, A. (2018) 'Cellular plasticity and the neuroendocrine phenotype in prostate cancer', *Nature Reviews Urology*. Nature Publishing Group, 15(5), pp. 271–286. doi: 10.1038/nrurol.2018.22.

Deng, Y. *et al.* (2015) 'Antibiotic monensin synergizes with EGFR inhibitors and oxaliplatin to suppress the proliferation of human ovarian cancer cells', *Scientific Reports*. Nature Publishing Group, 5, pp. 1–16. doi: 10.1038/srep17523.

Desjardins, P. and Conklin, D. (2010) 'NanoDrop microvolume quantitation of nucleic acids.', *Journal of visualized experiments: JoVE*. MyJoVE Corporation, (45). doi: 10.3791/2565.

Van Deun, J., Mestdagh, P., Sormunen, R., Cocquyt, V., Vermaelen, K., Vandesompele, J., Bracke, M., De Wever, O. and Hendrix, A. (2014) 'The impact of disparate isolation methods for extracellular vesicles on downstream RNA profiling', *Journal of Extracellular Vesicles*, 3(1). doi: 10.3402/jev.v3.24858.

Dietrich, A., Koi, L., Zöphel, K., Sihver, W., Kotzerke, J., Baumann, M. and Krause, M. (2015) 'Improving external beam radiotherapy by combination with internal irradiation', *British Journal of Radiology*. British Institute of Radiology, 88(1051). doi: 10.1259/bjr.20150042.

Dömötör, E., Abbott, N. J. and Adam-Vizi, V. (1999) 'Na⁺-Ca²⁺ exchange and its implications for calcium homeostasis in primary cultured rat brain microvascular endothelial cells', *Journal of Physiology*. Cambridge University Press, 515(1), pp. 147–155. doi: 10.1111/j.1469-7793.1999.147ad.x.

Doyle, L. M. and Wang, M. Z. (2019) 'Overview of Extracellular Vesicles, Their Origin, Composition, Purpose, and Methods for Exosome Isolation and Analysis', *Cells*, 8, p. 727. doi: 10.1016/b978-0-12-386050-7.50008-3.

Dragovic, R. A., Collett, G. P., Hole, P., Ferguson, D. J. P., Redman, C. W., Sargent, I. L. and Tannetta, D. S. (2015) 'Isolation of syncytiotrophoblast microvesicles and exosomes and their characterisation by multicolour flow cytometry and fluorescence Nanoparticle Tracking Analysis', *Methods*. Academic Press Inc., 87, pp. 64–74. doi: 10.1016/j.ymeth.2015.03.028.

Dragovic, R. A., Southcombe, J. H., Tannetta, D. S., Redman, C. W. G. and Sargent, I. L. (2013) 'Multicolor Flow Cytometry and Nanoparticle Tracking Analysis of Extracellular Vesicles in the Plasma of Normal Pregnant and Pre-eclamptic Women¹', *Biology of Reproduction*. Oxford University Press (OUP), 89(6), pp. 1–12. doi: 10.1095/biolreprod.113.113266.

Driedonks, T. A. P., Nijen Twilhaar, M. K. and Nolte-'t Hoen, E. N. M. (2018) 'Technical approaches to reduce interference of Fetal calf serum derived RNA in

the analysis of extracellular vesicle RNA from cultured cells.', *Journal of extracellular vesicles*. Taylor & Francis, 8(1), p. 1552059. doi: 10.1080/20013078.2018.1552059.

Duijvesz, D., Burnum-Johnson, K. E., Gritsenko, M. A., Hoogland, A. M., Vredenburg-Van Den Berg, M. S., Willemsen, R., Luider, T., Paša-Tolić, L. and Jenster, G. (2013) 'Proteomic Profiling of Exosomes Leads to the Identification of Novel Biomarkers for Prostate Cancer', *PLoS ONE*, 8(12), p. e82589. doi: 10.1371/journal.pone.0082589.

Dunn, M. W. and Kazer, M. W. (2011) 'Prostate Cancer Overview', *Seminars in Oncology Nursing*. W.B. Saunders, 27(4), pp. 241–250. doi: 10.1016/J.SONCN.2011.07.002.

Eitan, E., Zhang, S., Witwer, K. W. and Mattson, M. P. (2015) 'Extracellular vesicle-depleted fetal bovine and human sera have reduced capacity to support cell growth', *Journal of Extracellular Vesicles*. Taylor & Francis, 4(1), p. 26373. doi: 10.3402/jev.v4.26373.

Epstein, J. I., Zelefsky, M. J., Sjoberg, D. D., Nelson, J. B., Egevad, L., Magi-Galluzzi, C., Vickers, A. J., Parwani, A. V., Reuter, V. E., Fine, S. W., Eastham, J. A., Wiklund, P., Han, M., Reddy, C. A., Ciezki, J. P., Nyberg, T. and Klein, E. A. (2016) 'A Contemporary Prostate Cancer Grading System: A Validated Alternative to the Gleason Score', *European Urology*. Elsevier B.V., 69(3), pp. 428–435. doi: 10.1016/j.eururo.2015.06.046.

Essandoh, K., Yang, L., Wang, X., Huang, W., Qin, D., Hao, J., Wang, Y., Zingarelli, B., Peng, T. and Fan, G.-C. (2015) 'Blockade of exosome generation with GW4869 dampens the sepsis-induced inflammation and cardiac dysfunction.', *Biochimica et biophysica acta*. NIH Public Access, 1852(11), pp. 2362–2371. doi: 10.1016/j.bbadis.2015.08.010.

Fabbri, M. *et al.* (2012) 'MicroRNAs bind to Toll-like receptors to induce prometastatic inflammatory response', *Proceedings of the National Academy of*

Sciences of the United States of America. National Academy of Sciences, 109(31), pp. E2110–E2116. doi: 10.1073/pnas.1209414109.

Fader, C. M., Sánchez, D. G., Mestre, M. B. and Colombo, M. I. (2009) 'TI-VAMP/VAMP7 and VAMP3/cellubrevin: two v-SNARE proteins involved in specific steps of the autophagy/multivesicular body pathways', *Biochimica et Biophysica Acta - Molecular Cell Research*. Elsevier, 1793(12), pp. 1901–1916. doi: 10.1016/j.bbamcr.2009.09.011.

Feng, D., Zhao, W. L., Ye, Y. Y., Bai, X. C., Liu, R. Q., Chang, L. F., Zhou, Q. and Sui, S. F. (2010) 'Cellular internalization of exosomes occurs through phagocytosis', *Traffic*. John Wiley & Sons, Ltd, 11(5), pp. 675–687. doi: 10.1111/j.1600-0854.2010.01041.x.

Fitzner, D., Schnaars, M., Van Rossum, D., Krishnamoorthy, G., Dibaj, P., Bakhti, M., Regen, T., Hanisch, U. K. and Simons, M. (2011) 'Selective transfer of exosomes from oligodendrocytes to microglia by macropinocytosis', *Journal of Cell Science*. The Company of Biologists Ltd, 124(3), pp. 447–458. doi: 10.1242/jcs.074088.

Fleige, S. and Pfaffl, M. W. (2006) 'RNA integrity and the effect on the real-time qRT-PCR performance', *Molecular Aspects of Medicine*. Pergamon, 27, pp. 126–139. doi: 10.1016/J.MAM.2005.12.003.

Foj, L., Ferrer, F., Serra, M., Arévalo, A., Gavagnach, M., Giménez, N. and Filella, X. (2017) 'Exosomal and Non-Exosomal Urinary miRNAs in Prostate Cancer Detection and Prognosis', *The Prostate*, 77(6), pp. 573–583. doi: 10.1002/pros.23295.

Fraser, J. A., Sutton, J. E., Tazayoni, S., Bruce, I. and Poole, A. V. (2019) 'hASH1 nuclear localization persists in neuroendocrine transdifferentiated prostate cancer cells, even upon reintroduction of androgen', *Scientific Reports*. Nature Research, 9, p. 19076. doi: 10.1038/s41598-019-55665-y.

Frühbeis, C., Fröhlich, D., Kuo, W. P., Amphornrat, J., Thilemann, S., Saab, A. S., Kirchhoff, F., Möbius, W., Goebbels, S., Nave, K.-A., Schneider, A., Simons, M., Klugmann, M., Trotter, J. and Krämer-Albers, E.-M. (2013) 'Neurotransmitter-Triggered Transfer of Exosomes Mediates Oligodendrocyte–Neuron Communication', *PLoS Biology*. Edited by B. A. Barres. Public Library of Science, 11(7), p. e1001604. doi: 10.1371/journal.pbio.1001604.

Gardiner, C., Di Vizio, D., Sahoo, S., Théry, C., Witwer, K. W., Wauben, M. and Hill, A. F. (2016) 'Techniques used for the isolation and characterization of extracellular vesicles: results of a worldwide survey.', *Journal of extracellular vesicles*. Taylor & Francis, 5, p. 32945. doi: 10.3402/jev.v5.32945.

Gaupel, A.-C., Wang, W.-L. W., Mordan-McCombs, S., Yu Lee, E. C. and Tenniswood, M. (2013) 'Xenograft, Transgenic, and Knockout Models of Prostate Cancer', in *Animal Models for the Study of Human Disease*. Academic Press, pp. 973–995. doi: 10.1016/B978-0-12-415894-8.00039-7.

Git, A., Dvinge, H., Salmon-Divon, M., Osborne, M., Kutter, C., Hadfield, J., Bertone, P. and Caldas, C. (2010) 'Systematic comparison of microarray profiling, real-time PCR, and next-generation sequencing technologies for measuring differential microRNA expression', *RNA*. Cold Spring Harbor Laboratory Press, 16(5), pp. 991–1006. doi: 10.1261/rna.1947110.

Gkolfinopoulos, S., Tsapakidis, K., Papadimitriou, K., Papamichael, D. and Kountourakis, P. (2017) 'Chromogranin A as a valid marker in oncology: Clinical application or false hopes?', *World journal of methodology*. Baishideng Publishing Group Inc, 7(1), pp. 9–15. doi: 10.5662/wjm.v7.i1.9.

Gong, J., Lee, J., Akio, H., Schlegel, P. N. and Shen, R. (2007) 'Attenuation of Apoptosis by Chromogranin A-Induced Akt and Survivin Pathways in Prostate Cancer Cells', *Endocrinology*. Oxford University Press, 148(9), pp. 4489–4499. doi: 10.1210/en.2006-1748.

Graf, T. and Enver, T. (2009) 'Forcing cells to change lineages', *Nature*. Nature Publishing Group, 462(7273), pp. 587–594. doi: 10.1038/nature08533.

Gudbergsson, J. M. and Johnsen, K. B. (2019) 'Exosomes and autophagy: rekindling the vesicular waste hypothesis', *Journal of Cell Communication and Signaling*. Springer, 13(4), pp. 443–450. doi: 10.1007/s12079-019-00524-8.

Guo, B. B., Bellingham, S. A. and Hill, A. F. (2015) 'The neutral sphingomyelinase pathway regulates packaging of the prion protein into exosomes.', *The Journal of biological chemistry*. American Society for Biochemistry and Molecular Biology, 290(6), pp. 3455–3467. doi: 10.1074/jbc.M114.605253.

Guo, B. B., Bellingham, S. A. and Hill, A. F. (2016) 'Stimulating the Release of Exosomes Increases the Intercellular Transfer of Prions.', *The Journal of biological chemistry*. American Society for Biochemistry and Molecular Biology, 291(10), pp. 5128–37. doi: 10.1074/jbc.M115.684258.

Guo, H. *et al.* (2019) 'ONECUT2 is a driver of neuroendocrine prostate cancer', *Nature Communications*. Nature Publishing Group, 10(1), pp. 1–13. doi: 10.1038/s41467-018-08133-6.

Guo, J., Jayaprakash, P., Dan, J., Wise, P., Jang, G.-B., Liang, C., Chen, M., Woodley, D. T., Fabbri, M. and Li, W. (2017) 'PRAS40 Connects Microenvironmental Stress Signaling to Exosome-Mediated Secretion', *Molecular and Cellular Biology*, 37(19), pp. e00171-17. doi: 10.1128/MCB.

Gurunathan, S., Kang, M., Jeyaraj, M., Qasim, M. and Kim, J. (2019) 'Function, and Multifarious Therapeutic Approaches of Exosomes', *Cells*, 8(4), p. 307. doi: 10.3390/cells8040307.

Heid, C. A., Stevens, J., Livak, K. J. and Williams, P. M. (1996) 'Real Time Quantitative PCR', *Genome Research*, 6, pp. 986–994.

Heinlein, C. A. and Chang, C. (2002) 'The roles of androgen receptors and androgen-binding proteins in nongenomic androgen actions', *Molecular Endocrinology*. Narnia, 16(10), pp. 2181–2187. doi: 10.1210/me.2002-0070.

Heinlein, C. A. and Chang, C. (2004) 'Androgen receptor in prostate cancer', *Endocrine Reviews*. Oxford Academic, pp. 276–308. doi: 10.1210/er.2002-0032.

Hendrix, A., Maynard, D., Pauwels, P., Braems, G., Denys, H., Van Den Broecke, R., Lambert, J., Van Belle, S., Cocquyt, V., Gespach, C., Bracke, M., Seabra, M. C., Gahl, W. A., De Wever, O. and Westbroek, W. (2010) 'Effect of the secretory small GTPase Rab27B on breast cancer growth, invasion, and metastasis', *Journal of the National Cancer Institute*, 102(12), pp. 866–880. doi: 10.1093/jnci/djq153.

Hendrix, A. and de Wever, O. (2013) 'Rab27 GTPases distribute extracellular nanomaps for invasive growth and metastasis: Implications for prognosis and treatment', *International Journal of Molecular Sciences*. Multidisciplinary Digital Publishing Institute (MDPI), pp. 9883–9892. doi: 10.3390/ijms14059883.

Hessvik, N. P. and Llorente, A. (2018) 'Current knowledge on exosome biogenesis and release.', *Cellular and molecular life sciences : CMLS*. Springer, 75(2), pp. 193–208. doi: 10.1007/s00018-017-2595-9.

Horoszewicz, J. S., Leong, S. S., Kawinski, E., Karr, J. P., Rosenthal, H., Chu, T. M., Mirand, E. A. and Murphy, G. P. (1983) 'LNCaP model of human prostatic carcinoma.', *Cancer research*. American Association for Cancer Research, 43(4), pp. 1809–18.

Hosseini-Beheshti, E., Pham, S., Adomat, H., Li, N. and Tomlinson Guns, E. S. (2012) 'Exosomes as Biomarker Enriched Microvesicles: Characterization of Exosomal Proteins Derived from a Panel of Prostate Cell Lines with Distinct AR Phenotypes', *Molecular & Cellular Proteomics*, 11(10), pp. 863–885. doi: 10.1074/mcp.M111.014845.

Hotte, S. J. and Saad, F. (2010) 'Current management of castrate-resistant prostate cancer.', *Current oncology*. Multimed Inc., 17(2), pp. S72–S79. doi: 10.3747/co.v17i0.718.

Hu, C.-D., Choo, R. and Huang, J. (2015) 'Neuroendocrine differentiation in prostate cancer: a mechanism of radioresistance and treatment failure.', *Frontiers in oncology*. Frontiers Media SA, 5, p. 90. doi: 10.3389/fonc.2015.00090.

Ibrahim, T., Flamini, E., Mercatali, L., Sacanna, E., Serra, P. and Amadori, D. (2010) 'Pathogenesis of osteoblastic bone metastases from prostate cancer', *Cancer*. John Wiley & Sons, Ltd, 116(6), pp. 1406–1418. doi: 10.1002/cncr.24896.

Isgrò, M. A., Bottoni, P. and Scatena, R. (2015) 'Neuron-Specific Enolase as a Biomarker: Biochemical and Clinical Aspects', in *Advances in Cancer Biomarkers*. Springer, Dordrecht, pp. 125–143. doi: 10.1007/978-94-017-7215-0_9.

Ishizuya, Y., Uemura, M., Narumi, R., Tomiyama, E., Koh, Y., Matsushita, M., Nakano, K., Hayashi, Y., Wang, C., Kato, T., Hatano, K., Kawashima, A., Ujike, T., Fujita, K., Imamura, R., Adachi, J., Tomonaga, T. and Nonomura, N. (2020) 'The role of actinin-4 (ACTN4) in exosomes as a potential novel therapeutic target in castration-resistant prostate cancer', *Biochemical and Biophysical Research Communications*. Elsevier B.V., 523(3), pp. 588–594. doi: 10.1016/j.bbrc.2019.12.084.

Itoh, T., Ito, Y., Ohtsuki, Y., Ando, M., Tsukamasa, Y., Yamada, N., Naoe, T. and Akao, Y. (2012) 'Microvesicles released from hormone-refractory prostate cancer cells facilitate mouse pre-osteoblast differentiation', *Journal of Molecular Histology*, 43, pp. 509–515. doi: 10.1007/s10735-012-9415-1.

Jeppesen, D. K., Hvam, M. L., Primdahl-Bengtson, B., Boysen, A. T., Whitehead, B., Dyrskjøt, L., Ørntoft, T. F., Howard, K. A. and Ostfeld, M. S. (2014) 'Comparative analysis of discrete exosome fractions obtained by differential centrifugation', *Journal of Extracellular Vesicles*, 3, p. 25011. doi: 10.3402/jev.v3.25011.

Ji, H. (2010) 'Lysis of cultured cells for immunoprecipitation', *Cold Spring Harbor*

Protocols. Cold Spring Harbor Laboratory Press, 5(8), pp. 1–4. doi: 10.1101/pdb.prot5466.

Jin, H.-J., Kim, J. and Yu, J. (2013) 'Androgen receptor genomic regulation.', *Translational andrology and urology*. AME Publications, 2(3), pp. 157–177. doi: 10.3978/j.issn.2223-4683.2013.09.01.

Joncas, F. H., Lucien, F., Rouleau, M., Morin, F., Leong, H. S., Pouliot, F., Fradet, Y., Gilbert, C. and Toren, P. (2019) 'Plasma extracellular vesicles as phenotypic biomarkers in prostate cancer patients', *Prostate*, 79(15), pp. 1767–1776. doi: 10.1002/pros.23901.

Karantanos, T., Corn, P. G. and Thompson, T. C. (2013) 'Prostate cancer progression after androgen deprivation therapy: mechanisms of castrate resistance and novel therapeutic approaches.', *Oncogene*. NIH Public Access, 32(49), pp. 5501–11. doi: 10.1038/onc.2013.206.

Keerthikumar, S., Chisanga, D., Ariyaratne, D., Al Saffar, H., Anand, S., Zhao, K., Samuel, M., Pathan, M., Jois, M., Chilamkurti, N., Gangoda, L. and Mathivanan, S. (2016) 'ExoCarta: A Web-Based Compendium of Exosomal Cargo', *Journal of Molecular Biology*. Academic Press, 428(4), pp. 688–692. doi: 10.1016/j.jmb.2015.09.019.

Ketola, K., Vainio, P., Fey, V., Kallioniemi, O. and Iljin, K. (2010) 'Monensin Is a Potent Inducer of Oxidative Stress and Inhibitor of Androgen Signaling Leading to Apoptosis in Prostate Cancer Cells', *Molecular Cancer Therapeutics*. American Association for Cancer Research, 9(12), pp. 3175–3185. doi: 10.1158/1535-7163.MCT-10-0368.

Kibbe, W. A. (2007) 'OligoCalc: an online oligonucleotide properties calculator', *Nucleic Acids Research*, 35, pp. 43–46. doi: 10.1093/nar/gkm234.

Kim, D.-K., Kang, B., Kim, O. Y., Choi, D., Lee, J., Kim, S. R., Go, G., Yoon, Y. J., Kim, J. H., Jang, S. C., Park, K.-S., Choi, E.-J., Kim, K. P., Desiderio, D. M.,

Kim, Y.-K., Lötvall, J., Hwang, D. and Gho, Y. S. (2013) 'EVpedia: an integrated database of high-throughput data for systemic analyses of extracellular vesicles', *Journal of Extracellular Vesicles*. Co-Action Publishing, 2, p. 20384. doi: 10.3402/jev.v2i0.20384.

Kim, S.-H., Kim, K.-Y., Yu, S.-N., Park, S.-G., Yu, H.-S., Seo, Y.-K. and Ahn, S.-C. (2016) 'Monensin Induces PC-3 Prostate Cancer Cell Apoptosis via ROS Production and Ca²⁺ Homeostasis Disruption.', *Anticancer research*. International Institute of Anticancer Research, 36(11), pp. 5835–5843. doi: 10.21873/anticanres.11168.

Kosaka, N., Iguchi, H., Yoshioka, Y., Takeshita, F., Matsuki, Y. and Ochiya, T. (2010) 'Secretory mechanisms and intercellular transfer of microRNAs in living cells', *Journal of Biological Chemistry*. American Society for Biochemistry and Molecular Biology, 285(23), pp. 17442–17452. doi: 10.1074/jbc.M110.107821.

Ku, S. Y., Rosario, S., Wang, Y., Mu, P., Seshadri, M., Goodrich, Z. W., Goodrich, M. M., Labbé, D. P., Cortes Gomez, E., Wang, J., Long, H. W., Xu, B., Brown, M., Loda, M., Sawyers, C. L., Ellis, L. and Goodrich, D. W. (2017) 'Rb1 and Trp53 cooperate to suppress prostate cancer lineage plasticity, metastasis, and antiandrogen resistance HHS Public Access', *Science*, 355(6320), pp. 78–83. doi: 10.1126/science.aah4199.

Kumar, D., Gupta, D., Shankar, S. and Srivastava, R. K. (2014) 'Biomolecular characterization of exosomes released from cancer stem cells: Possible implications for biomarker and treatment of cancer', *Oncotarget*, 6(5), pp. 3280–3291.

Labrecque, M. P. *et al.* (2019) 'Molecular profiling stratifies diverse phenotypes of treatment-refractory metastatic castration-resistant prostate cancer', *Journal of Clinical Investigation*. American Society for Clinical Investigation, 129(10), pp. 4492–4505. doi: 10.1172/JCI128212.

Laemmli, U. K. (1970) 'Cleavage of structural proteins during the assembly of the

head of bacteriophage T4', *Nature*, 227(5259), pp. 680–685. doi: 10.1038/227680a0.

Lane, R. E., Korbie, D., Anderson, W., Vaidyanathan, R. and Trau, M. (2015) 'Analysis of exosome purification methods using a model liposome system and tunable-resistive pulse sensing', *Scientific Reports*, 5. doi: 10.1038/srep07639.

Lee, J. K., Phillips, J. W., Smith, B. A., Gustafson, W. C., Huang, J. and Witte Correspondence, O. N. (2016) 'N-Myc Drives Neuroendocrine Prostate Cancer Initiated from Human Prostate Epithelial Cells', *Cancer Cell*, 29, pp. 536–547. doi: 10.1016/j.ccell.2016.03.001.

Lee, T. H., Chennakrishnaiah, S., Audemard, E., Montermini, L., Meehan, B. and Rak, J. (2014) 'Oncogenic ras-driven cancer cell vesiculation leads to emission of double-stranded DNA capable of interacting with target cells', *Biochemical and Biophysical Research Communications*. Academic Press Inc., 451(2), pp. 295–301. doi: 10.1016/j.bbrc.2014.07.109.

Lehrich, B. M., Liang, Y., Khosravi, P., Federoff, H. J. and Fiandaca, M. S. (2018) 'Fetal Bovine Serum-Derived Extracellular Vesicles Persist within Vesicle-Depleted Culture Media', *International journal of molecular sciences*, 19(11), p. 3538. doi: 10.3390/ijms19113538.

Levina, E., Ji, H., Chen, M., Baig, M., Oliver, D., Ohouo, P., Lim, C.-U., Schools, G., Carmack, S., Ding, Y., Broude, E. V, Roninson, I. B., Buttyan, R. and Shtutman, M. (2015) 'Identification of novel genes that regulate androgen receptor signaling and growth of androgen-deprived prostate cancer cells', *Oncotarget*, 6(15), pp. 13088–13104.

Li, I. and Nabet, B. Y. (2019) 'Exosomes in the tumor microenvironment as mediators of cancer therapy resistance', *Molecular Cancer*. BioMed Central, 18, pp. 1–10. doi: 10.1186/s12943-019-0975-5.

Li, P., Kaslan, M., Lee, S. H., Yao, J. and Gao, Z. (2017) 'Progress in Exosome

Isolation Techniques.', *Theranostics*. Ivyspring International Publisher, 7(3), pp. 789–804. doi: 10.7150/thno.18133.

Li, W., Hu, Y., Jiang, T., Han, Y., Han, G., Chen, J. and Li, X. (2014) 'Rab27A regulates exosome secretion from lung adenocarcinoma cells A549: involvement of EPI64', *APMIS*. Blackwell Munksgaard, 122(11), pp. 1080–1087. doi: 10.1111/apm.12261.

Lin, L.-C., Gao, A. C., Lai, C.-H., Hsieh, J.-T. and Lin, H. (2017) 'Induction of neuroendocrine differentiation in castration resistant prostate cancer cells by adipocyte differentiation-related protein (ADRP) delivered by exosomes', *Cancer Letters*. Elsevier, 391, pp. 74–82. doi: 10.1016/J.CANLET.2017.01.018.

Lipianskaya, J., Cohen, A., Chen, C. J., Hsia, E., Squires, J., Li, Z., Zhang, Y., Li, W., Chen, X., Xu, H. and Huang, J. (2014) 'Androgen-deprivation therapy-induced aggressive prostate cancer with neuroendocrine differentiation', *Asian Journal of Andrology*. Medknow Publications, 16(4), pp. 541–544. doi: 10.4103/1008-682X.123669.

Liu, A. Y. and True, L. D. (2002) 'Characterization of Prostate Cell Types by CD Cell Surface Molecules', *American Journal of Pathology*, 160(1), pp. 37–43.

Livak, K. J. and Schmittgen, T. D. (2001) 'Analysis of Relative Gene Expression Data Using Real-Time Quantitative PCR and the $2^{-\Delta\Delta CT}$ Method', *Methods*, 25(4), pp. 402–408. doi: 10.1006/meth.2001.1262.

Livshits, M. A., Khomyakova, E., Evtushenko, E. G., Lazarev, V. N., Kulemin, N. A., Semina, S. E., Generozov, E. V and Govorun, V. M. (2015) 'Isolation of exosomes by differential centrifugation: Theoretical analysis of a commonly used protocol', *Scientific Reports*, 32(5), p. 17319. doi: 10.1038/srep17319.

Lonergan, P. E. and Tindall, D. J. (2011) 'Androgen receptor signaling in prostate cancer development and progression.', *Journal of carcinogenesis*. Wolters Kluwer -- Medknow Publications, 10, p. 20. doi: 10.4103/1477-3163.83937.

Lötvall, J., Hill, A. F., Hochberg, F., Buzas, E. I., Di Vizio, D., Gardiner, C., Gho,

Y. S., Kurochkin, I. V., Mathivanan, S., Quesenberry, P., Sahoo, S., Tahara, H., Wauben, M. H., Witwer, K. W. and Théry, C. (2014) 'Minimal experimental requirements for definition of extracellular vesicles and their functions: a position statement from the International Society for Extracellular Vesicles', *Journal of Extracellular Vesicles*, 3, p. 26913. doi: 10.3402/jev.v3.26913.

Ludwig, A.-K. *et al.* (2018) 'Precipitation with polyethylene glycol followed by washing and pelleting by ultracentrifugation enriches extracellular vesicles from tissue culture supernatants in small and large scales', *Journal of Extracellular Vesicles*. Taylor & Francis, 7(1), p. 1528109. doi: 10.1080/20013078.2018.1528109.

Ludwig, N., Whiteside, T. L. and Reichert, T. E. (2019) 'Challenges in Exosome Isolation and Analysis in Health and Disease', *International Journal of Molecular Sciences*, 20(19), p. 4684. doi: 10.3390/ijms20194684.

Macia, E., Ehrlich, M., Massol, R., Boucrot, E., Brunner, C. and Kirchhausen, T. (2006) 'Dynasore, a Cell-Permeable Inhibitor of Dynamin', *Developmental Cell*. Elsevier, 10(6), pp. 839–850. doi: 10.1016/j.devcel.2006.04.002.

Maina, P. K., Shao, P., Liu, Q., Fazli, L., Tyler, S., Nasir, M., Dong, X. and Qi, H. H. (2016) 'c-MYC drives histone demethylase PHF8 during neuroendocrine differentiation and in castration-resistant prostate cancer.', *Oncotarget*. Impact Journals, LLC, 7(46), pp. 75585–75602. doi: 10.18632/oncotarget.12310.

Malla, B., Aebbersold, D. M. and Dal Pra, A. (2018) 'Protocol for serum exosomal miRNAs analysis in prostate cancer patients treated with radiotherapy', *Journal of Translational Medicine*. BioMed Central, 16, p. 223. doi: 10.1186/s12967-018-1592-6.

Mao, H.-L., Zhu, Z.-Q. and Chen, C. D. (2009) 'The androgen receptor in hormone-refractory prostate cancer.', *Asian journal of andrology*. Wolters Kluwer -- Medknow Publications, 11, pp. 69–73. doi: 10.1038/aja.2008.14.

Marcu, M., Radu, E. and Sajin, M. (2010) 'Neuroendocrine transdifferentiation of prostate carcinoma cells and its prognostic significance', *Romanian Journal of Morphology and Embryology*, 51(1), pp. 7–12.

Markowska, A., Kaysiewicz, J., Markowska, J. and Huczyński, A. (2019) 'Doxycycline, salinomycin, monensin and ivermectin repositioned as cancer drugs', *Bioorganic and Medicinal Chemistry Letters*. Elsevier Ltd, 29(13), pp. 1549–1554. doi: 10.1016/j.bmcl.2019.04.045.

Mateescu, B. *et al.* (2017) 'Obstacles and opportunities in the functional analysis of extracellular vesicle RNA - An ISEV position paper', *Journal of Extracellular Vesicles*. Taylor & Francis, 6(1), p. 1286095. doi: 10.1080/20013078.2017.1286095.

Mathivanan, S., Fahner, C. J., Reid, G. E. and Simpson, R. J. (2012) 'ExoCarta 2012: database of exosomal proteins, RNA and lipids', *Nucleic Acid Research*, 40, pp. D1241–D1244. doi: 10.1093/nar/gkr828.

Mcgough, I. J. and Vincent, J.-P. (2016) 'Exosomes in developmental signalling', *The Company of Biologists*, 143, pp. 2482–2493. doi: 10.1242/dev.126516.

Meacham, C. E. and Morrison, S. J. (2013) 'Tumour heterogeneity and cancer cell plasticity', *Nature*. Howard Hughes Medical Institute, 501(7467), pp. 328–337. doi: 10.1038/nature12624.

Menck, K., Sönmezer, C., Stefan Worst, T., Schulz, M., Helene Dihazi, G., Streit, F., Erdmann, G., Kling, S., Boutros, M., Binder, C. and Christina Gross, J. (2017) 'Neutral sphingomyelinases control extracellular vesicles budding from the plasma membrane', *Journal of Extracellular Vesicles*, 6, p. 1378056. doi: 10.1080/20013078.2017.1378056.

Messenger, S. W., Woo, S. S., Sun, Z. and Martin, T. F. J. (2018) 'A Ca²⁺ - stimulated exosome release pathway in cancer cells is regulated by Munc13-4', *Journal of Cell Biology*, 217(8), pp. 2877–2890. doi: 10.1083/jcb.201710132.

Mittelbrunn, M. and Sánchez-Madrid, F. (2012) 'Intercellular communication: Diverse structures for exchange of genetic information', *Nature Reviews Molecular Cell Biology*. Europe PMC Funders, 13(5), pp. 328–335. doi: 10.1038/nrm3335.

Mizutani, K., Terazawa, R., Kameyama, K., Kato, T., Horie, K., Tsuchiya, T., Seike, K., Ehara, H., Fujita, Y., Kawakami, K., Ito, M. and Deguchi, T. (2014) 'Isolation of prostate cancer-related exosomes.', *Anticancer research*. International Institute of Anticancer Research, 34(7), pp. 3419–3424.

Montecalvo, A., Larregina, A. T., Shufesky, W. J., Stolz, D. B., Sullivan, M. L. G., Karlsson, J. M., Baty, C. J., Gibson, G. A., Erdos, G., Wang, Z., Milosevic, J., Tkacheva, O. A., Divito, S. J., Jordan, R., Lyons-Weiler, J., Watkins, S. C. and Morelli, A. E. (2012) 'Mechanism of transfer of functional microRNAs between mouse dendritic cells via exosomes', *Blood*. American Society of Hematology, 119(3), pp. 756–766. doi: 10.1182/blood-2011-02-338004.

Morelli, A. E., Larregina, A. T., Shufesky, W. J., Sullivan, M. L. G., Stolz, D. B., Papworth, G. D., Zahorchak, A. F., Logar, A. J., Wang, Z., Watkins, S. C., Falo, L. D. and Thomson, A. W. (2004) 'Endocytosis, intracellular sorting, and processing of exosomes by dendritic cells', *Blood*. American Society of Hematology, 104(10), pp. 3257–3266. doi: 10.1182/blood-2004-03-0824.

Mosmann, T. (1983) 'Rapid colorimetric assay for cellular growth and survival: Application to proliferation and cytotoxicity assays', *Journal of Immunological Methods*, 65(1–2), pp. 55–63. doi: 10.1016/0022-1759(83)90303-4.

Mozzi, A., Guerini, F. R., Forni, D., Costa, A. S., Nemni, R., Baglio, F., Cabinio, M., Riva, S., Pontremoli, C., Clerici, M., Sironi, M. and Cagliani, R. (2017) 'REST, a master regulator of neurogenesis, evolved under strong positive selection in humans and in non human primates', *Scientific Reports*. Nature Publishing Group, 7(1), p. 9530. doi: 10.1038/s41598-017-10245-w.

Mueller, O., Lightfoot, S. and Schroeder, A. (2016) *RNA Integrity Number (RIN)-*

Standardization of RNA Quality Control Application.

Mulcahy, L. A., Pink, R. C. and Carter, D. R. F. (2014) 'Routes and mechanisms of extracellular vesicle uptake.', *Journal of extracellular vesicles*. Taylor & Francis, 3, p. 24641. doi: 10.3402/jev.v3.24641.

Muralidharan-Chari, V., Clancy, J. W., Sedgwick, A. and D'Souza-Schorey, C. (2010) 'Microvesicles: Mediators of extracellular communication during cancer progression', *Journal of Cell Science*, 123(10), pp. 1603–1611. doi: 10.1242/jcs.064386.

Nakamura, K., Sawada, K., Kinose, Y., Yoshimura, A., Toda, A., Nakatsuka, E., Hashimoto, K., Mabuchi, S., Morishige, K. I., Kurachi, H., Lengyel, E. and Kimura, T. (2017) 'Exosomes promote ovarian cancer cell invasion through transfer of CD44 to peritoneal mesothelial cells', *Molecular Cancer Research*. American Association for Cancer Research Inc., 15(1), pp. 78–92. doi: 10.1158/1541-7786.MCR-16-0191.

Nanbo, A., Kawanishi, E., Yoshida, R. and Yoshiyama, H. (2013) 'Exosomes Derived from Epstein-Barr Virus-Infected Cells Are Internalized via Caveola-Dependent Endocytosis and Promote Phenotypic Modulation in Target Cells', *Journal of Virology*. American Society for Microbiology, 87(18), pp. 10334–10347. doi: 10.1128/jvi.01310-13.

Van Niel, G., D'Angelo, G. and Raposo, G. (2018) 'Shedding light on the cell biology of extracellular vesicles', *Nature Reviews Molecular Cell Biology*. Nature Publishing Group, 19(4), pp. 213–228. doi: 10.1038/nrm.2017.125.

Nierode, G. J., Gopal, S., Kwon, P., Clark, D. S., Schaffer, D. V. and Dordick, J. S. (2019) 'High-throughput identification of factors promoting neuronal differentiation of human neural progenitor cells in microscale 3D cell culture', *Biotechnology and Bioengineering*, 116, pp. 168–180. doi: 10.1002/bit.26839.

Nishimura, M., Nikawa, T., Kawano, Y., Nakayama, M. and Ikeda, M. (2008) 'Effects of dimethyl sulfoxide and dexamethasone on mRNA expression of

housekeeping genes in cultures of C2C12 myotubes', *Biochemical and Biophysical Research Communications*. Academic Press, 367(3), pp. 603–608. doi: 10.1016/j.bbrc.2008.01.006.

Novilla, M. N. (2011) 'Ionophores', in *Reproductive and Developmental Toxicology*. Elsevier Inc., pp. 373–384. doi: 10.1016/B978-0-12-382032-7.10029-3.

Ortega, F. G., Roefs, M. T., de Miguel Perez, D., Kooijmans, S. A., de Jong, O. G., Sluijter, J. P., Schiffelers, R. M. and Vader, P. (2019) 'Interfering with endolysosomal trafficking enhances release of bioactive exosomes', *Nanomedicine: Nanotechnology, Biology, and Medicine*. Elsevier Inc., 20, p. 102014. doi: 10.1016/j.nano.2019.102014.

Ostenfeld, M. S. *et al.* (2014) 'Cellular disposal of miR23b by RAB27-dependent exosome release is linked to acquisition of metastatic properties', *Cancer Research*. American Association for Cancer Research Inc., 74(20), pp. 5758–5771. doi: 10.1158/0008-5472.CAN-13-3512.

Ostrowski, M. *et al.* (2010) 'Rab27a and Rab27b control different steps of the exosome secretion pathway', *Nature Cell Biology*. Nature Publishing Group, 12, pp. 19–30. doi: 10.1038/ncb2000.

Pan, J., Ding, M., Xu, K., Yang, C. and Mao, L.-J. (2017) 'Exosomes in diagnosis and therapy of prostate cancer.', *Oncotarget*. Impact Journals, LLC, 8(57), pp. 97693–97700. doi: 10.18632/oncotarget.18532.

Panigrahi, G. K., Praharaj, P. P., Peak, T. C., Long, J., Singh, R., Rhim, J. S., Abd Elmageed, Z. Y. and Deep, G. (2018) 'Hypoxia-induced exosome secretion promotes survival of African-American and Caucasian prostate cancer cells.', *Scientific reports*. Nature Publishing Group, 8(1), p. 3853. doi: 10.1038/s41598-018-22068-4.

Patel, G. K., Chugh, N. and Tripathi, M. (2019) 'Neuroendocrine differentiation of

prostate cancer— An intriguing example of tumor evolution at play’, *Cancers*. MDPI AG, 11(10), p. 1405. doi: 10.3390/cancers11101405.

Peak, T. C., Panigrahi, G. K., Praharaj, P. P., Su, Y., Shi, L., Chyr, J., Rivera-Chávez, J., Flores-Bocanegra, L., Singh, R., Vander Griend, D. J., Oberlies, N. H., Kerr, B. A., Hemal, A., Bitting, R. L. and Deep, G. (2020) ‘Syntaxin 6-mediated exosome secretion regulates enzalutamide resistance in prostate cancer’, *Molecular Carcinogenesis*. John Wiley and Sons Inc., 59, pp. 62–72. doi: 10.1002/mc.23129.

Peinado, H. *et al.* (2012) ‘Melanoma exosomes educate bone marrow progenitor cells toward a pro-metastatic phenotype through MET’, *Nature Medicine*, 18(6), pp. 883–891. doi: 10.1038/nm.2753.

Petrylak, D. P., Tangen, C. M., Hussain, M. H. A., Lara, P. N., Jones, J. A., Taplin, M. E., Burch, P. A., Berry, D., Moinpour, C., Kohli, M., Benson, M. C., Small, E. J., Raghavan, D. and Crawford, E. D. (2004) ‘Docetaxel and Estramustine Compared with Mitoxantrone and Prednisone for Advanced Refractory Prostate Cancer’, *New England Journal of Medicine*. Massachusetts Medical Society , 351(15), pp. 1513–1520. doi: 10.1056/NEJMoa041318.

Pezaro, C., Woo, H. H. and Davis, I. D. (2014) ‘Prostate cancer: measuring PSA’, *Internal Medicine Journal*. Blackwell Publishing, 44(5), pp. 433–440. doi: 10.1111/imj.12407.

Pritchard, C. C., Cheng, H. H. and Tewari, M. (2012) ‘MicroRNA profiling: Approaches and considerations’, *Nature Reviews Genetics*. Nature Publishing Group, 13(5), pp. 358–369. doi: 10.1038/nrg3198.

Ranno, S., Motta, M., Rampello, E., Risino, C., Bennati, E. and Malaguarnera, M. (2005) ‘The chromogranin-A (CgA) in prostate cancer’, *Archives of Gerontology and Geriatrics*. Elsevier, 43(1), pp. 117–126. doi: 10.1016/J.ARCHGER.2005.09.008.

Rapa, I., Ceppi, P., Bollito, E., Rosas, R., Cappia, S., Bacillo, E., Porpiglia, F., Berruti, A., Papotti, M. and Volante, M. (2008) 'Human ASH1 expression in prostate cancer with neuroendocrine differentiation', *Modern Pathology*. Nature Publishing Group, 21(6), pp. 700–707. doi: 10.1038/modpathol.2008.39.

Raposo, A. A. S. F., Vasconcelos, F. F., Drechsel, D., Marie, C., Johnston, C., Dolle, D., Bithell, A., Gillotin, S., van den Berg, D. L. C., Ettwiller, L., Flicek, P., Crawford, G. E., Parras, C. M., Berninger, B., Buckley, N. J., Guillemot, F. and Castro, D. S. (2015) 'Ascl1 Coordinately Regulates Gene Expression and the Chromatin Landscape during Neurogenesis.', *Cell reports*. Elsevier, 10(9), pp. 1544–1556. doi: 10.1016/j.celrep.2015.02.025.

Raposo, G. and Stoorvogel, W. (2013) 'Extracellular vesicles: Exosomes, microvesicles, and friends', *Journal of Cell Biology*, pp. 373–383. doi: 10.1083/jcb.201211138.

Rawla, P. (2019) 'Epidemiology of Prostate Cancer', *Review World J Oncol*, 10(2), pp. 63–89. doi: 10.14740/wjon1191.

Read, J., Ingram, A., Al Saleh, H. A., Platko, K., Gabriel, K., Kapoor, A., Pinthus, J., Majeed, F., Qureshi, T. and Al-Nedawi, K. (2017) 'Nuclear transportation of exogenous epidermal growth factor receptor and androgen receptor via extracellular vesicles', *European Journal of Cancer*. Elsevier Ltd, 70, pp. 62–74. doi: 10.1016/j.ejca.2016.10.017.

Rider, M. A., Hurwitz, S. N., Meckes, D. G. and Jr. (2016) 'ExtraPEG: A Polyethylene Glycol-Based Method for Enrichment of Extracellular Vesicles.', *Scientific reports*. Nature Publishing Group, 6, p. 23978. doi: 10.1038/srep23978.

Ritch, C. R. and Cookson, M. S. (2016) 'Advances in the management of castration resistant prostate cancer.', *BMJ (Clinical research ed.)*. British Medical Journal Publishing Group, 355, p. i4405. doi: 10.1136/bmj.i4405.

La Rosa, S., Marando, A., Gatti, G., Rapa, I., Volante, M., Papotti, M., Sessa, F. and Capella, C. (2013) 'Achaete-scute homolog 1 as a marker of poorly differentiated neuroendocrine carcinomas of different sites: a validation study using immunohistochemistry and quantitative real-time polymerase chain reaction on 335 cases', *Human Pathology*. W.B. Saunders, 44(7), pp. 1391–1399. doi: 10.1016/J.HUMPATH.2012.11.013.

Roudier, M. P., True, L. D., Higano, C. S., Vesselle, H., Ellis, W., Lange, P. and Vessella, R. L. (2003) 'Phenotypic heterogeneity of end-stage prostate carcinoma metastatic to bone', *Human Pathology*. W.B. Saunders, 34(7), pp. 646–653. doi: 10.1016/S0046-8177(03)00190-4.

Sampson, N., Neuwirt, H., Puhr, M., Klocker, H. and Eder, I. E. (2013) 'In vitro model systems to study androgen receptor signaling in prostate cancer', *Endocrine-Related Cancer*, 20(2), pp. R49–R64. doi: 10.1530/ERC-12-0401.

Saraon, P., Jarvi, K. and Diamandis, E. P. (2011) 'Molecular alterations during progression of prostate cancer to androgen independence.', *Clinical chemistry*. Clinical Chemistry, 57(10), pp. 1366–75. doi: 10.1373/clinchem.2011.165977.

Sartor, A. O. (2011) 'Progression of metastatic castrate-resistant prostate cancer: impact of therapeutic intervention in the post-docetaxel space', *Journal of Hematology & Oncology*. BioMed Central, 4(1), p. 18. doi: 10.1186/1756-8722-4-18.

Savina, A., Fader, C. M., Damiani, M. T. and Colombo, M. I. (2005) 'Rab11 Promotes Docking and Fusion of Multivesicular Bodies in a Calcium-Dependent Manner', *Traffic*. John Wiley & Sons, Ltd (10.1111), 6(2), pp. 131–143. doi: 10.1111/j.1600-0854.2004.00257.x.

Savina, A., Furlán, M., Vidal, M. and Colombo, M. I. (2003) 'Exosome release is regulated by a calcium-dependent mechanism in K562 cells', *Journal of Biological Chemistry*. American Society for Biochemistry and Molecular Biology, 278(22), pp. 20083–20090. doi: 10.1074/jbc.M301642200.

Schmidt, O. and Teis, D. (2012) 'The ESCRT machinery', *Current Biology*. Cell Press, 22(4), p. R116. doi: 10.1016/j.cub.2012.01.028.

Schwarzenbach and Heidi (2017) 'Methods for quantification and characterization of microRNAs in cell-free plasma/serum, normal exosomes and tumor-derived exosomes', *Translational Cancer Research*, 7(2), pp. S253–S263. doi: 10.21037/16263.

Sedelaar, J. P. M. and Isaacs, J. T. (2009) 'Tissue culture media supplemented with 10% fetal calf serum contains a castrate level of testosterone.', *The Prostate*. NIH Public Access, 69(16), pp. 1724–9. doi: 10.1002/pros.21028.

Servier Medical Art. 2020. *SMART - Servier Medical ART*. [online] Available at: <<https://smart.servier.com>>.

Shang, Y., Myers, M. and Brown, M. (2002) 'Formation of the androgen receptor transcription complex', *Molecular Cell*. Cell Press, 9(3), pp. 601–610. doi: 10.1016/S1097-2765(02)00471-9.

Shao, H., Im, H., Castro, C. M., Breakefield, X., Weissleder, R. and Lee, H. (2018) 'New Technologies for Analysis of Extracellular Vesicles', *Chemical Reviews*. American Chemical Society, 118(4), pp. 1917–1950. doi: 10.1021/acs.chemrev.7b00534.

Sharifi, N., Dahut, W. L., Steinberg, S. M., Figg, W. D., Tarassoff, C., Arlen, P. and Gulley, J. L. (2005) 'A retrospective study of the time to clinical endpoints for advanced prostate cancer', *BJU International*. John Wiley & Sons, Ltd, 96(7), pp. 985–989. doi: 10.1111/j.1464-410X.2005.05798.x.

Sharifi, N., Gulley, J. L. and Dahut, W. L. (2005) 'Androgen Deprivation Therapy for Prostate Cancer', *JAMA*. American Medical Association, 294(2), p. 238. doi: 10.1001/jama.294.2.238.

Shelke, G. V., Lässer, C., Gho, Y. S. and Lötvall, J. (2014) 'Importance of

exosome depletion protocols to eliminate functional and RNA-containing extracellular vesicles from fetal bovine serum.’, *Journal of Extracellular Vesicles*. Taylor & Francis, 3, p. 24783. doi: 10.3402/jev.v3.24783.

Shen, B., Fang, Y., Wu, N. and Gould, S. J. (2011) ‘Biogenesis of the posterior pole is mediated by the exosome/microvesicle protein-sorting pathway’, *Journal of Biological Chemistry*. American Society for Biochemistry and Molecular Biology, 286(51), pp. 44162–44176. doi: 10.1074/jbc.M111.274803.

Shen, R., Dorai, T., Szaboles, M., Katz, A. E., Olsson, C. A. and Buttyan, R. (1997) ‘Transdifferentiation of cultured human prostate cancer cells to a neuroendocrine cell phenotype in a hormone-depleted medium.’, *Urologic oncology*, 3(2), pp. 67–75. doi: 10.1016/s1078-1439(97)00039-2.

Sheridan, C. (2016) ‘Exosome cancer diagnostic reaches market’, *Nature biotechnology*. Nature Publishing Group, 34(4), pp. 359–360. doi: 10.1038/nbt0416-359.

Shi, Y., Han, J. J., Tennakoon, J. B., Mehta, F. F., Merchant, F. A., Burns, A. R., Howe, M. K., McDonnell, D. P. and Frigo, D. E. (2013) ‘Androgens promote prostate cancer cell growth through induction of autophagy’, *Molecular Endocrinology*. The Endocrine Society, 27(2), pp. 280–295. doi: 10.1210/me.2012-1260.

Sikora, M. J., Johnson, M. D., Lee, A. V. and Oesterreich, S. (2016) ‘Endocrine Response Phenotypes Are Altered by Charcoal-Stripped Serum Variability’, *Endocrinology*. Narnia, 157(10), pp. 3760–3766. doi: 10.1210/en.2016-1297.

Soares Martins, T., Catita, J., Martins Rosa, I., B da Cruz Silva, O. A. and Gabriela Henriques, A. (2018) ‘Exosome isolation from distinct biofluids using precipitation and column-based approaches’, *PLoS ONE*, 13(6), p. e0198820. doi: 10.1371/journal.pone.0198820.

Soekmadji, C., Riches, J. D., Russell, P. J., Ruelcke, J. E., McPherson, S., Wang, C., Hovens, C. M., Corcoran, N. M., BioResource, T. A. P. C. C., Hill, M. M. and

Nelson, C. C. (2017) 'Modulation of paracrine signaling by CD9 positive small extracellular vesicles mediates cellular growth of androgen deprived prostate cancer', *Oncotarget*. Impact Journals, LLC, 8(32), pp. 52237–52255. doi: 10.18632/oncotarget.11111.

Soundararajan, R., Paranjape, A. N., Maity, S., Aparicio, A. and Mani, S. A. (2018) 'EMT, stemness and tumor plasticity in aggressive variant neuroendocrine prostate cancers', *Biochimica et Biophysica Acta - Reviews on Cancer*. Elsevier, 1870(2), pp. 229–238. doi: 10.1016/j.bbcan.2018.06.006.

Spiotto, M. T. and Chung, T. D. K. (2000) 'STAT3 mediates IL-6-induced neuroendocrine differentiation in prostate cancer cells', *The Prostate*. John Wiley & Sons, Ltd, 42(3), pp. 186–195. doi: 10.1002/(SICI)1097-0045(20000215)42:3<186::AID-PROS4>3.0.CO;2-E.

Su, M.-J., Parayath, N. N. and Amiji, M. M. (2018) '11 - Exosome-Mediated Communication in the Tumor Microenvironment', in *Diagnostic and Therapeutic Applications of Exosomes in Cancer*, pp. 187–218. doi: 10.1016/B978-0-12-812774-2.00011-0.

Suarez, C. D., Deng, X. and Hu, C.-D. (2014) 'Targeting CREB inhibits radiation-induced neuroendocrine differentiation and increases radiation-induced cell death in prostate cancer cells', *Am J Cancer Res*, 4(6), pp. 850–861.

Subedi, P., Schneider, M., Philipp, J., Azimzadeh, O., Metzger, F., Moertl, S., Atkinson, M. J. and Tapio, S. (2019) 'Comparison of methods to isolate proteins from extracellular vesicles for mass spectrometry-based proteomic analyses', *Analytical Biochemistry*. Academic Press Inc., 584, p. 113390. doi: 10.1016/j.ab.2019.113390.

Sumida, K., Igarashi, Y., Toritsuka, N., Matsushita, T., Abe-Tomizawa, K., Aoki, M., Urushidani, T., Yamada, H. and Ohno, Y. (2011) 'Effects of DMSO on gene expression in human and rat hepatocytes.', *Human & experimental toxicology*. SAGE Publications Sage UK: London, England, 30(10), pp. 1701–9. doi:

10.1177/0960327111399325.

Svensson, K. J., Christianson, H. C., Wittrup, A., Bourseau-Guilmain, E., Lindqvist, E., Svensson, L. M., Mörgelin, M. and Belting, M. (2013) 'Exosome uptake depends on ERK1/2-heat shock protein 27 signaling and lipid raft-mediated endocytosis negatively regulated by caveolin-1', *Journal of Biological Chemistry*. American Society for Biochemistry and Molecular Biology, 288(24), pp. 17713–17724. doi: 10.1074/jbc.M112.445403.

Szatanek, R., Baj-Krzyworzeka, M., Zimoch, J., Lekka, M., Siedlar, M. and Baran, J. (2017) 'The Methods of Choice for Extracellular Vesicles (EVs) Characterization.', *International journal of molecular sciences*. Multidisciplinary Digital Publishing Institute (MDPI), 18(6). doi: 10.3390/ijms18061153.

Szatanek, R., Baran, J., Siedlar, M. and Baj-Krzyworzeka, M. (2015) 'Isolation of extracellular vesicles: Determining the correct approach (Review)', *International Journal of Molecular Medicine*. Spandidos Publications, 36, pp. 11–17. doi: 10.3892/ijmm.2015.2194.

Tai, Y.-L., Lin, C.-J., Li, T.-K., Shen, T.-L., Hsieh, J.-T. and Chen, B. P. C. (2020) 'The role of extracellular vesicles in prostate cancer with clinical applications', *Endocrine-Related Cancer*. Bioscientifica, 27(5), pp. 133–144. doi: 10.1530/erc-20-0021.

Takasugi, M., Okada, R., Takahashi, A., Virya Chen, D., Watanabe, S. and Hara, E. (2017) 'Small extracellular vesicles secreted from senescent cells promote cancer cell proliferation through EphA2', *Nature Communications*. Nature Publishing Group, 8(1), pp. 1–11. doi: 10.1038/ncomms15728.

Tan, M. H. E., Li, J., Xu, H. E., Melcher, K. and Yong, E. (2015) 'Androgen receptor: structure, role in prostate cancer and drug discovery.', *Acta pharmacologica Sinica*. Nature Publishing Group, 36, pp. 3–23. doi: 10.1038/aps.2014.18.

Tang, Y.-T., Huang, Y.-Y., Zheng, L., Qin, S.-H., Xu, X.-P., An, T.-X., Xu, Y., Wu,

Y.-S., Hu, X.-M., Ping, B.-H. and Wang, Q. (2017a) 'Comparison of isolation methods of exosomes and exosomal RNA from cell culture medium and serum', *International journal of molecular medicine*. Spandidos Publications, 40(3), pp. 834–844. doi: 10.3892/ijmm.2017.3080.

Tang, Y.-T., Huang, Y.-Y., Zheng, L., Qin, S.-H., Xu, X.-P., An, T.-X., Xu, Y., Wu, Y.-S., Hu, X.-M., Ping, B.-H. and Wang, Q. (2017b) 'Comparison of isolation methods of exosomes and exosomal RNA from cell culture medium and serum', *International Journal of Molecular Medicine*. Spandidos Publications, 40(3), pp. 834–844. doi: 10.3892/ijmm.2017.3080.

Taylor, S., Wakem, M., Dijkman, G., Alsarraj, M. and Nguyen, M. (2010) 'A practical approach to RT-qPCR—Publishing data that conform to the MIQE guidelines', *Methods*, 50, pp. s1–s5. doi: 10.1016/j.ymeth.2010.01.005.

Terry, S. and Beltran, H. (2014) 'The Many Faces of Neuroendocrine Differentiation in Prostate Cancer Progression', *Frontiers in Oncology*. Frontiers, 4, p. 60. doi: 10.3389/fonc.2014.00060.

Tetta, C., Ghigo, E., Silengo, L., Deregibus, M. C. and Camussi, G. (2013) 'Extracellular vesicles as an emerging mechanism of cell-to-cell communication', *Endocrine*. Springer, 44, pp. 11–19. doi: 10.1007/s12020-012-9839-0.

Théry, C. (2011) 'Exosomes: secreted vesicles and intercellular communications.', *F1000 Biology Reports*. Faculty of 1000 Ltd, 3(15), pp. 1–8. doi: 10.3410/B3-15.

Théry, C. *et al.* (2018) 'Minimal information for studies of extracellular vesicles 2018 (MISEV2018): a position statement of the International Society for Extracellular Vesicles and update of the MISEV2014 guidelines', *Journal of Extracellular Vesicles*. Andrew F Hill, 7, p. 1535750. doi: 10.1080/20013078.2018.1535750.

Théry, C., Amigorena, S., Raposo, G. and Clayton, A. (2006) 'Isolation and

Characterization of Exosomes from Cell Culture Supernatants and Biological Fluids', *Current Protocols in Cell Biology*. Wiley-Blackwell, 30(1), pp. 3.22.1-3.22.29. doi: 10.1002/0471143030.cb0322s30.

Towbin, H., Staehelin, T. and Gordon, J. (1979) 'Electrophoretic transfer of proteins from polyacrylamide gels to nitrocellulose sheets: Procedure and some applications (ribosomal proteins/radioimmunoassay/fluorescent antibody assay/peroxidase-conjugated antibody/autoradiography)', *Biochemistry*, 76(9), pp. 4350–4354.

Trajkovic, K., Hsu, C., Chiantia, S., Rajendran, L., Wenzel, D., Wieland, F., Schwille, P., Brügger, B. and Simons, M. (2008) 'Ceramide triggers budding of exosome vesicles into multivesicular endosomes', *Science*, 319(5867), pp. 1244–1247. doi: 10.1126/science.1153124.

Tricarico, C., Clancy, J. and D'Souza-Schorey, C. (2017) 'Biology and biogenesis of shed microvesicles', *Small GTPases*. Taylor and Francis Inc., 8(4), pp. 220–232. doi: 10.1080/21541248.2016.1215283.

Turturici, G., Tinnirello, R., Sconzo, G. and Geraci, F. (2014) 'Extracellular membrane vesicles as a mechanism of cell-to-cell communication: Advantages and disadvantages', *American Journal of Physiology - Cell Physiology*. American Physiological Society, 306(7), pp. 621–633. doi: 10.1152/ajpcell.00228.2013.

Vader, P., Breakefield, X. O. and Wood, M. J. A. (2014) 'Extracellular vesicles: emerging targets for cancer therapy.', *Trends in molecular medicine*. Elsevier, 20(7), pp. 385–93. doi: 10.1016/j.molmed.2014.03.002.

Verma, Mukesh, Patel, P. and Verma, Mudit (2011) 'Biomarkers in Prostate Cancer Epidemiology', *Cancers*. Molecular Diversity Preservation International, 3(4), pp. 3773–3798. doi: 10.3390/cancers3043773.

Vlaeminck-Guillem, V. (2018) 'Extracellular Vesicles in Prostate Cancer Carcinogenesis, Diagnosis, and Management', *Frontiers in Oncology*. Frontiers,

8, p. 222. doi: 10.3389/fonc.2018.00222.

Wang, T., Gilkes, D. M., Takano, N., Xiang, L., Luo, W., Bishop, C. J., Chaturvedi, P., Green, J. J. and Semenza, G. L. (2014) 'Hypoxia-inducible factors and RAB22A mediate formation of microvesicles that stimulate breast cancer invasion and metastasis.', *Proceedings of the National Academy of Sciences of the United States of America*. National Academy of Sciences, 111(31), pp. E3234–E3242. doi: 10.1073/pnas.1410041111.

Wang, Xiaobin, Wang, Xi, Zhu, Z., Li, W., Yu, G., Jia, Z. and Wang, Xiangwei (2019) 'Prostate carcinoma cell-derived exosomal MicroRNA-26a modulates the metastasis and tumor growth of prostate carcinoma', *Biomedicine & Pharmacotherapy*. Elsevier Masson, 117, p. 109109. doi: 10.1016/J.BIOPHA.2019.109109.

Wang, Xin *et al.* (2018) 'Monensin inhibits cell proliferation and tumor growth of chemo-resistant pancreatic cancer cells by targeting the EGFR signaling pathway', *Scientific Reports*. Nature Publishing Group, 8, p. 17914. doi: 10.1038/s41598-018-36214-5.

Wei, Z., Batagov, A. O., Carter, D. R. F. and Krichevsky, A. M. (2016) 'Fetal Bovine Serum RNA Interferes with the Cell Culture derived Extracellular RNA', *Scientific Reports*. Nature Publishing Group, 6(1), p. 31175. doi: 10.1038/srep31175.

Welton, J. L., Webber, J. P., Botos, L.-A., Jones, M. and Clayton, A. (2015) 'Ready-made chromatography columns for extracellular vesicle isolation from plasma.', *Journal of extracellular vesicles*. Taylor & Francis, 4, p. 27269. doi: 10.3402/jev.v4.27269.

Wiedenmann, B., Franke, W. W., Kuhn, C., Moll, R. and Gould, V. E. (1986) 'Synaptophysin: a marker protein for neuroendocrine cells and neoplasms.', *Proceedings of the National Academy of Sciences of the United States of America*. National Academy of Sciences, 83(10), pp. 3500–4. doi:

10.1073/pnas.83.10.3500.

Willms, E., Johansson, H. J., Mäger, I., Lee, Y., Blomberg, K. E. M., Sadik, M., Alaarg, A., Smith, C. I. E., Lehtiö, J., EL Andaloussi, S., Wood, M. J. A. and Vader, P. (2016) 'Cells release subpopulations of exosomes with distinct molecular and biological properties', *Scientific Reports*. Nature Publishing Group, 6, p. 22519. doi: 10.1038/srep22519.

Wilson, Cornelia M., Naves, T., Vincent, F., Melloni, B., Bonnaud, F., Lalloué, F. and Jauberteau, M. O. (2014) 'Sortilin mediates the release and transfer of exosomes in concert with two tyrosine kinase receptors', *Journal of Cell Science*. Company of Biologists Ltd, 127(18), pp. 3983–3997. doi: 10.1242/jcs.149336.

Wilson, Cornelia M, Naves, T., Vincent, F., Melloni, B., Bonnaud, F., Lalloué, F. and Jauberteau, M.-O. (2014) 'Sortilin mediates the release and transfer of exosomes in concert with two tyrosine kinase receptors.', *Journal of cell science*. The Company of Biologists Ltd, 127, pp. 3983–97. doi: 10.1242/jcs.149336.

Witwer, K. W., Buzás, E. I., Bemis, L. T., Bora, A., Lässer, C., Lötvall, J., Nolte-’t Hoen, E. N., Piper, M. G., Sivaraman, S., Skog, J., Théry, C., Wauben, M. H. and Hochberg, F. (2013) 'Standardization of sample collection, isolation and analysis methods in extracellular vesicle research.', *Journal of extracellular vesicles*. Taylor & Francis, 2, p. 20360. doi: 10.3402/jev.v2i0.20360.

Wong, M. L. and Medrano, J. F. (2005) 'Real-time PCR for mRNA quantitation', *BioTechniques*. Future Science Ltd London, UK , 39(1), pp. 75–85. doi: 10.2144/05391RV01.

Xu, J., Camfield, R. and Gorski, S. M. (2018) 'The interplay between exosomes and autophagy-partners in crime', *Journal of Cell Science*, 131, p. jcs215210. doi: 10.1242/jcs.215210.

Xu, Y., Qin, S., An, T., Tang, Y., Huang, Y. and Zheng, L. (2017) 'MiR-145 detection in urinary extracellular vesicles increase diagnostic efficiency of

prostate cancer based on hydrostatic filtration dialysis method', *The Prostate*. John Wiley and Sons Inc., 77(10), pp. 1167–1175. doi: 10.1002/pros.23376.

Yang, J. M. and Gould, S. J. (2013) 'The cis-acting signals that target proteins to exosomes and microvesicles', *Biochemical Society Transactions*. Biochem Soc Trans, 41, pp. 277–282. doi: 10.1042/BST20120275.

Yuan, T. C., Veeramani, S., Lin, F. F., Kondrikou, D., Zelivianski, S., Igawa, T., Karan, D., Batra, S. K. and Lin, M. F. (2006) 'Androgen deprivation induces human prostate epithelial neuroendocrine differentiation of androgen-sensitive LNCaP cells', *Endocrine-Related Cancer*, 13(1), pp. 151–167. doi: 10.1677/erc.1.01043.

Yuan, T. C., Veeramani, S. and Lin, M. F. (2007) 'Neuroendocrine-like prostate cancer cells: Neuroendocrine transdifferentiation of prostate adenocarcinoma cells', *Endocrine-Related Cancer*, 14(3), pp. 531–547. doi: 10.1677/ERC-07-0061.

Zaborowski, M. P., Balaj, L., Breakefield, X. O. and Lai, C. P. (2015) 'Extracellular Vesicles: Composition, Biological Relevance, and Methods of Study', *BioScience*, 65(8), pp. 783–797. doi: 10.1093/biosci/biv084.

Zhang, M., Jin, K., Gao, L., Zhang, Z., Li, F., Zhou, F. and Zhang, L. (2018) 'Methods and Technologies for Exosome Isolation and Characterization', *Small Methods*. John Wiley & Sons, Ltd, 2(9), p. 1800021. doi: 10.1002/smtd.201800021.

Zhang, X., Coleman, I. M., Brown, L. G., True, L. D., Kollath, L., Lucas, J. M., Lam, H. M., Dumpit, R., Corey, E., Chéry, L., Lakely, B., Higano, C. S., Montgomery, B., Roudier, M., Lange, P. H., Nelson, P. S., Vessella, R. L. and Morrissey, C. (2015) 'SRRM4 expression and the loss of REST activity may promote the emergence of the neuroendocrine phenotype in castration-resistant prostate cancer', *Clinical Cancer Research*. American Association for Cancer Research Inc., 21(20), pp. 4698–4708. doi: 10.1158/1078-0432.CCR-15-0157.

Zhang, Y., Li, X., Becker, K. A. and Gulbins, E. (2009) 'Ceramide-enriched membrane domains-Structure and function', *Biochimica et Biophysica Acta - Biomembranes*. Elsevier, 1788, pp. 178–183. doi: 10.1016/j.bbamem.2008.07.030.

Zhang, Y., Liu, Y., Liu, H. and Tang, W. H. (2019) 'Exosomes: Biogenesis, biologic function and clinical potential', *Cell and Bioscience*. BioMed Central Ltd., 9(19), pp. 1–18. doi: 10.1186/s13578-019-0282-2.

Zhao, H., Ma, T.-F., Lin, J., Liu, L.-L., Sun, W.-J., Guo, L.-X., Wang, S.-Q., Otecko, N. O. and Zhang, Y.-P. (2018) 'Identification of valid reference genes for mRNA and microRNA normalisation in prostate cancer cell lines.', *Scientific reports*. Nature Publishing Group, 8(1), p. 1949. doi: 10.1038/s41598-018-19458-z.

Zöller, M. (2009) 'Tetraspanins: Push and pull in suppressing and promoting metastasis', *Nature Reviews Cancer*, 9(1), pp. 40–55. doi: 10.1038/nrc2543.